FINAL PROJECT REPORT

HYDRAULIC MODEL STUDY

WASTEWATER INFLUENT SPLITTER CHAMBER
PROJECT 88

SOUTHERLY WASTEWATER TREATMENT PLANT
COLUMBUS, OHIO

By

Steven J. Wright
Daniel B. Schläpfer
Razik Al-Saigh

THE UNIVERSITY OF MICHIGAN
DEPARTMENT OF CIVIL ENGINEERING
ANN ARBOR, MICHIGAN

JANUARY, 1988

TABLE OF CONTENTS

INTRODUCTION

This report describes a hydraulic model study conducted to examine the nature of the flow within the influent splitter chamber to be constructed at the existing Southerly Wastewater Treatment Plant in Columbus, Ohio. The study was performed in the Hydraulics Laboratory of the Civil Engineering Department at The University of Michigan. The scale model was constructed at 1/7.5 of the prototype size and subjected to a variety of flow conditions to be expected at the WWTP under present and future conditions. As used above and elsewhere in this report, *prototype* refers to the dimensions and conditions existing in the actual splitter chamber. The model study examined the nature of the flow in the proposed splitter chamber for purposes of defining potential problems with respect to flow distribution, grit deposition, and guide vane vibration. This report describes the details of this study. In the description of the model and the results, *right* always refer to the flow system in the sense of an observer standing at the upstream end and looking in the direction of flow or downstream.

GENERAL SYSTEM DETAIL

The treatment plant is expected to operate at 1988 flows of up to 150 million gallons per day (MGD) in the present proposed configuration with average flows in the range of 70-90 MGD and a minimum flow of approximately 50 MGD. By the year 2015, the maximum flow is expected to be on the order of 300 MGD with average flows of 120-176 MGD. Provisions for handling the ultimate capacity of 300 MGD have been designed into the proposed influent splitter chamber. The wastewater influent enters through a pumping station, through the proposed influent splitter chamber, and into independent preaeration tanks. In the early years of the wastewater treatment plant operation, a temporary inlet conduit will direct this inflow into the splitter chamber with a provision for switching over to a different entrance conduit at a later date. These different inlets are referred to as the 1988 entrance and the 2015 entrance, respectively. At the 1988 capacity of 150 MGD, a total of three discharge conduits will

receive the flow from the splitter chamber and divert it into the appropriate preaeration tanks; to handle the 2015 flows, four such conduits will be in place. In the 1988 configuration, one of the conduits will divert the flow into four aeration tanks while the other two will service six tanks; this results in an unequal flow distribution among the various conduits.

The splitter chamber is composed of an inlet channel which ends at the guide vane section. Adjustable vanes installed within the splitter chamber are intended to attain more uniform flow distribution among the treatment trains. These vanes may be adjusted up to ± 45° from the direction parallel to the inflow channel. The flow then passes into separate channels which expand in width and decrease in depth in the direction of flow such that a constant velocity is approximately maintained along each channel. Hydraulic control in the splitter chamber is maintained by overflow weirs at the entrance to the separate outlet conduits. The flow distribution can be controlled by slide gates along the weir crests which regulate the flow by controlling the weir crest length in discrete increments. Each outflow section may also be isolated by stop gates within the influent splitter chamber.

Wastewater influent flows as a pressurized flow through the inlet conduits until a short distance upstream from the guide vane, the exact location depending upon the flow rate. A free surface is present through the remainder of the splitter chamber.

The grit entering the influent chamber is estimated to have a specific gravity of 2.65, to lie in the size range that will pass a 30 mesh screen but retained on a 100 mesh one, and to have an influent concentration of 200 mg/l.

Matters of potential concern addressed by the model study include:

1. The general flow patterns and flow distribution within the splitter chamber
2. The required vane settings to obtain optimum flow distributions
3. The ability to use a single vane setting over a range of flow rates
4. The possible occurrence of locations exhibiting excessive sedimentation
5. Potential problems with vane vibration due to vortex shedding on the vanes.

FINDINGS

During the course of this investigation, the following results were developed:

- With the 1988 entrance, flow velocities in the inlet channel are higher along the east wall as a result of the bend in the inlet conduit. This results in a tendency for higher flows to occur in the easterly outlet trains and lower flows in the west train. By adjusting the guide vanes, the flow distributions in the outlet conduits can be equalized. There are likely to be several different sets of vane angles that would give essentially equivalent flow distributions for a given flow; thus there is not likely to be a unique solution. In general, a single vane setting will give satisfactory flow distributions for the range of discharges studied. With all three trains in operation, only the flow of 70 MGD is not within the measurement accuracy of the desired flow distribution for a single vane setting. An anomaly in the trends of the flow distribution occurs between the flows of 50 and 70 MGD and is probably associated with the flow through the bend as it approaches the vanes.

When only two trains are in operation, it is not always possible at the lower flow rates to achieve the desired flow split. This holds for the case with the west and center trains in operation or with the center and east trains . However, the deviations are relatively minor and the flow can be controlled for the higher plant flow rates in which the flow distribution will be more critical.

- With the 2015 entrance, the inlet conduit does not turn through such a large bend and the approach flow velocities are more uniform upstream but tend to become more nonuniform across the channel in the downstream direction. Without the vanes, the center two trains tend to receive the higher flows at the expense of the outer two. Also, flow tends to concentrate in the easterly trains when compared to the westerly ones. Again, with the guide vanes, it is possible to regulate the flow to achieve the desired flow distributions. A single vane setting appears feasible for achieving the required flow distribution when all four trains are in operation as the deviation from the intended flow in any one train is within 2 percent of the plant flow in all cases and within 1 percent for all but the highest flow rate tested. Similar results were obtained

for all combinations with three trains open and the deviations in the flow split with a single vane setting were less than 1 percent for nearly all conditions examined.

- With respect to possible flow induced vibrations due to vortex shedding from the gates, there does not appear any significant possibility for problems. According to a free vibration analysis of the proposed vane, the frequency associated with the lowest vibration modes are greater than 65 Hz whereas the highest prototype shedding frequency estimated from the model study is approximately 0.15 Hz. Therefore, any design considerations regarding the vane bearings, etc. need not be concerned with the phenomenon of vortex shedding.

- The model studies of sediment movement through the splitter chamber indicate a significant potential for sedimentation. The model sediment was selected based upon a sample collected from the grit chamber preceding the present pumping station. This may represent too large of a grit size for that which will enter the splitter chamber, especially in light of the fact that the present grit chambers will be upgraded in the wastewater treatment plant expansion. However, it was observed that the sediment introduced into the model settled almost immediately with the 1988 entrance and the lower plant flow rates. With the larger plant flow rates and the 1988 entrance condition, most of the sediment was deposited on the upslope downstream from the vanes and at most, only 30 percent of the sediment passed through the splitter chamber. The increased flows associated with the 2015 entrance resulted in less sediment deposition but even with the 300 MGD flow, only about 60 percent of the sediment passed through the splitter chamber.

- The measurements of water level in the approach sections to the overflow weirs indicated consistent but small variations in the water surface levels across the channels and that these could generally be correlated with the relative distribution of flows in the individual trains. The selection of suitable water level sensing stations was based upon the observations of sedimentation patterns (to avoid regions of high deposition) and to obtain minimal variations in observed water levels among the various trains for a given flow condition.

MODEL DESCRIPTION

Modelling Criteria

Physical models to examine flow patterns in free surface flow are performed using Froude number similarity, which fixes the relations between model and prototype conditions once the physical model scale has been selected. Dynamic similarity requires keeping all Froude numbers defined by $V/(gL)^{1/2}$ equal in the model and prototype, where V refers to any representative fluid velocity, g the acceleration due to gravity, and L is any system length. The relations between prototype and model parameters are related to the scale ratio $\mathbf{L_r}$ which is the geometric ratio between any length in the prototype and the corresponding one in the model ($\mathbf{L_r}$ = $\text{Length}_{\text{prototype}}/\text{Length}_{\text{model}}$). For a Froude scaled model, the following relations must hold:

PARAMETER		RATIO
Length	$\mathbf{L_r}$	$\mathbf{L_r}$
Velocity	$\mathbf{V_r}$	$\mathbf{L_r^{1/2}}$
Discharge	$\mathbf{Q_r}$	$\mathbf{L_r^{5/2}}$
Pressure	$\mathbf{P_r}$	$\mathbf{L_r}$

Problems associated with vortex shedding from the vanes, however, depends upon the internal nature of the flow and requires similarity of Reynolds numbers in order to achieve dynamic similarity. The relations between prototype and model parameters are related to the scale ratio $\mathbf{L_r}$ by the following relations (assuming that water is the working fluid in both model and prototype and that variations in fluid viscosity are unimportant):

PARAMETER		RATIO
Velocity	$\mathbf{V_r}$	$\mathbf{L_r^{-1}}$
Discharge	$\mathbf{Q_r}$	$\mathbf{L_r}$
Pressure	$\mathbf{P_r}$	$\mathbf{L_r^{-2}}$

Finally, if the deposition of particles within the splitter chamber is to be examined, the essential parameter is that of the settling velocity of the representative particles carried with the flow. In order to maintain dynamic similarity of settling characteristics, the ratio of particle settling velocity to any other representative flow velocity should remain constant between prototype and model. Since settling velocity is a function of both particle diameter and density, similarity can be maintained by adjusting the model particle submerged weight which in turn depends upon particle size and specific gravity in order to maintain the similarity requirement.

Because of differences between the Froude and Reynolds number modelling criteria, it is not possible to satisfy dynamic similarity for flow distribution and vortex shedding at the vanes in the same model. Therefore, a separate model was constructed to study the latter component of the problem. This was not a complete system model since the Froude scaled model (which modelled the entire splitter chamber) provided the general details on the approach velocities to the vanes and the vortex shedding characteristics were found in a Reynolds scaled model of the region in the vicinity of the vanes only. The sediment deposition problems were studied in the complete Froude scaled model only. The proposed study therefore consisted of a complete model in which the general flow conditions were examined on the basis of Froude number similarity and a separate model of the flow at an individual vane which was scaled according to the Reynolds number similarity criterion.

Model Testing Facilities

The model study was conducted in the Civil Engineering Hydraulics Laboratory at The University of Michigan. The model was supplied from a constant head water supply containing a recirculating water supply system capable of delivering a flow rate of up to about 7.0 cubic feet per second (cfs). At the 1:7.5 scale ratio for the Froude scaled model, the maximum discharge (corresponding to 300 MGD) required in the model was approximately 3.0 cfs.

Model Construction

A complete model of the influent splitter chamber along with the influent conduit was constructed at a model scale of 1:7.5 and operated according to Froude scaling criteria. The model was constructed according to the dimensions detailed in the various blueprints provided by URS Dalton. Since the 1988 flow will enter through a different inlet conduit than that for the future (2015) flows, both inlets were constructed with the provision for bulkheading either of them as required. The extent of the physical model is indicated in the plan view in Fig. 1 and also in the photographs of the overall model in Fig. 2. All relevant internal details in the splitter chamber were modelled according to the information provided in the design blueprints. This includes the deflector vanes, internal walls, and all internal gates. The only deviation was in the deflector vanes which were constructed with a constant thickness, Fig. 3, which corresponded to the maximum vane thickness and the correct total length. Figure 4 is a photograph of the guide vanes in place in the model. The model extended to the weir crests at the outlet to the splitter chamber since the weir crests provide the hydraulic control for the flow within the splitter chamber. Provisions were made for installing gates over portions of the weir crest length as indicated in Fig. 5 which indicates the downstream weir crest completely open in one case and with the two side gates in place in the other. The rest of the model consisted of a inlet flow metering device (upstream venturi meter) and associated piping, separate flow metering devices (weir boxes) on each outlet train, an injection system for the model grit particles, and an outflow system to return the flow to the building storage tanks.

The flow was introduced into the model through an 8 inch PVC manifold attached to the supply line as indicated in Fig. 6. The manifold consisted of connections for either entrance and the one not being used for the entrance condition studied was sealed. An 8 inch gate valve at the upstream end of the manifold was used to regulate the flow. The inflow pipe was constructed to enter vertically downwards into the model in a short mixing chamber, after which the model flow was basically equivalent to the prototype situation. The mixing chamber was constructed 5-10 flow depths ahead of

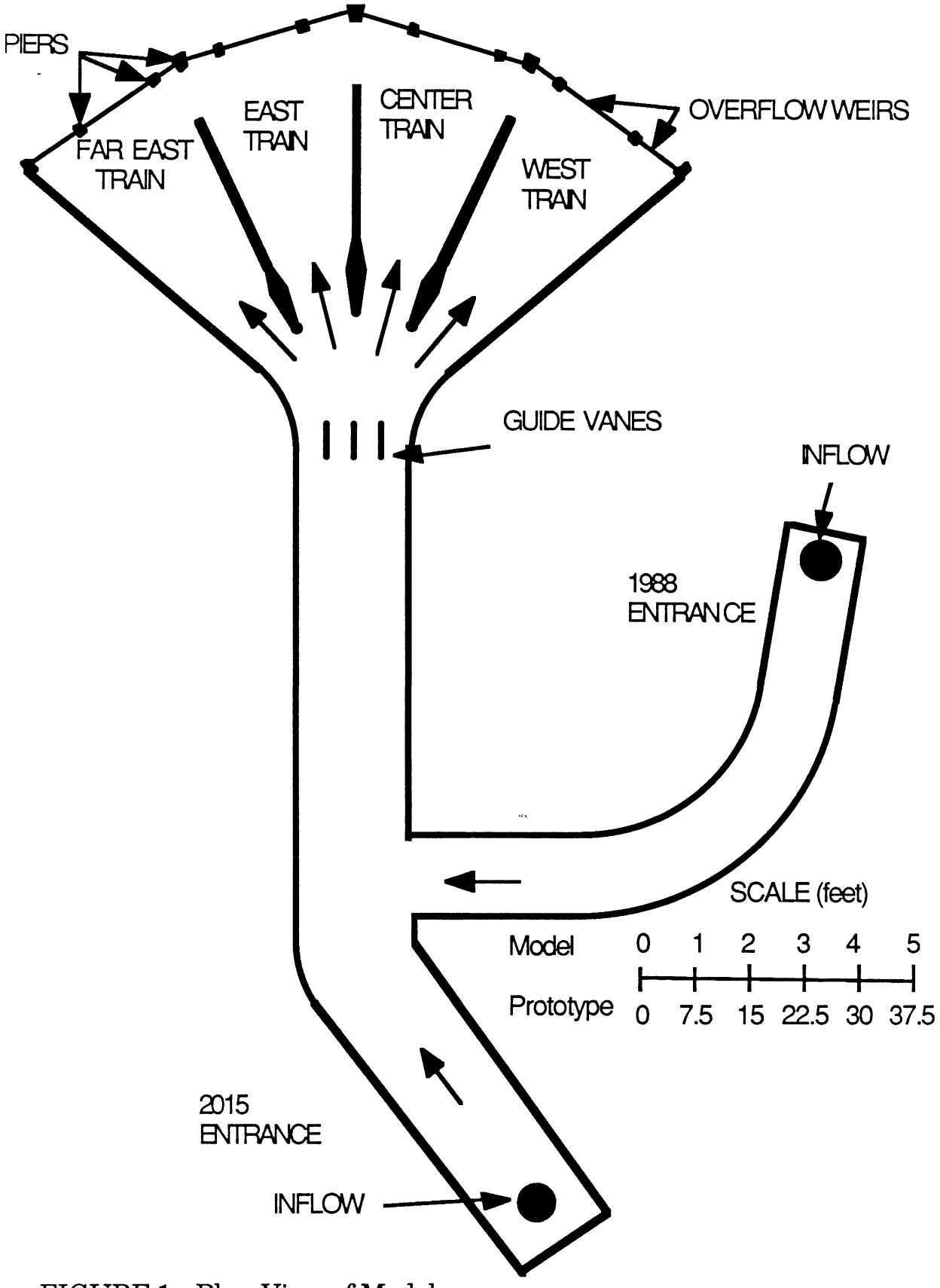

FIGURE 1. Plan View of Model.

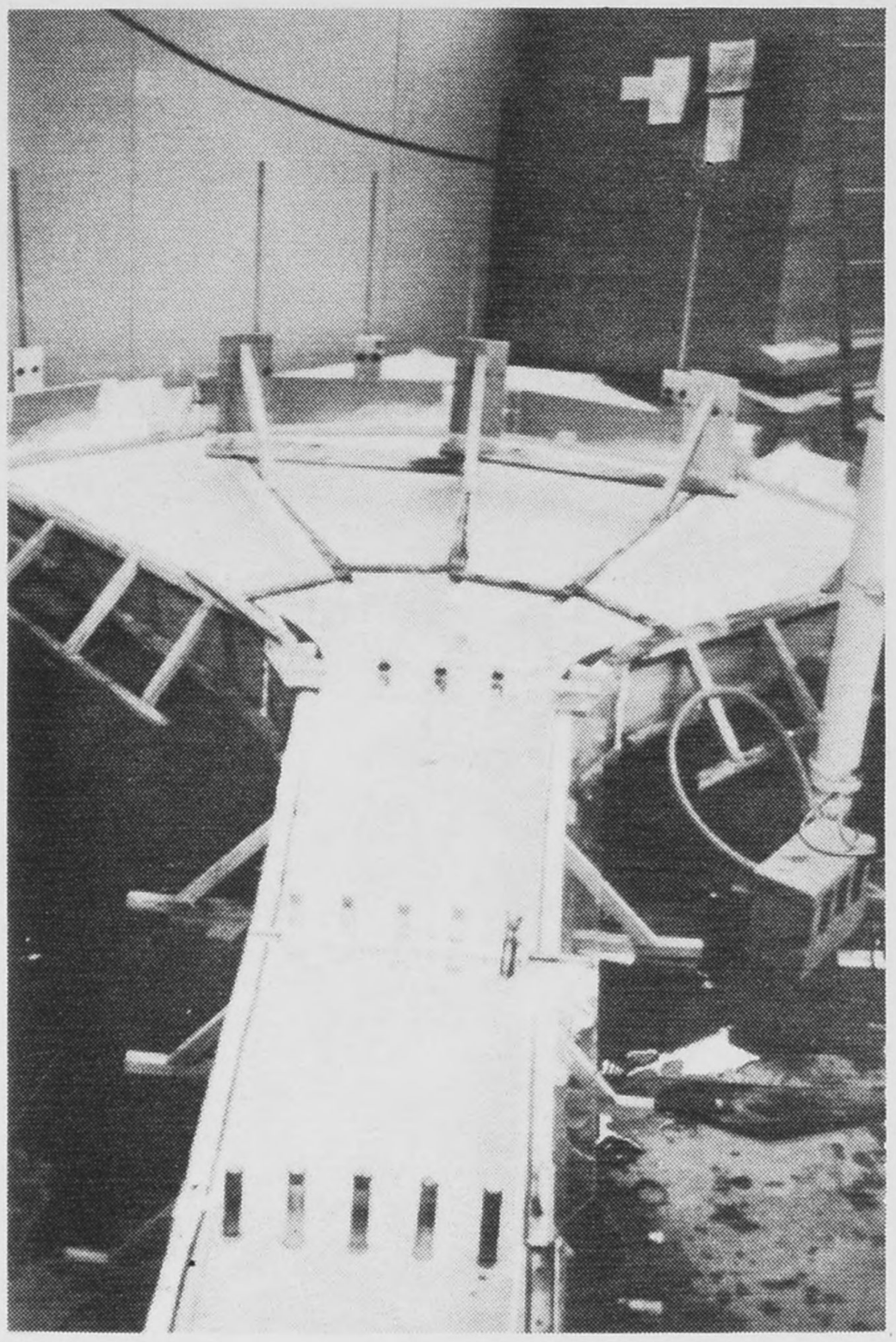

Figure 2. View of Splitter Chamber Model From Upstream End.

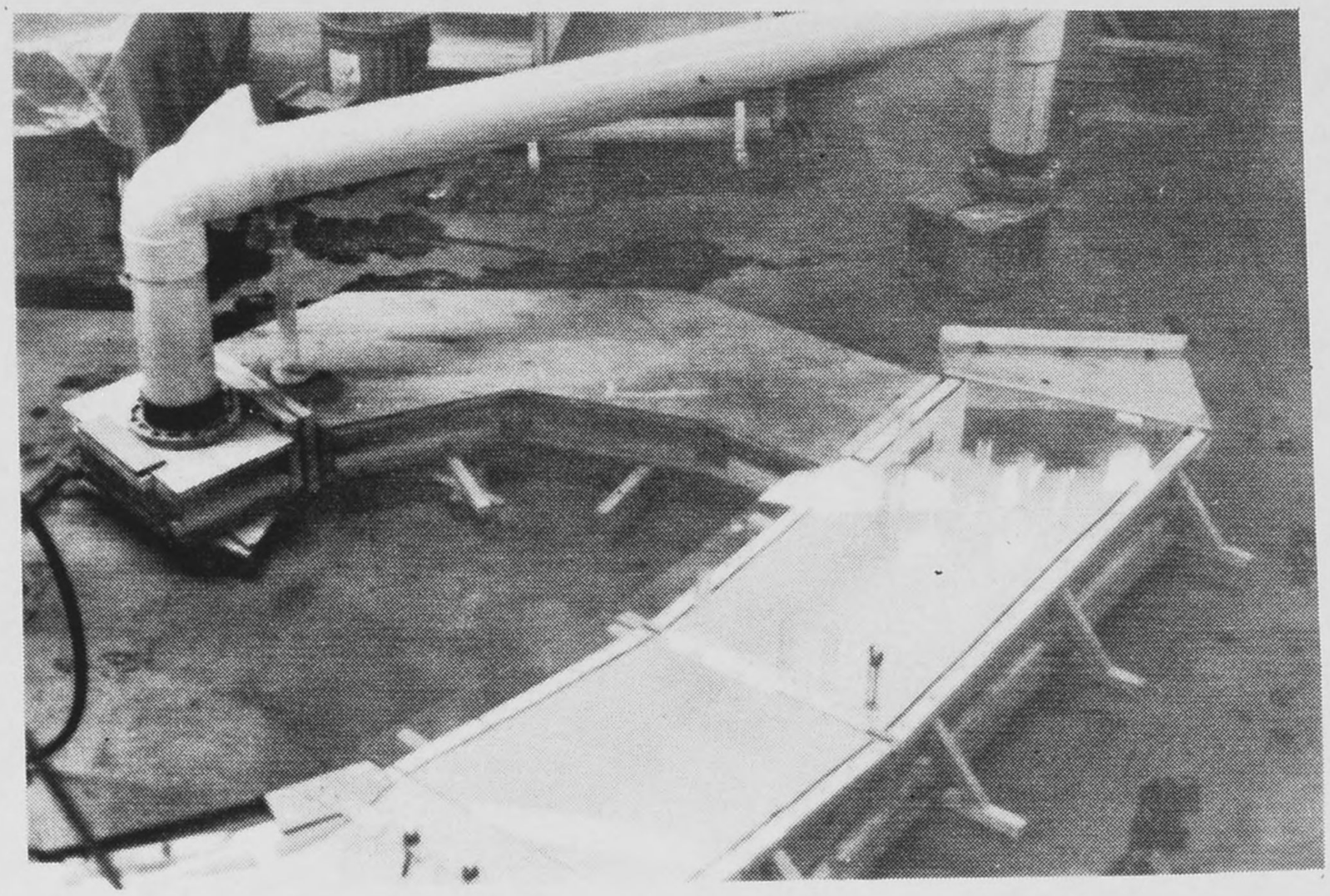

1988 Entrance

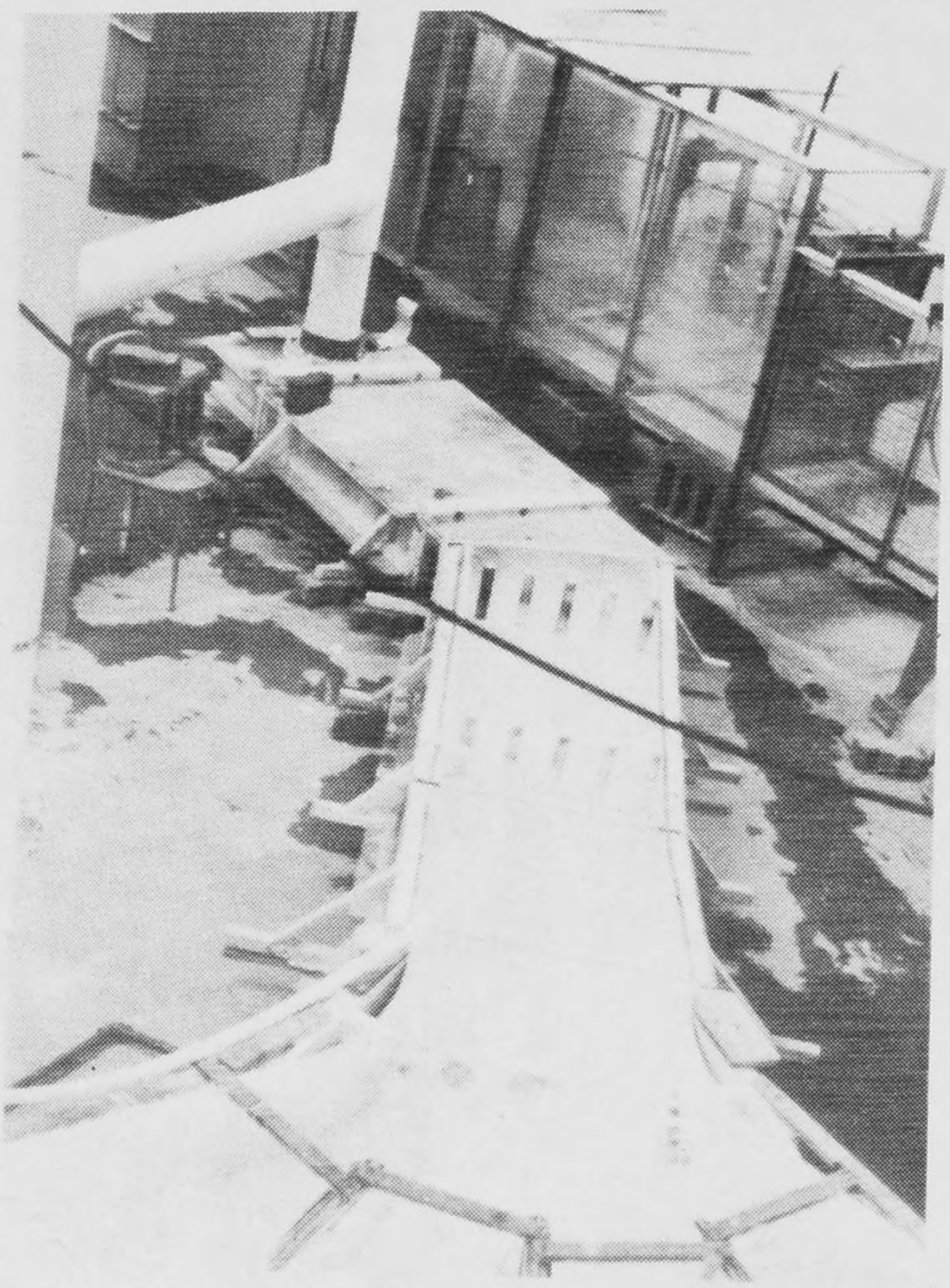

2015 Entrance

Figure 2. View of Splitter Chamber Model.

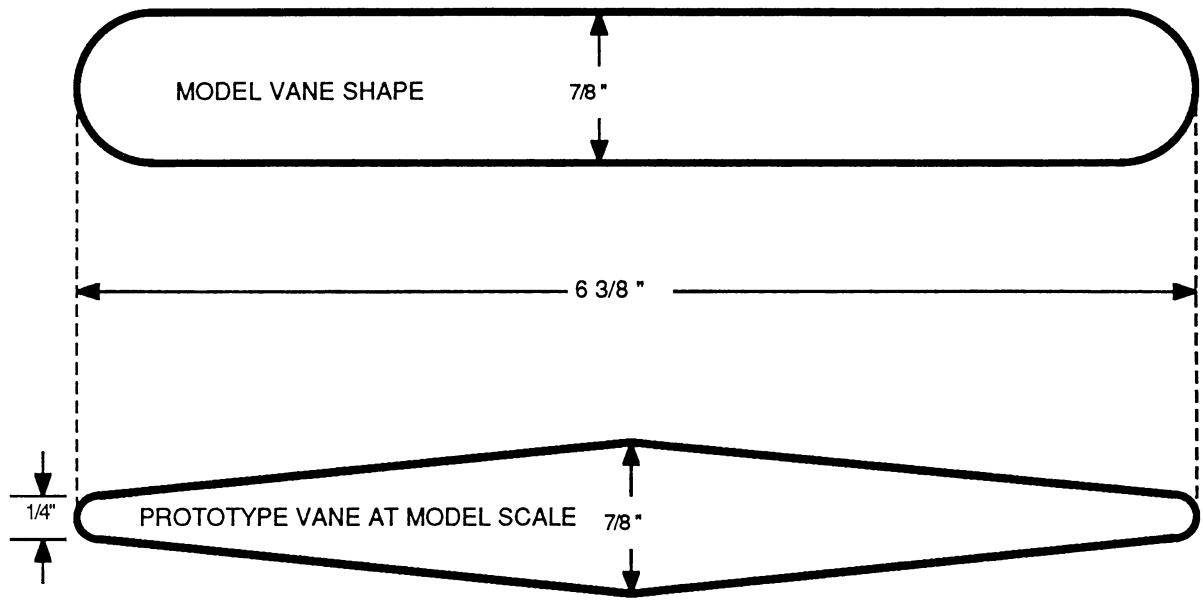

Figure 3. Cross-Section of Model and Prototype Vanes at Model Scale.

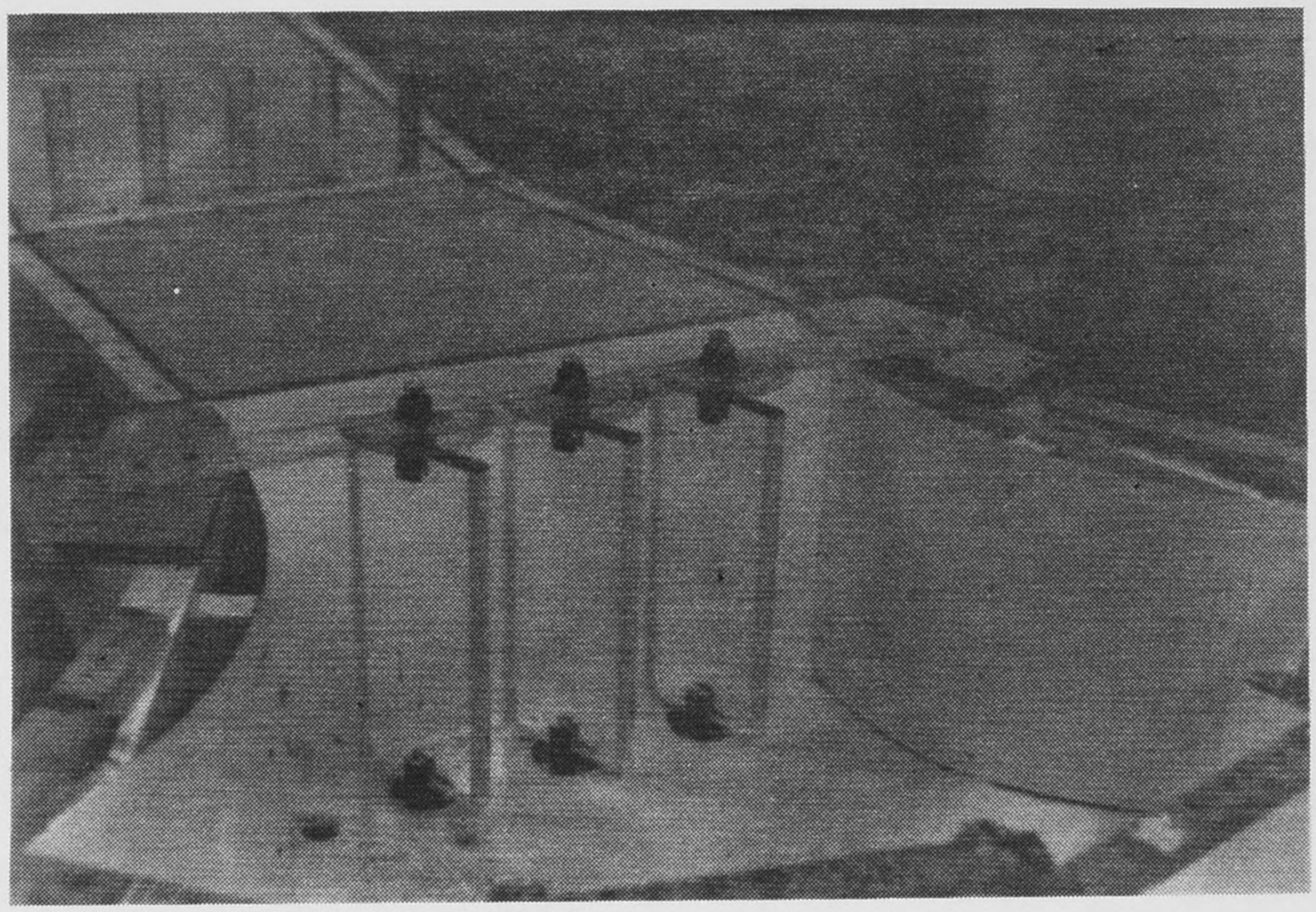

Figure 4. View of Guide Vanes Installed in Model.

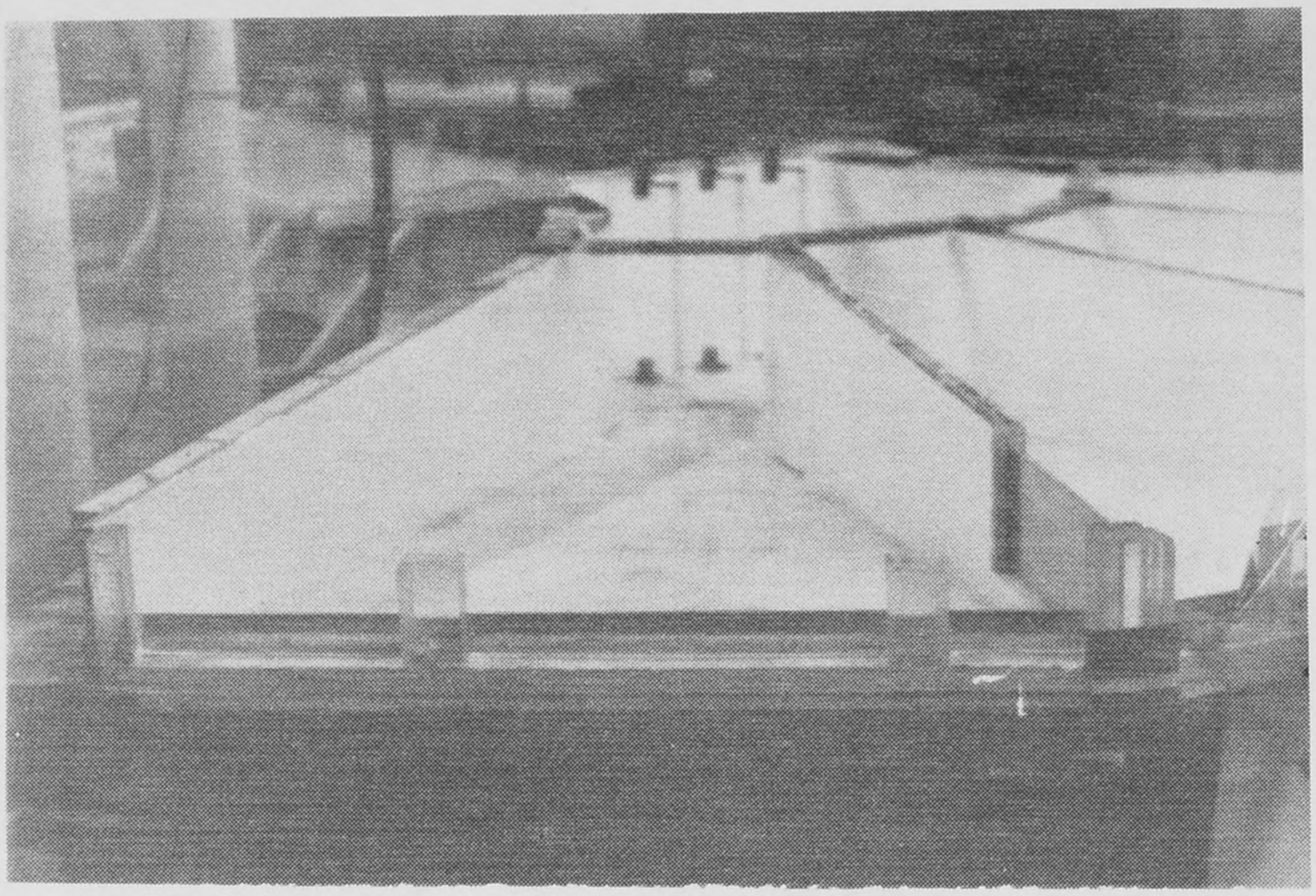

a.) With Entire Crest Length Open.

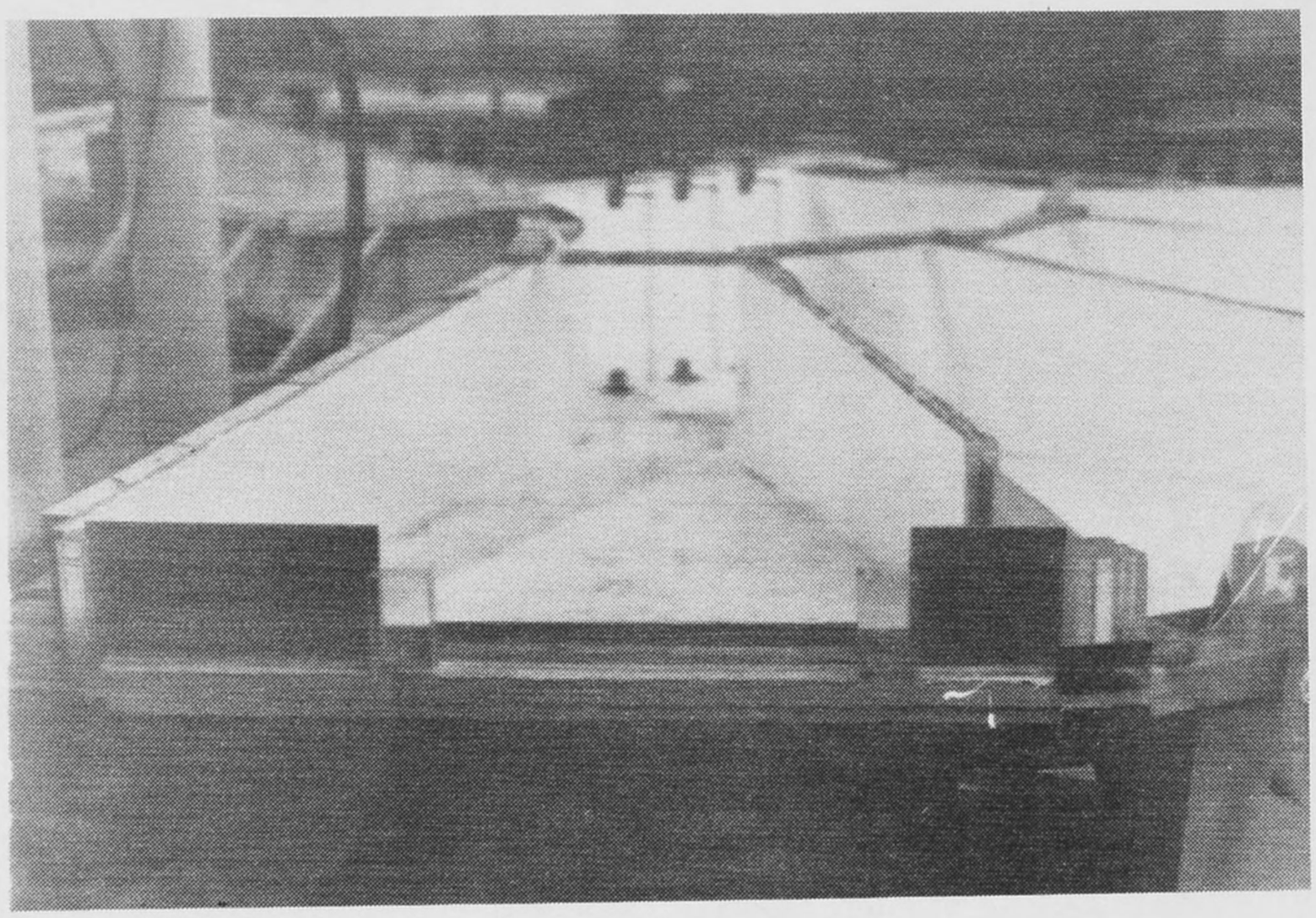

b.) With Two Side Gates in Place

Figure 5. View of Downstream Weir Crest in Model.

Figure 6. View of Supply Manifold.

the bends in the model so that the flow entering the bend would be straight and parallel to the channel sides.

The basic model construction was of exterior plywood which was subsequently painted white to obtain the most contrast for dye and sediment injections. Specific portions of the model which involved curved surfaces along bends were constructed with sheet metal to provide the necessary curvature. The vanes were constructed of plexiglass to maintain better dimensional stability. The covered portion of the splitter chamber was covered with a plexiglass lid to allow visual observation of the flow within that region. Access ports (open plexiglass cylinders of 1 1/2 inch diameter glued to the lid) to inject dye for flow visualization and to measure velocities were installed in the lid.

Vortex Shedding Model

A separate facility was constructed to examine the question of vortex shedding from a model of the prototype vane. As stated previously, Reynolds number similarity is required to study this phenomenon. In order to reproduce appropriately scaled model velocities, a water tunnel was converted for use to study the flow around a single vane. The model vane was constructed at a scale of 1:10 and at the dimensions provided in the initial shop drawings provided with a submittal date of June 10,1987. Subsequent telephone conversations provided information that the final prototype vane would have the cross-sectional detail indicated in Fig. 3.

The vane section was installed in a water tunnel which had a 0.5 ft wide by 1 ft high cross section. Flow to the tunnel was provided through a 0.5 ft round section with a transition to the 0.5 x 1 ft cross-section and came from the laboratory constant head supply as indicated in Fig. 7. Flow straighteners (honeycomb) were placed upstream and downstream from the test section to obtain uniform flow. The top and bottom of the tunnel was constructed of clear plexiglass and the vane position could be adjusted externally to any desired angle of attack relative to the incident flow. A pressure transducer mounted downstream and behind the vane was used to observe the pressure fluctuations in the wake and to determine the vortex shedding frequency.

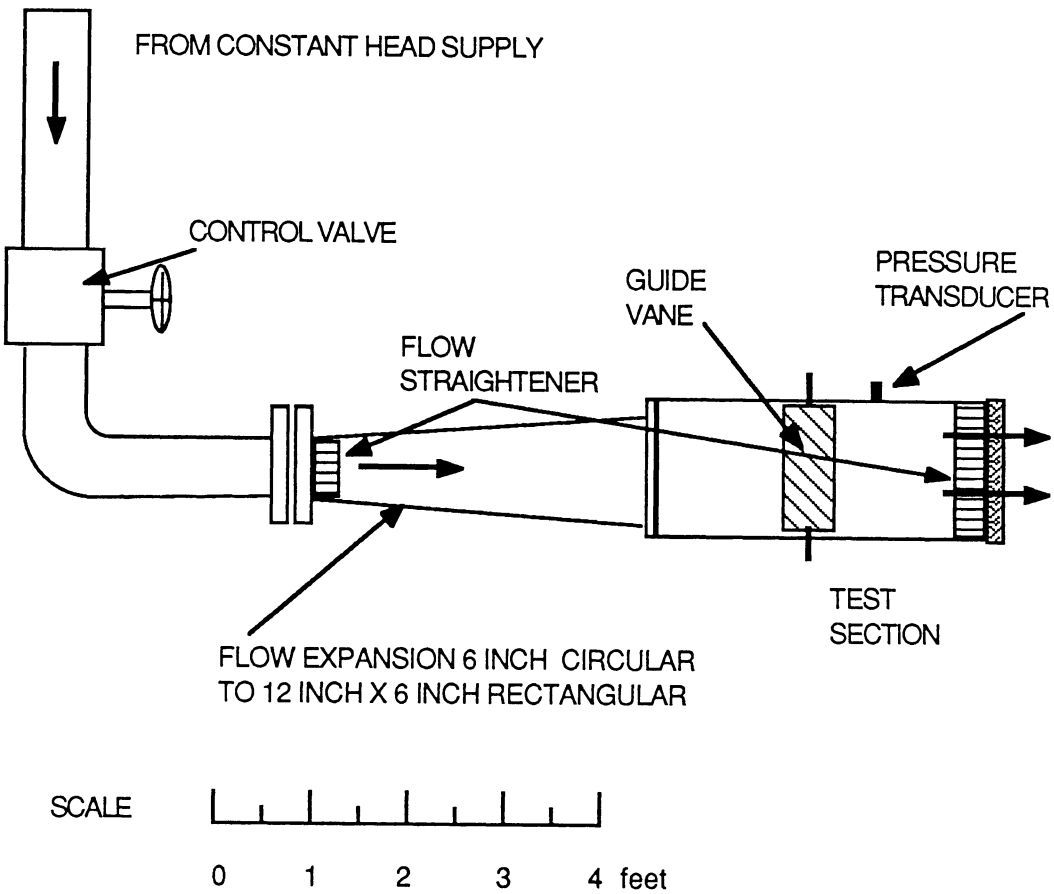

Figure 7. Schematic of Water Tunnel for Vortex Shedding Experiments.

Instrumentation

Flow Metering

Flow rates were measured in the model both in the combined inlet flow and in the separate flows exiting the splitter chamber. The inlet flows were measured with a venturi meter with a 5 inch diameter throat that is installed in the 12 inch supply line from the constant head tank. The pressure difference is recorded by means of a differential mercury manometer. This meter was calibrated prior to the model study since the installation is fairly old and known shifts in the calibration curve have been noted over time. Calibrations are performed by means of a weigh tank. The calibration equation generated by means of a linear regression to the logarithms of the manometer deflection discharge data was

$$Q\ (\text{cfs}) = 1.085\ R\ (\text{inches of mercury})^{0.5225}$$

The calibration is probably accurate to within 1-2 percent, but one difficulty is that the lowest flows used in the study are at low manometer deflections. The manometer deflection for the lowest flow of 50 MGD is 0.25 inches, for example, so there is a possibility for up to about ten percent error in the determination of discharge in this range. The relative error in flow decreases significantly with increasing discharge, however. However, the venturi meter flow rates were used for setting an estimated flow rates and the actual total flow rates were measured with the weir boxes installed on the downstream end of the model.

The weir boxes were sized to fit under the lip of the downstream end of the model with a separate box for each discharge train. The weir shape was designed to pass the entire range of flows with the largest feasible weir head. The weir crest was constructed from a sheet of machined aluminum with a total width of 11 inches and sides as indicated in Fig. 8; a weir box is shown in the photographs of Fig. 9. The upper plate serves to deflect the flow to the back of the weir box and serves to provide a lid for the flow at the highest flow rates. A stilling well connected to the side of the box was used to determine the weir head; the levels in the stilling wells were observed to fluctuate somewhat with time. Because of this complex geometry and the fact that the

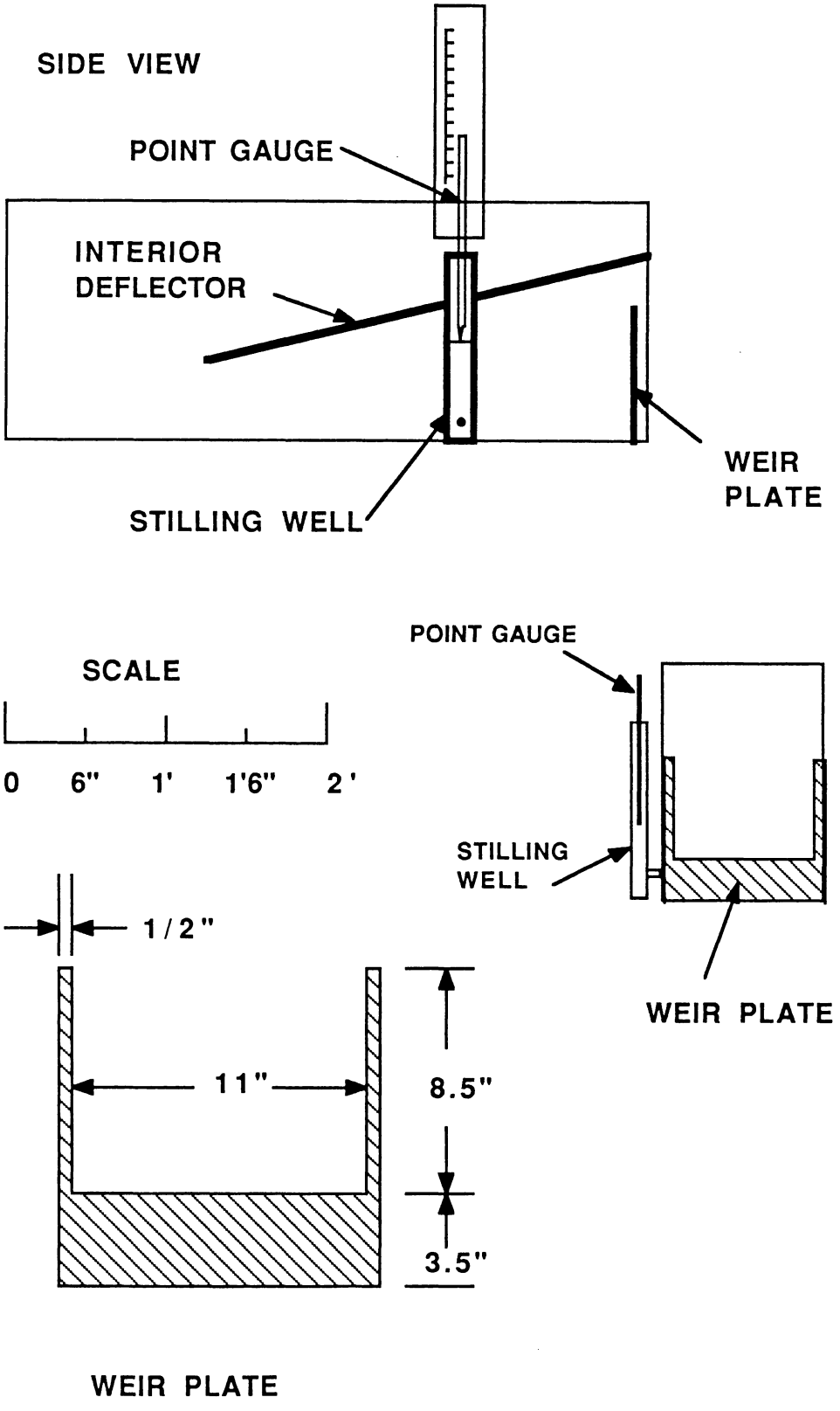

Figure 8. Details of Weir Box Construction.

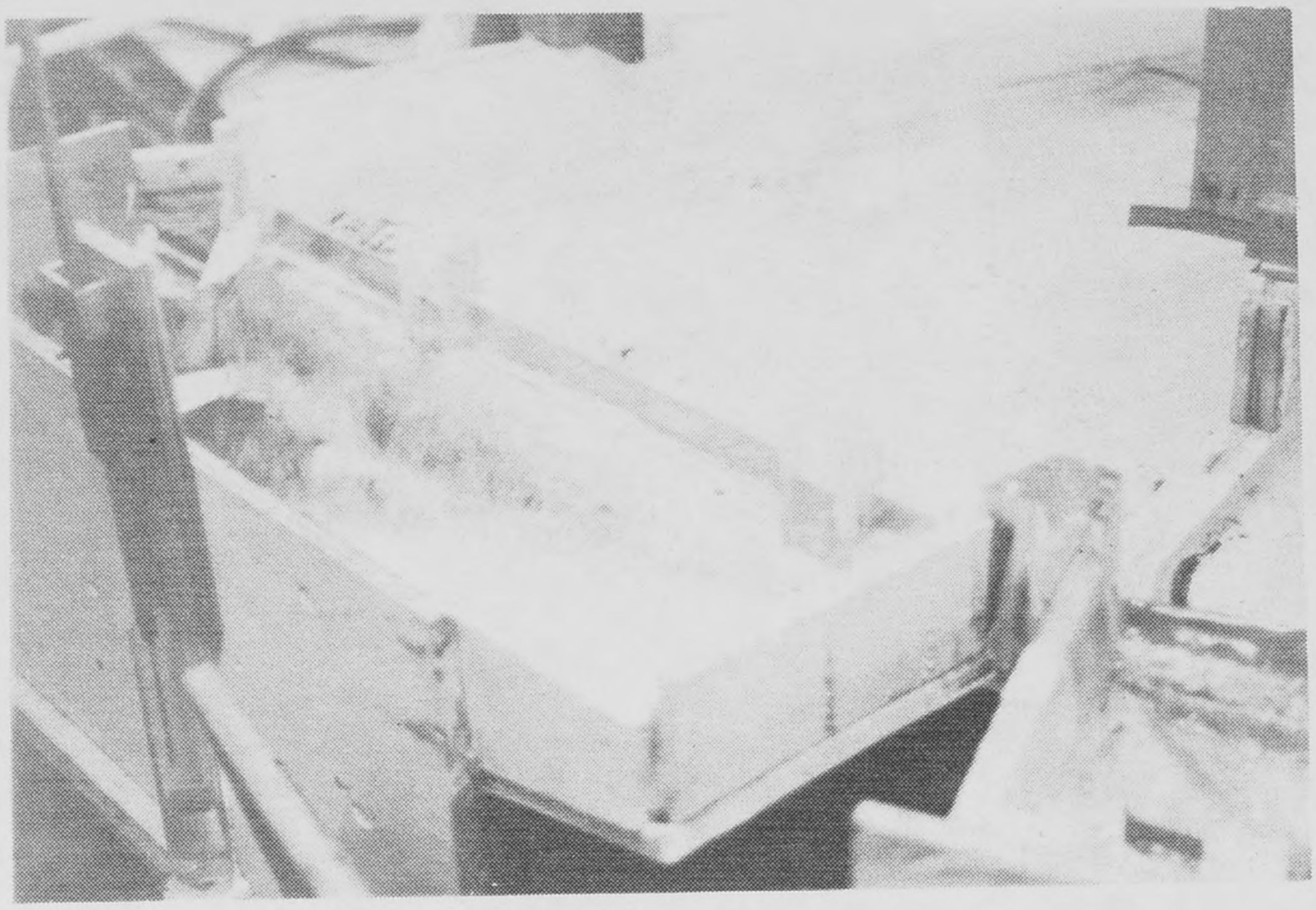

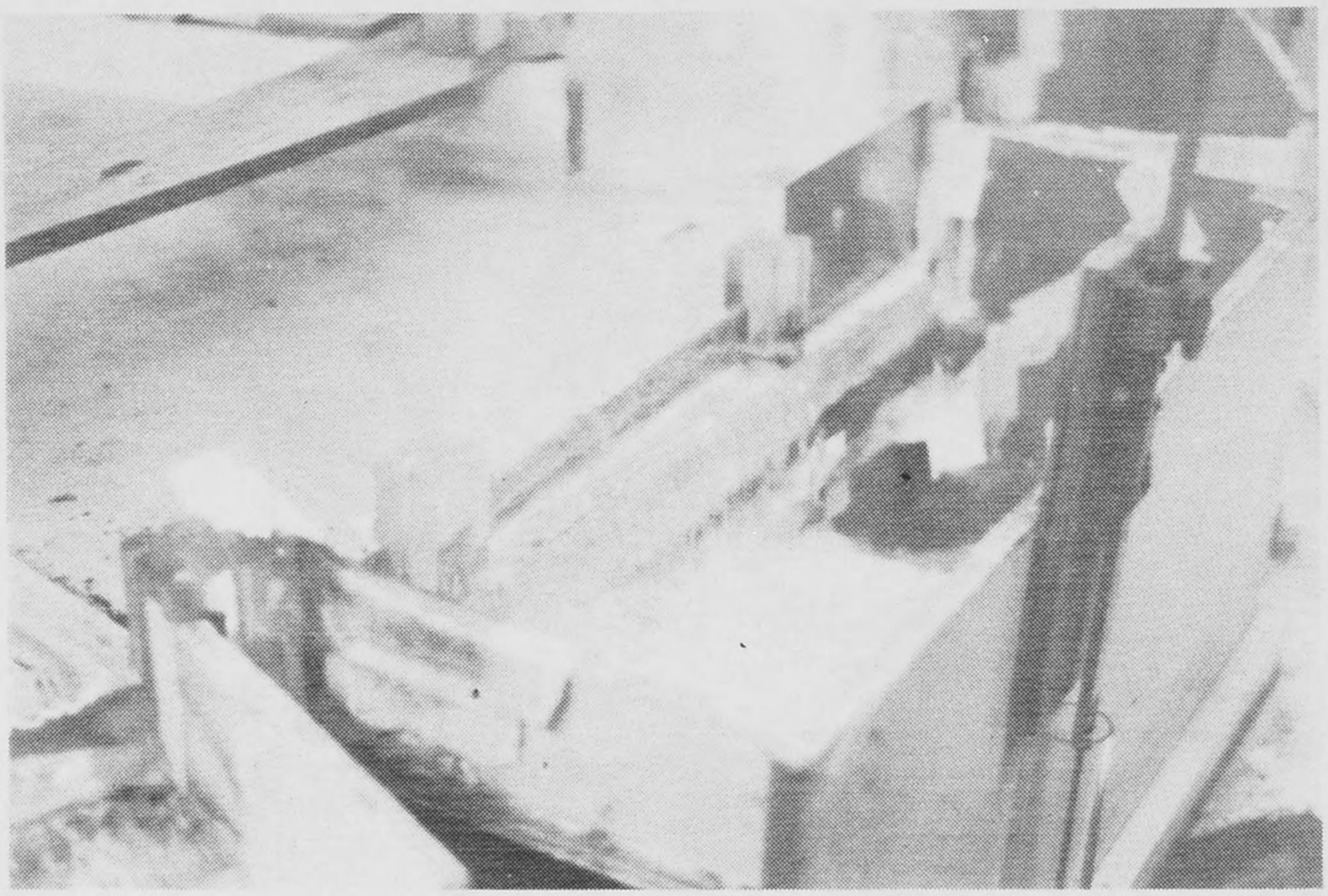

Figure 9. Photographs of Weir Boxes.

approach velocity was quite high, the weirs were calibrated in order to establish their depth-discharge relations. After some trials with alternate calibration approaches, it was ultimately decided to calibrate the boxes in place. Three boxes were isolated from the model and the fourth was allowed to pass the entire flow. The discharge was supplied from an alternate supply line with a calibrated venturi meter with a 3.5 inch diameter throat. Each weir box was calibrated in turn with this procedure. The four calibration curves are essentially the same; the calibration for Box 3 is presented in Fig. 10. These calibrations are considered accurate to within about 2 percent and limited to the accuracy of the stilling well head readings. The accuracy estimate is determine by repeated readings with the same weir box and comparisons of continuity checks with the 12 inch venturi meter. In general, the sum of the weir box flows tended to provide a total flow that was slightly greater than the venturi reading, but the deviation was fairly consistent throughout the experimental program.

Velocity Measurement

A Nixon Stream-Flo mini-propeller meter was used to make all velocity measurements. The propeller on the meter is 1 cm in diameter and therefore resolves the flow at this spatial scale. It can measure flow velocities down to about 3 cm/sec, but cannot resolve flow direction. Therefore, the velocity measurements obtained in the wake regions downstream from a separation point will be ambiguous in this regard. The propeller meter was calibrated against a second, previously calibrated velocity meter at higher velocities prior to the commencement of the model study. This calibration was found to be quite accurate, but it did not extend to low velocities. However, the locations with low velocities are those in a wake region and are subject to uncertainty with respect to flow direction as well. The counting circuit for the propeller meter averages over a 10 second interval, which was too short to adequately resolve the relatively low frequency scale turbulence due to vortex shedding in the wake of the entrance bend so 10 successive readings were averaged, resulting in a total 100 second averaging period. This was found to be suitable for obtaining a consistent

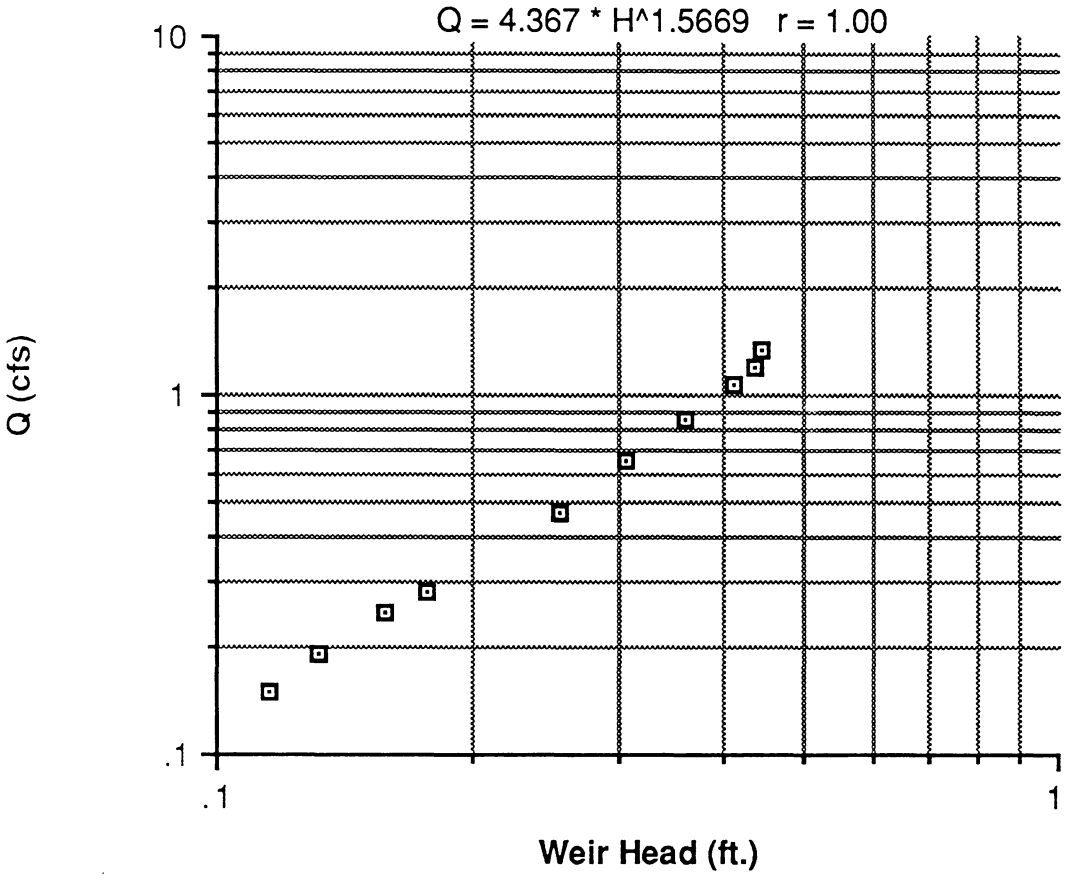
Q = 4.367 * H^1.5669 r = 1.00
10
1
.1
.1
1
Q (cfs)
Weir Head (ft.)

average velocity. All velocity measurements recorded are with the propeller meter axis parallel to the channel sides.

Water levels

All water levels were recorded with point gages with a resolution of 0.001 feet. The accuracy of individual readings may not have been this good because often fluctuations in water surface levels due to turbulence influenced the water level determinations. For the weir box flows, readings were probably accurate to within about 0.005 feet. The water levels in the influent chamber were probably accurate to about 0.002 feet.

Sediment

After some initial trials, the model sediment selected for use in the model study was a black silicon carbide powder obtained from a grinding supplies distributor. This allowed acquisition of a suitable size distribution to model the range of prototype settling velocities and obtain a product with a color that was suitable for photographic purposes. The specific gravity of the silicon carbide is specified to be 3.2.

The prototype grit is specified to have a specific gravity of 2.65, to lie in the size range that will pass a 30 mesh screen but retained on a 100 mesh one, and to have an influent concentration of 200 mg/l. These conditions were reproduced at a suitable scale in the model to ensure the maintenance of dynamic similarity. The range of prototype settling velocities is estimated from the Sedimentation Engineering Manual (1) for the corresponding sieve diameters of 0.149 and 0.595 mm to be 1.5 - 9.3 cm/sec. Model settling velocities are reduced by a factor of the square root of the length scale ratio (7.5) and thus range between 0.55 and 3.4 cm/sec. Using the specific gravity and required settling velocities, the range of model diameters was determined to be 0.06 - 0.19 mm.

The specific product used was a 120 grit "#37 Crystolon" silicon carbide powder produced by Norton Company. A sieve analysis of a representative sample yielded the size distribution indicated in Fig. 11. Since most of the material passes the 100 mesh sieve but is retained on the 120 mesh, the representative diameter of the majority of the sediment is 0.125-0.149 mm. Almost all of the sediment is above 0.088 mm so the

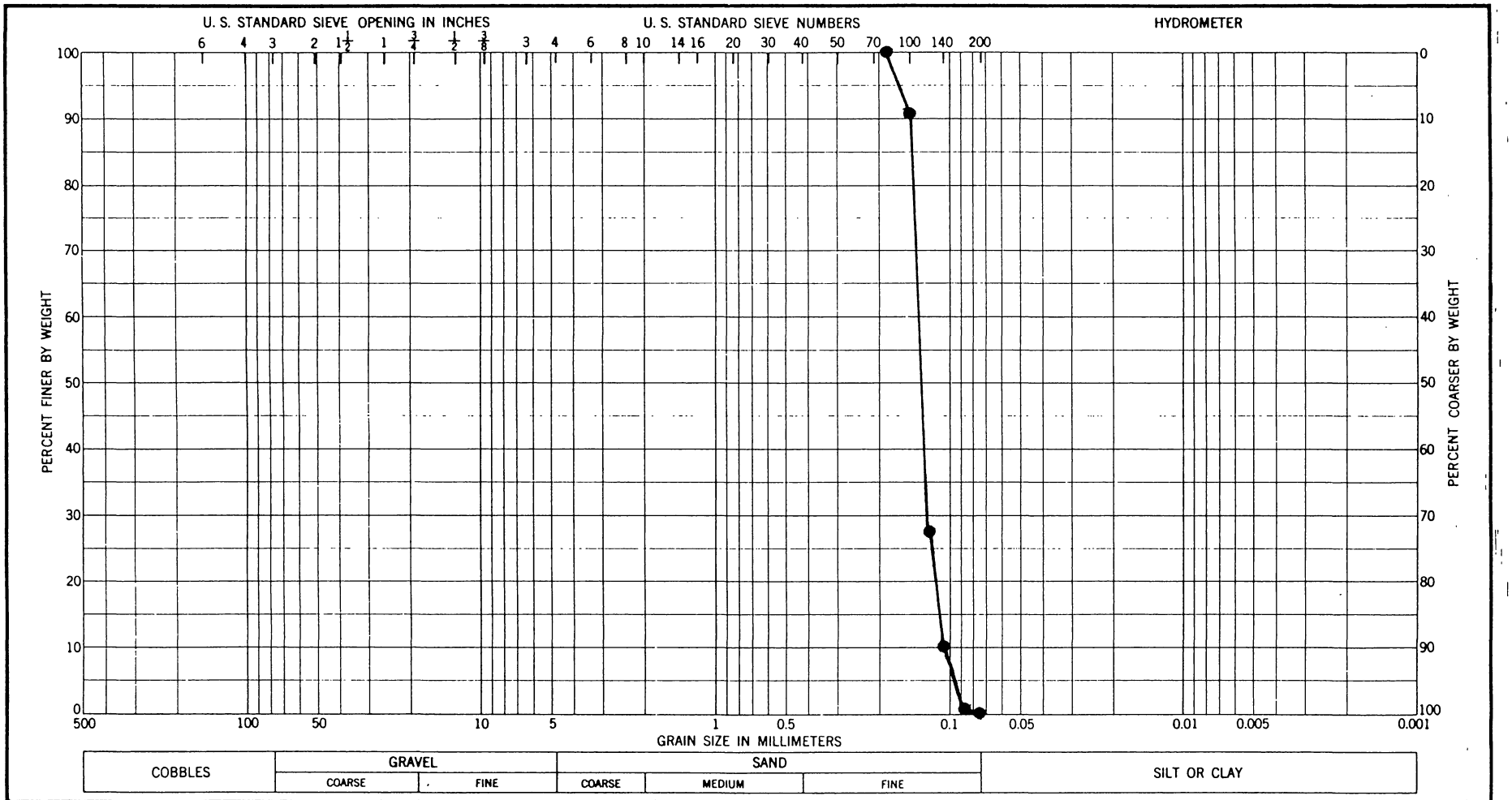

Sample No.	Elev or Depth	Classification	Nat w %	LL	PL	PI

GRADATION CURVES

Project URS Dalton, Project 88
Model Sediment
Area Crystolon ± 37, 120 grit
Boring No.
Date 7/14/87

Figure 11. Gradation Curve for Model Sediment.

silicon carbide is approximately at the middle of the required range. Without more detailed information on the size distribution of the grit at the WWTP, a better match of particles cannot be attained.

Pressure Measurements

All pressure measurements were made with a 0-2 psi Sensotec miniature strain gage pressure transducer. The actual pressure fluctuations were generally much less than the given range, so the signal had to be amplified to an acceptable level to be fed as an analog signal to either a spectrum analyzer or a strip chart recorder. The spectrum analyzer was initially used to obtain the frequency peaks with significant energy content. It was found that there were several different frequency peaks, each associated with a different turbulent flow phenomenon. Consequently, it was necessary to rely upon previous measurements on flow past flat plates at an angle of attack to determine the appropriate frequency range associated with the vortex shedding. The time required for the spectrum analyzer to adequately resolve a signal was found to be excessive and ultimately, the frequencies were estimated by averaging over about 10 cycles in a strip chart record of the pressure transducer output. Since the expected prototype shedding frequencies are not even close to the natural vibration frequencies of a vane, the results are sufficiently accurate for purposes of discussion.

Photographs

In addition to the other recorded data, a series of color slides and black and white photographs were taken of various aspects of the flow that were felt to be visually interesting and informative about the nature of the flow. Copies of these are appended as part of this report. Also obtained was a video tape, recorded on a VHS format video camera which recorded various aspects of the dye injection surveys and the sediment injection experiments. An edited version of the tape is also provided as part of the report submission.

Model Calibration

In addition to calibration of the various flow meters, several efforts were made to ensure that the model setup was appropriate and that the testing procedure was valid.

Specific efforts employed included:

1.) Surveying the bottom of the splitter chamber to ensure that it was set as level as possible. All ten points surveyed in the horizontal portion of the influent channel were within 0.007 feet of a level plane and all but one within 0.003 feet. This corresponds to a maximum deviation of approximately 5/8 inch prototype and therefore is probably better than the construction tolerance in the prototype. The floor elevations at the overflow weirs were surveyed in the corner of each train to verify that they were also set to an equivalent degree of accuracy.

2.) Verifying that consistent flows could be obtained with the weir boxes and the inlet venturi meter. That is, since there were two independent points of discharge measurement in the flow train, it is possible to get an independent check on the discharge. This was performed to ensure that the flows at high discharges could be metered accurately and indicated no difficulty.

3.) Setting the overflow weir crests to ensure that all were at equal elevations and verifying that the flow distribution would be uniform in the absence of nonuniform approach flow velocities. This was accomplished by placing a fiber mat across the channel at the upstream sides of the dividing walls to produce sufficient head drop such that no upstream effect could be felt and the flow is determined by the conditions in the individual channels. The results of the flow distribution measurements are presented in Fig. 12 and are basically within the accuracy of the flow measurements as no obvious trend in the deviations is apparent.

4.) Checking to see what effect the detail of the vane shape would have on the flow distribution. This was done after the details of the correct prototype vane shape were provided. Wooden vanes of the correct shape were constructed and tested over a range of flow rates for two different vane positions; 1.) parallel to the influent channel ($\theta = 0°$) and 2.) rotated 45° clockwise from this position ($\theta = 45°$, the maximum vane deflection). Experiments were performed by setting the flow with the wooden vanes in place, performing the flow measurements, pulling the vanes and replacing with the model plexiglass vanes, and re-measuring the flow. This was done in order to minimize any

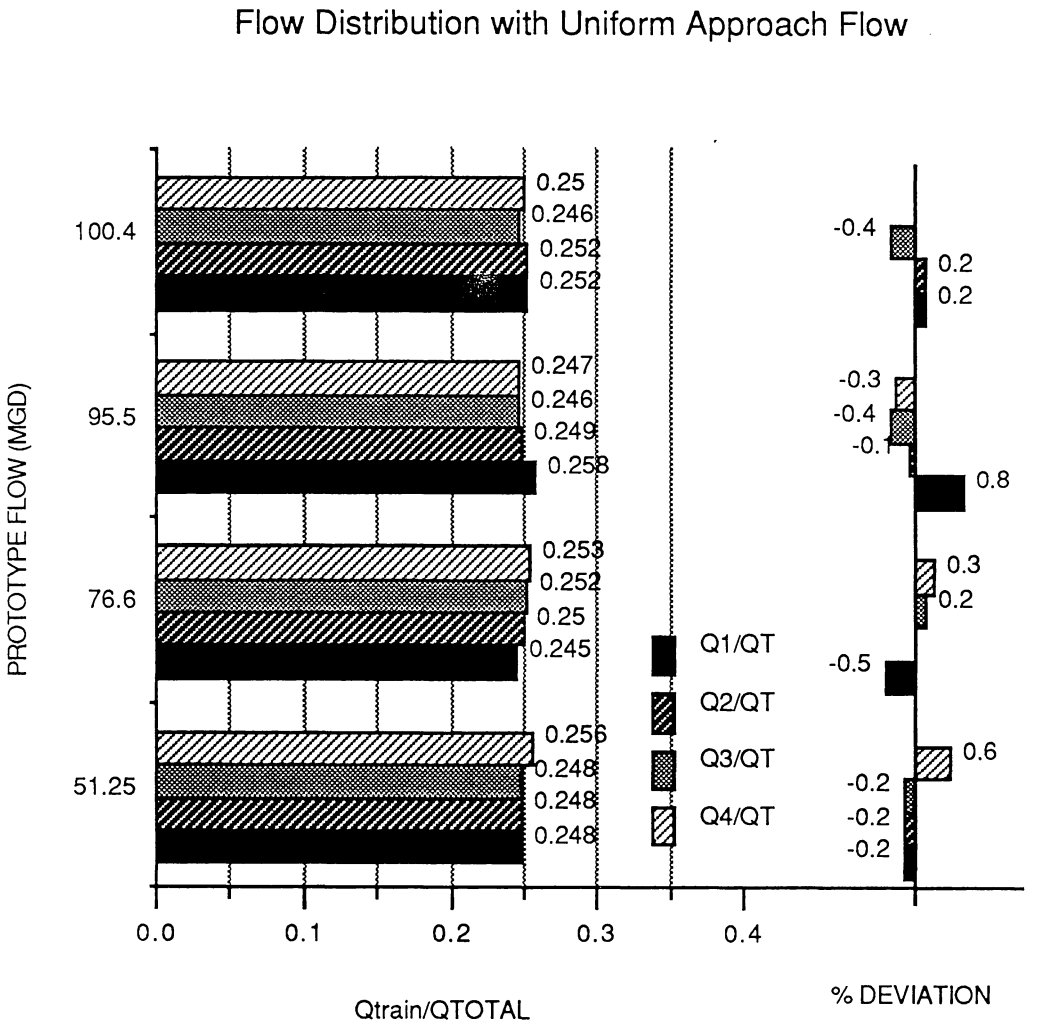

Figure 12. Flow Distribution with Uniform Approach Flow Conditions.

error in reproducing the exact flow condition. Results of these measurements are presented in Fig. 13 and while there may be some trends present, the differences between the two sets of vanes are less than 2 percent. Therefore, the effect of using the model vane shape over the range of operating conditions is judged to be minimal in terms of the measured flow distributions.

TESTING PROCEDURES

Flow Distribution

The following procedure was taken for any one flow state. A flow state was defined as any combination of outlet trains in operation over a specified range of flow rates.

1. Set the desired flow rate; this was done using the inlet venturi meter. All flow distributions are not related to this specific value since the sum of the flows from the individual weir boxes did not necessarily match the recorded venturi flow. Since all information presented is in terms of fractional flows (of the total summed through the individual weir boxes), the exact flow rate was unimportant so long as it is within a few percent of the desired flow. After this flow was set, the readings for the individual weir boxes were recorded and converted into discharges. If there was a significant discrepancy between the sum of the weir box flows and the inlet discharge, the source of this error was determined and the setting of the flow was repeated.

2. Remove the control vanes from the model and determine the flow distribution for the various flow rates to be considered in the particular testing sequence. This step was not performed with most of the 2015 flow states.

3. Re-install the vanes and go through a trial-and-error sequence of establishing the optimum vane settings. Initial vane settings were guided solely by experience with previous flow rates. After the initial flow distribution was obtained, the results were compared to the no-vane condition and subjective decisions regarding adjustments in the vane settings were made. This process was repeated until it was either established that the desired flow distribution could not be achieved or until the recorded flow

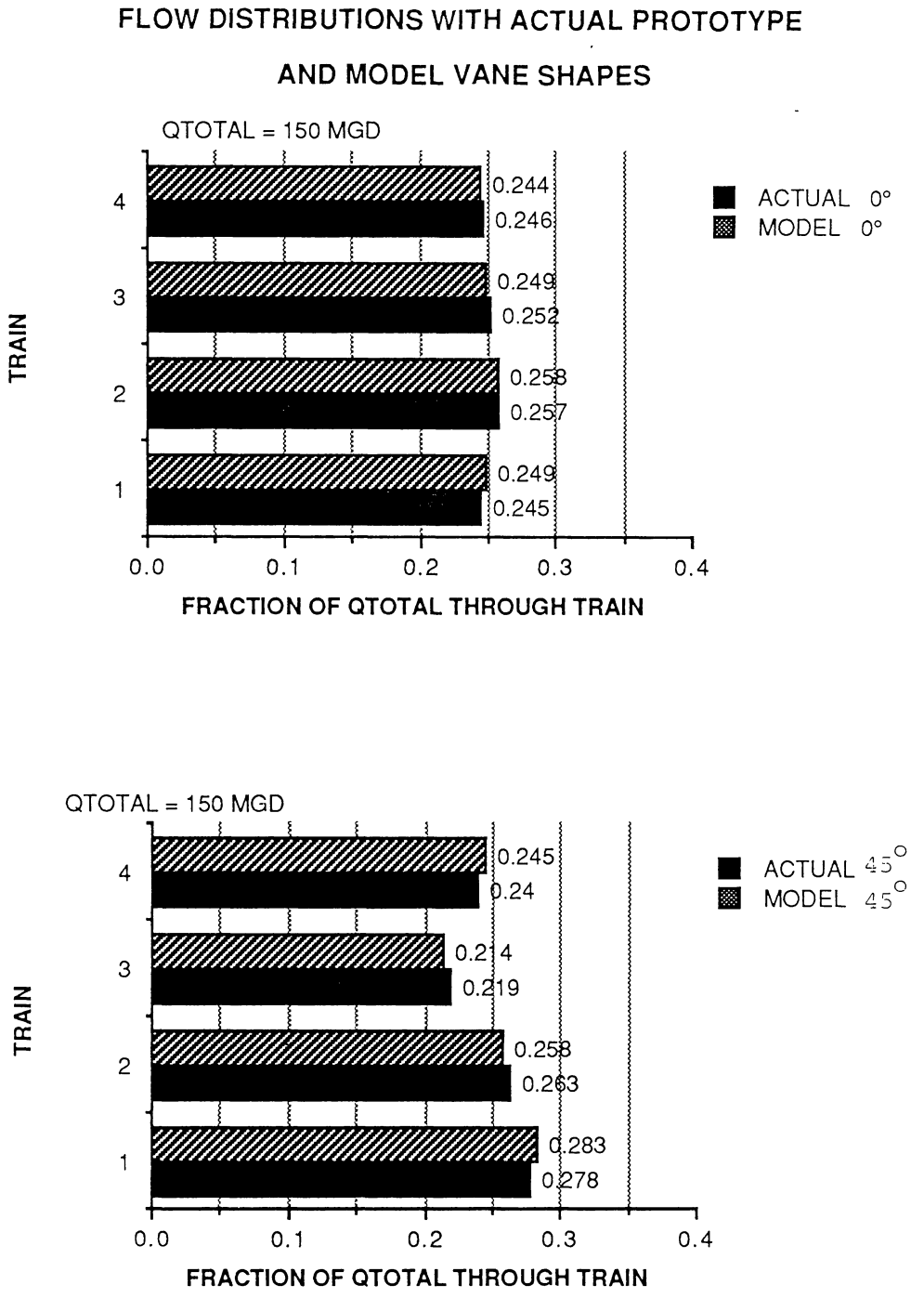

Figure 13. Comparison of Flow Distributions with Actual Prototype and Model Vane Shapes.

distribution was equal to the desired one to better than the estimated accuracy of measurement of about 2 percent. Repeat for all other flow rates.

4. Once the optimum vane settings have been obtained for a single downstream configuration, examine the results and subjectively select a single vane setting that is likely to be satisfactory over the entire range of flows. Record the flow distribution for these vane settings. Make minor adjustments if it appears to be fruitful.

Water Level Variation and Velocity Measurements

Once the optimal flow distributions were obtained for the flow state with all trains in operation for each of the 1988 entrance (three) and the 2015 entrance (four), the entire range of discharges for each were subjected to measurements of approach velocity in the inlet channel and the water level variations near the overflow weir. Velocity measurements were recorded at five equally spaced positions across the channel at the two sections indicated in Fig. 14. The velocity measurement sections are referred to as "UPSTREAM" and "DOWNSTREAM" and the measurement stations are numbered 1 through five passing across the channel from right to left looking downstream. Velocity measurements were made at four vertical locations at each station.

The water surface was observed to be fairly calm in all experiments. Therefore water level elevations were recorded at the locations indicated in Fig. 15 which were selected on the basis of verbal communications with URS Dalton personnel that indicated that the water level measurements would have to be taken close to either wall in each outflow train. Visual observations at the upstream end of the trains showed a much more complicated flow pattern with more surface disturbance and separation zones in various locations. The nature of the surface in indicated in the photographs in Fig. 16. Thus, the downstream sections were judged to give better flow level indications. The procedure employed in the measurements was to take a point gage reading of the water surface when the model was filled but not spilling water over the overflow weirs. This gives a zero level that subsequent readings are referred to. With the established flow rate, the water surface levels were again measured and the

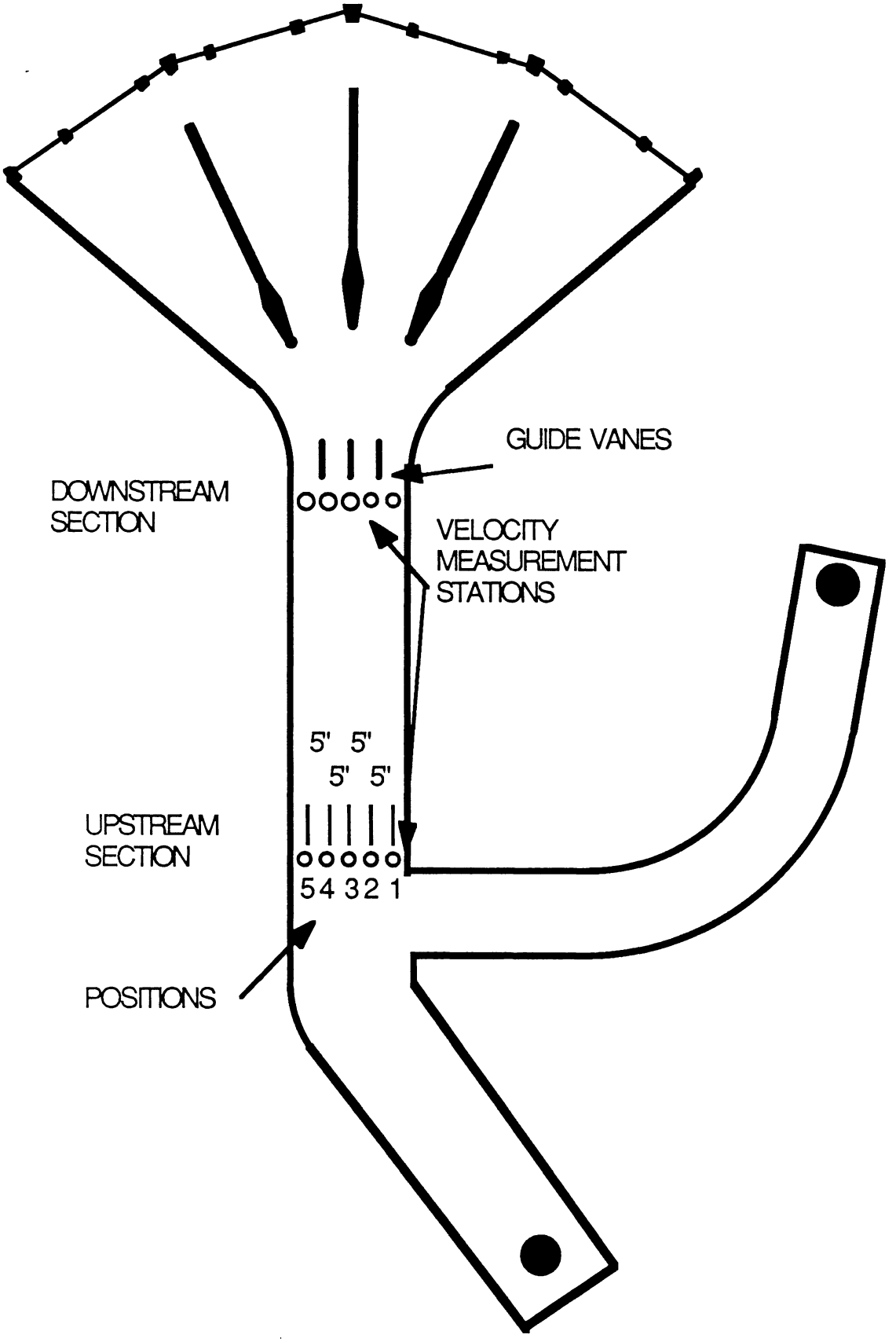

Figure 14. Velocity Measurement Stations.

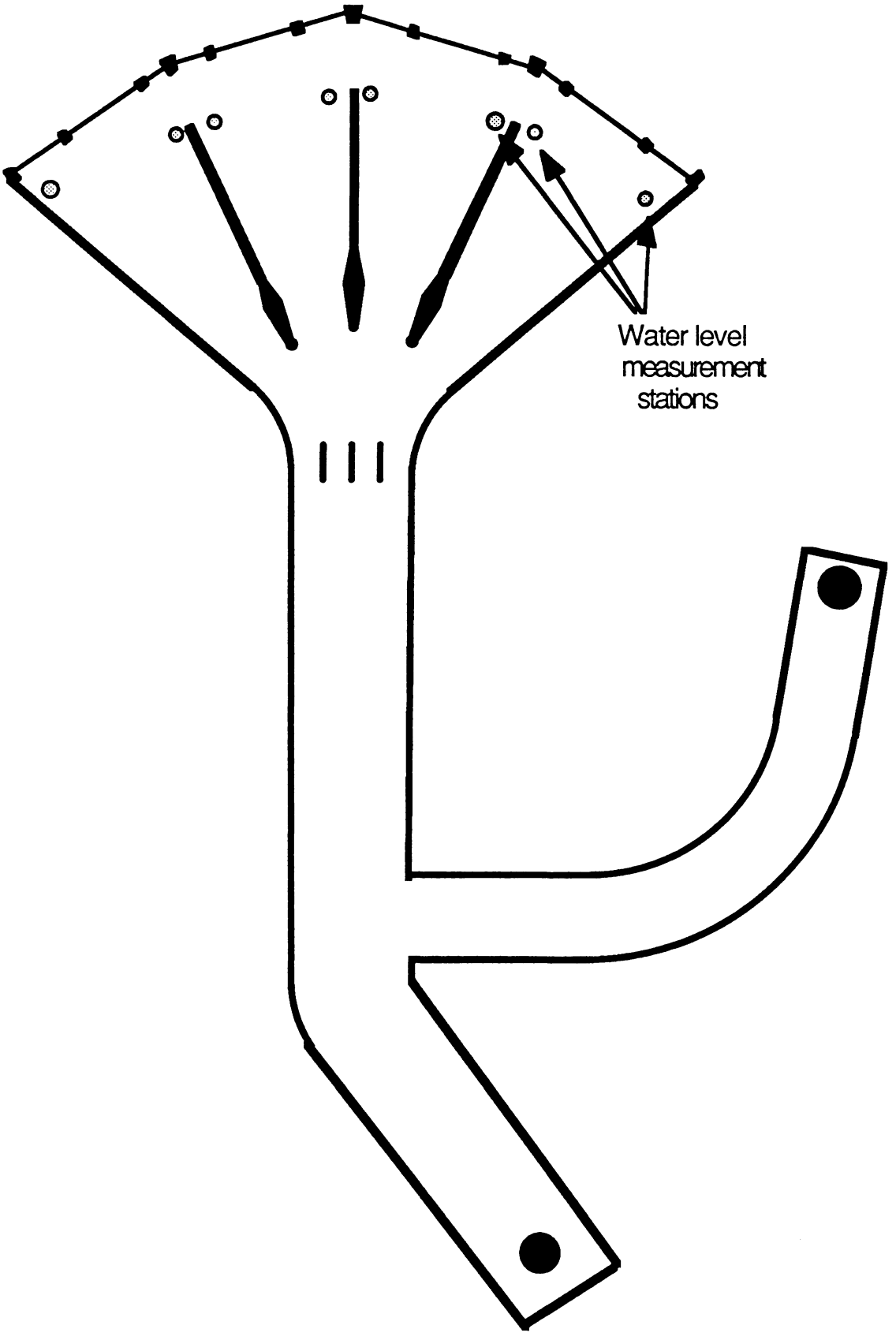

Figure 15. Water Level Sensor Locations.

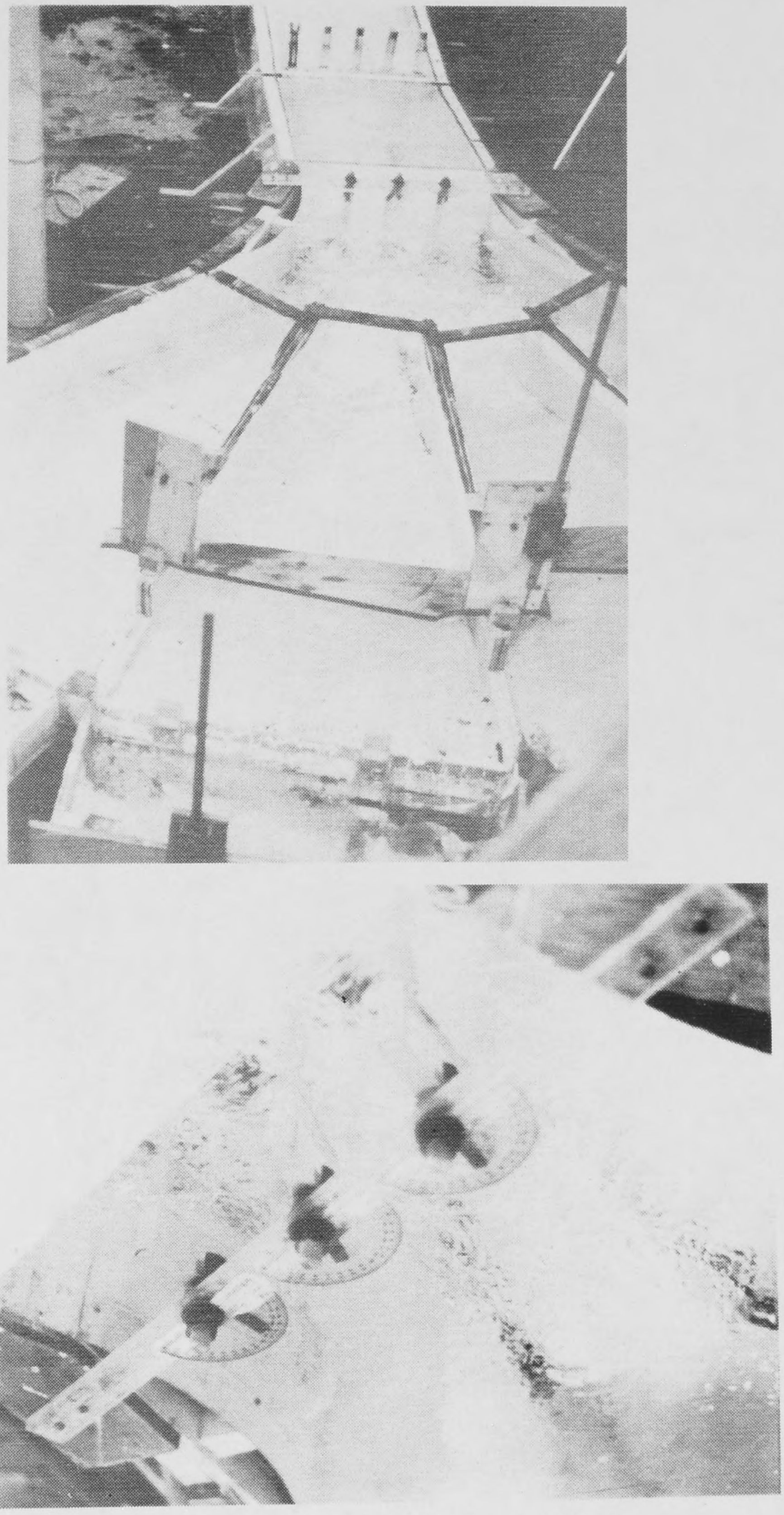

Figure 16. Water Surface Downstream from Guide Vanes.

difference between these levels and the zero levels computed to provide the weir heads.

At the lowest flow rates (less than about 110 MGD), no detectable water surface level variations across any one train could be measured. At the higher flow rates, variations of up to 0.004 ft (0.36 inches prototype) were recorded. This variation is felt to be greater than the inherent accuracy of the measurement, and the deviations are consistent in that one side of the train would consistently be higher than the other for nearly all flow rates studied and the deviation tended to increase with higher flows.

Sediment injection

Because it was difficult to meter the sediment into the inflow at an exact rate, it was decided to use a constant injection rate for all experiments at a rate that was approximately consistent with the specified influent concentration. In most experiments, 5 pounds of sediment were introduced which was a sufficient quantity to clearly observe the regions of significant deposition. This sediment was filtered through a funnel fitted with a series of screens to regulate the inflow rate and into a vertical tube mounted on the top of the physical model just downstream from the inflow pipe where the turbulence mixed it rapidly with the flow. At a typical model flow rate of 1 cfs or 28.4 liters/sec, it would take 400 seconds or 6-7 minutes to transport 5 lbs of sediment through the system at an average concentration of 200 mg/l. This was the target for the injection rate and it was maintained through all experiments. The actual sediment deposition will not be dependent upon the exact concentration so this procedure was quite suitable.

The entire 5 pounds of sediment was introduced and the flow allowed to continue an additional 2 minutes beyond the cessation of sediment inflow. The flow was then rapidly shut down and the sediment removed according to location within the splitter chamber. The regions surveyed indicated in Fig. 17 include:

A.) The region upstream from the vanes

B.) The region downstream from the vanes but upstream from the channel split into separate channels

C,D,E,F.) Each independent outlet channel

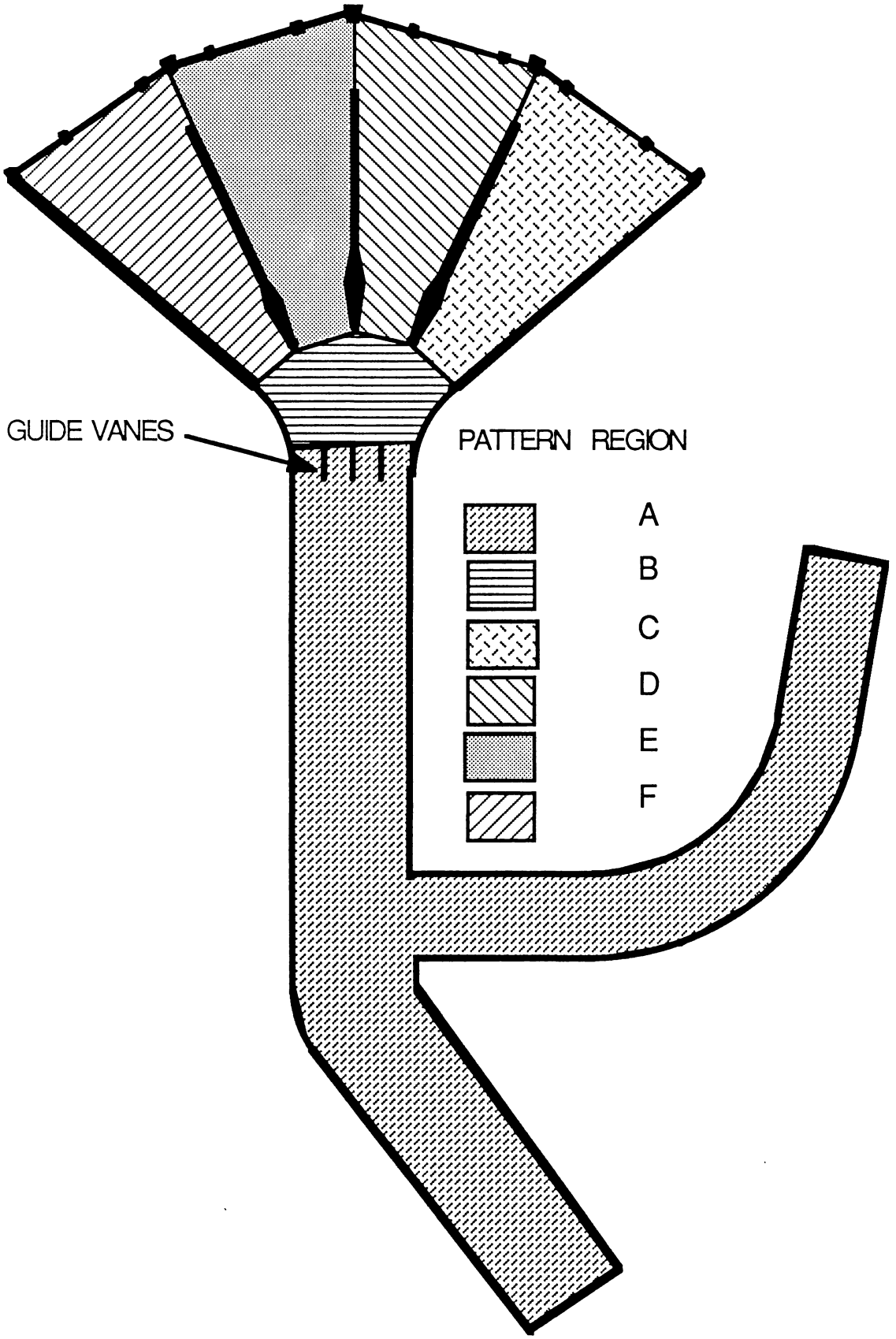

Figure 17. Sediment Sampling Regions.

The sediment was then removed from each region with a vacuum, dried and weighed, and the relative amount found in each region was recorded. The sediment that was deposited at the far upstream end of the influent chamber had to be flushed with a higher velocity into a region where it could be recovered; this was always the last step in any measurement. With the exception of the very first experiment in which the procedure was still being developed, it is felt that virtually all of the sediment retained within the splitter chamber was collected. In that particular experiment, at a prototype flow of 50 MGD, it is felt that virtually no sediment left the chamber since there was scarcely any deposition downstream from the control vanes.

The sediment injections were performed over the range of discharges specified for the particular entrance condition. Since the deposition was felt to be largely dependent upon the approach velocity to the vanes, separate experiments were not performed for all combinations of downstream controls. Nor were all vane orientations considered. Instead, the particular combination of vane positions that had been found to provide the optimum flow distribution for each flow rate was set and the injection made.

Vortex Shedding Frequencies

In order to estimate vortex shedding frequencies in the prototype, measurements were performed at a variety of flow velocities. In this way, the change of the *Strouhal Number* $\omega L \cos\alpha/U$ with flow Reynolds Number could be determined. The Strouhal number as used in this study is defined by the average approach velocity U, vane length L (48 inches prototype) and the vortex shedding frequency ω, and α is the angle between the vane and the approach flow. In most studies, S_t is found to be independent of the Reynolds number and therefore the constant value can be used to predict the shedding frequency at any approach velocity. This has been found to be approximately the case in the study by Abernathy (2) who examined flow past flat plates oriented at an angle α to the free stream. Not only were the Strouhal Numbers approximately constant with Reynolds number, they also varied only slightly with vane orientation. Therefore, similar results could be anticipated in the present study and it was decided to perform a few tests at various flow rates for each of two different

vane angles and compare with the flat plate results. These were found to give similar results and since the predicted prototype shedding frequencies were not close to the predicted natural vibration frequencies of the vane, no further testing was performed.

Natural Vibration Frequencies

A finite element analysis of the vane shape was performed to identify the first few modes associated with the natural frequencies of the vane. In this analysis, the presence of internal ribs was ignored and this would only raise the resonant frequencies. Otherwise, the vane detail was modelled correctly in that it was assumed to be constructed of 1/2 inch steel plate with 1/2 inch thick tubing welded to form the rounded tips as indicated in Fig. 3. Since we have no details on the bearings and connections to the bearing shaft, it was assumed that these were rigid connections. The results of the computer analysis are presented in Appendix A. The first five modes of oscillation are depicted graphically and the corresponding frequencies were computed to be:

MODE NUMBER	FREQUENCY (Hz)	PERIOD (seconds)
1	65.6	0.01524
2	75.3	0.01328
3	87.9	0.01138
4	95.8	0.01044
5	96.3	0.01039

These frequencies are higher than the expected frequencies due to vortex shedding in the prototype by over two orders of magnitude and it is therefore expected that vortex shedding will be an insignificant problem in the prototype with respect to the structural integrity of the vanes and bearings.

TESTING RESULTS

Notation Convention

In order to facilitate discussion of results in an orderly fashion, a convention referring to the discharge trains and vanes was independently developed. This

convention is summarized in Fig. 18. In particular, the discharge trains are labeled as 1 through 4 in going from west through east in the prototype installation. The correspondence between this numbering system is thus

Train	URS Designation
1	West
2	Center
3	East
4	Far East

In the results reported, deviations from desired flow distributions are presented. These are expressed as a percentage of **total plant flow**, rather than the individual outlet train flows. This presentation was selected as being easier to visualize as a flow rate magnitude to compare among the different flow configurations and may be converted to a percentage of the desired individual train flow by dividing by the fraction of the total flow that the particular train is intended to pass.

The vanes were designated as A, B, and C in a similar orientation going west through east in the prototype configuration, also see Fig. 18. The vane angles are reference to a datum in which 0° is defined by the vanes oriented parallel to the inlet channel. As the vane is rotated clockwise, the vane angle increases to an angle of 90° as the vane is aligned perpendicular to the approach flow. Thus, permissible vane angles will range between -45° and 45°.

Test Conditions

In consultation with URS Dalton and City of Columbus personnel, a series of test conditions were defined. The document of February 19, 1987 prepared by URS Dalton with remarks by William Poteet from the City of Columbus Public Utilities and Aviation Department describing the proposed testing schedule is reproduced herein as follows:

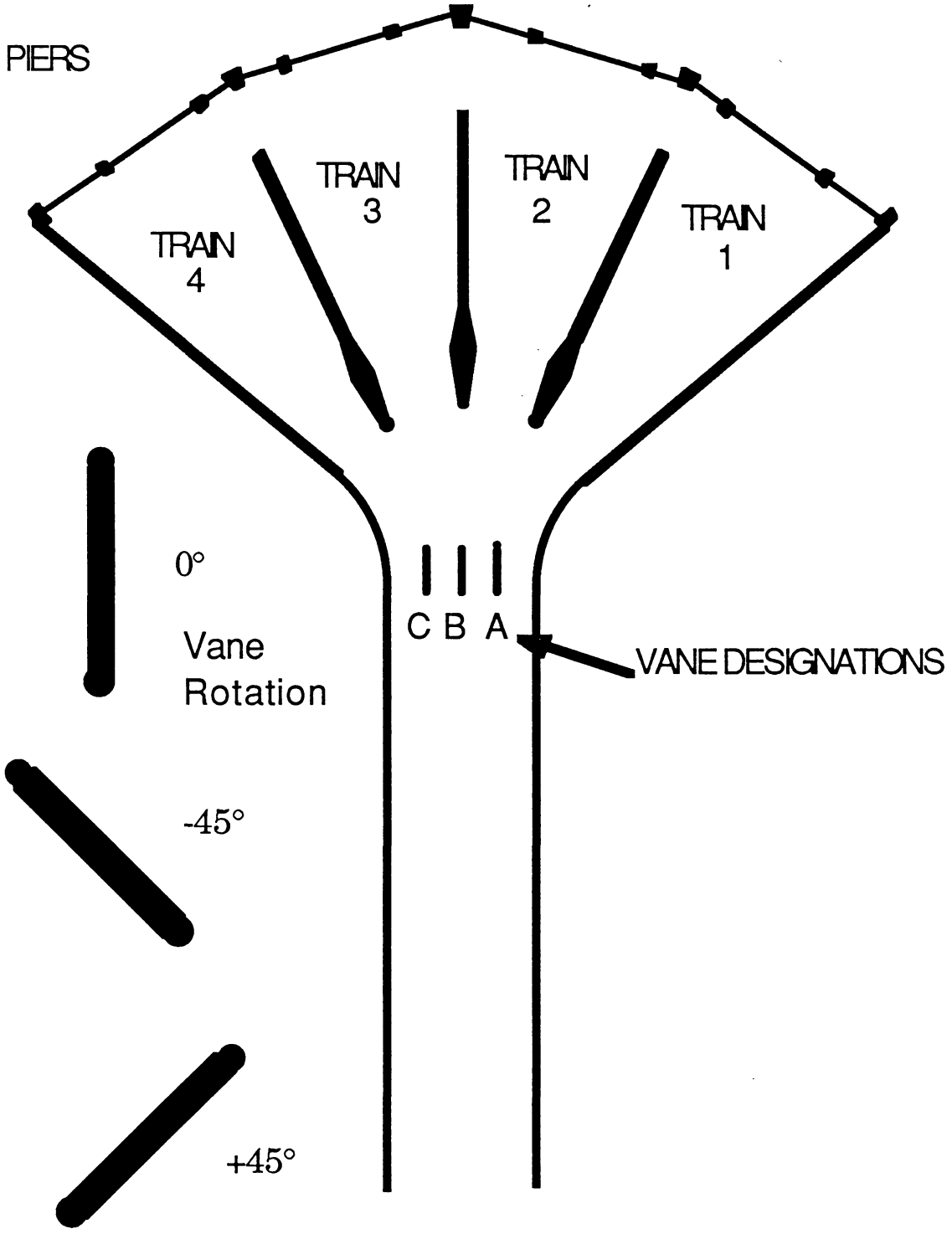

Figure 18. Notation Convention for Guide Vanes and Trains.

General

Initially in 1988, the influent splitter chamber will be required to split flows among each of three treatment trains known as West, Center and East. West and East train each consist of six aeration tanks and Center consists of four aeration tanks; thus with all three trains in operation, the required proportions of flow are: West - 6/16 of total; Center - 4/16 of total; East - 6/16 of total. This constant ratio is to be achieved by shortening the Center weir with a temporary gate. It is desirable to determine a constant positioning of the vanes such that this ratio of flow splitting is maintained through a range of input flows varying from 50 to 150 MGD. An additional requirement is to achieve similar optimum splitting between two trains (one train out of service) and determine the vane positions for the full range of input flow conditions also.

Ultimately in 2015, the treatment plant will consist of four trains of six aeration tanks each. It is to be demonstrated that the influent splitter chamber splits flows in the ratio of 1/4:1/4:1/4:1/4, to determine the optimum vane position for the 170 MGD flow, and for this same flow with three of four rains operating (one train out of service). The flows in 2015 are expected to vary from 150 to 300 MGD.

It is desired to use a water surface level measuring device in each segment of the flow splitter to determine the flow over each weir. An optimum location of such devices is to be studied for each flow condition. Also, grit deposition for each flow condition is to be studied.

Part I of this model study shall examine the functioning of the flow splitter under 1988 and 2015 flow conditions, to determine the general linearity of the device, and to determine immediately any modifications which may be necessary or desirable to achieve the type of operation required, since the flow splitter is currently under construction in the field.

Part II of this model study shall produce a complete set of operating curves for the flow splitter that relate the configuration of the device, the positions of the vanes, the input and output flows, and the optimum locations of water surface level measuring devices.

PART 1 of STUDY

CONDITION 1:

Year 1988, three treatment trains receiving flow as follows: West - 6/16 of total; Center - 4/16 of total; East - 6/16 of total. Total flows as follows: 50, 70, 90, 110, 130, and 150 MGD:

A. Determine vane positions ϕ_x for optimum flow distribution at 90 MGD.

B. Determine flow distributions at ϕ_x for each of the other flows listed above.

C. Determine vane positions for optimum flow distribution for each of the other flows.

Vanes may vary through a range of ±45° from center.

For each of the above flow conditions, determine grit deposition. Display results both

graphically and in tabular form.

CONDITION 2:

Year 1988, two treatment trains operating, and flow splitter distributing flow as follows: West train, 1/2 of total flow; East train, 1/2 of total flow. Total flows as follows: 50, 70, 90, 110, 130, and 150 MGD.

A. Run same series of flow distribution, vane position, grit deposition, and depth measurement location tests as described in Condition I. Again, display results in both graphic and tabular forms.

B. Repeat A. for East train out of service.

C. Repeat A. for West train out of service.

CONDITION 3:

Year 2015, using the 2015 inlet channel, four treatment trains in operation, receiving 1/4 of the total flow to each train. Total flows as follows: 150, 170, 200, 220, 250, and 300 MGD.

A. Determine vane positions ϕ_x for optimum flow distribution at 170 MGD.

B. Determine flow distributions at ϕ_x for each of the other flows listed above.

C. Determine vane positions for optimum flow distribution for each of the other flows.

Vane positions may vary through a range of ±45° from center. For each of the above flow conditions, determine optimum position for depth measurement over weirs for each sector of flow splitter. For each of the above flow conditions, determine grit deposition. Display results both graphically and in tabular form.

CONDITION 4:

Year 2015, three treatment trains operating, and flow splitter distributing total flow 1/3 to each West train, East train and Far East train. Total flows as follows: 150, 170, 200, 220, 250, and 300 MGD:

A. Run same series of flow distribution, vane position, grit deposition. and depth measurement location as described in Condition 3. Again, display results in both graphic and tabular forms.

B. Repeat A. for West train out of service.

C. Repeat A. for East train out of service

D. Repeat A. for Far East train out of service.

PART II OF STUDY:

Establish complete operating curves for the influent flow splitter for all flows in 1988 and 2015 with all treatment trains operating (three in 1988 and four in 2015). Establish complete operating curves for the influent flow splitter for all flows in 1988 and 2015 for all combinations of one treatment train out of service.

In the remainder of this report, specific test conditions shall be referred to as enumerated in the above protocol, e.g. Test Condition 2B refers to that series of tests involving the 1988 entrance with the flow split evenly between Trains 1 and 2 (or West and Center in the above document). Variations on this testing protocol were developed during the testing upon consultation with URS Dalton personnel. The most relevant of these relates to Test Conditions 2B and 2C. In these flow states, Train 2 was presumed to only service four aeration tanks while the remaining trains serviced six. Therefore the desired flow distribution was 4/16 of the total to Train 2 and 6/16 to the remaining two trains. This is more representative of the expected treatment plant operation over the near future. The same relative flow split was maintained for those flow states with one train blocked.

An additional change to the testing protocol was in regards to the requirements stated in 1B, 3B and similar flows with one train blocked. It was observed during the course of the testing that the flow distribution was relatively insensitive to vane position at lower flow rates compared to the highest flows. Therefore, the vane position that gave the optimum flow distribution at 90 MGD in 1A, for example, may not give very good flow distributions at a flow of 150 MGD. However, a vane setting similar to the optimum one at a flow of 110 or 130 MGD would give a reasonable flow distribution over the entire range of flow rates and that a single vane setting would give a reasonable flow distribution for all flows. Therefore, the experimental objective became to find a single vane setting that gave a satisfactory flow distribution at all flow rates. This generally resulted in near optimal flow distributions at the intermediate flow rates with somewhat greater deviations at the highest and lowest flows.

General Flow Pattern and Velocity Distributions

1988 Entrance

Velocity profile data is presented for the lowest (50 MGD) and highest (150 MGD) plant flow rates in Figs. 19 and 20, respectively and indicate qualitatively similar trends. These profiles are for flow conditions with Trains 1,2, and 3 in operation and with the optimal vane settings reported in the next section to obtain an appropriate flow split in each outlet conduit. Looking downstream, the velocities on the left side of the channel are several times larger than on the right side. The velocities on the right side of the channel are near the resolution of the velocity meter and could be in any direction. Flow visualization indicated that both the upstream and downstream measurement sections are in a recirculation zone on the right side of the channel and this is consistent with the velocity measurements. Fig. 21a shows the result of dye injected near the upstream end of the channel on the right side and indicates the general extent of this wake zone. Approximately one-half of the total discharge passes through the left-most one-quarter of the flow cross section at the upstream end and this is probably only slightly decreased at the downstream section. Fig. 21b indicates upstream flow along the right hand side of the channel as far downstream as the guide vane section. The flow is very intermittent there with alternating current directions and relatively low frequency fluctuations. As the flow approaches the vanes, the total depth begins to increase and this is probably the major influence on the decrease in flow velocity along the left side of the channel.

After the flow passes the guide vane sections, there is a considerable amount of turbulence in the immediate wake of the guide vanes. Flow separation off the leading edge of the internal dividing walls was observed in many instances, with a wake extending the entire length of the downstream channels in some instances. Dye injection indicated some situations where reverse flow occurred, especially along the east wall of Trains 2 and 3. Different velocity magnitudes were observed in the upstream sections of the separate channels with the center trains generally exhibiting higher velocities. This resulted in net flow out of these center trains at the connecting

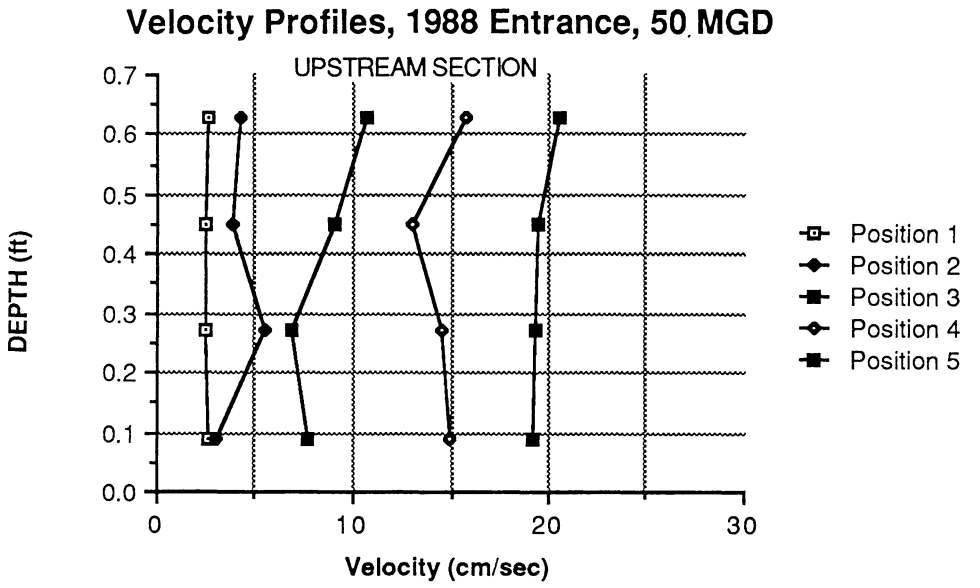

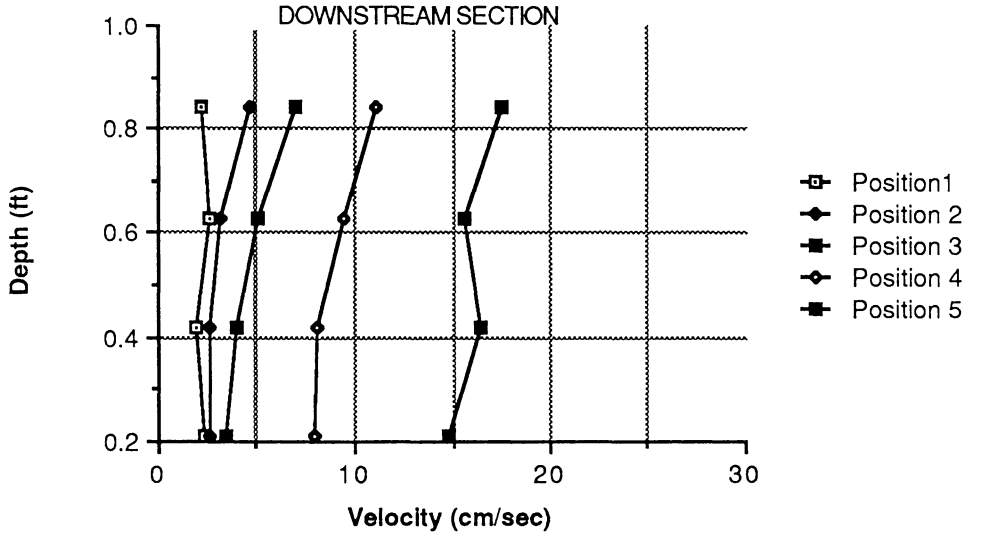

Figure 19. Velocity Distributions, 1988 Entrance, 50 MGD.

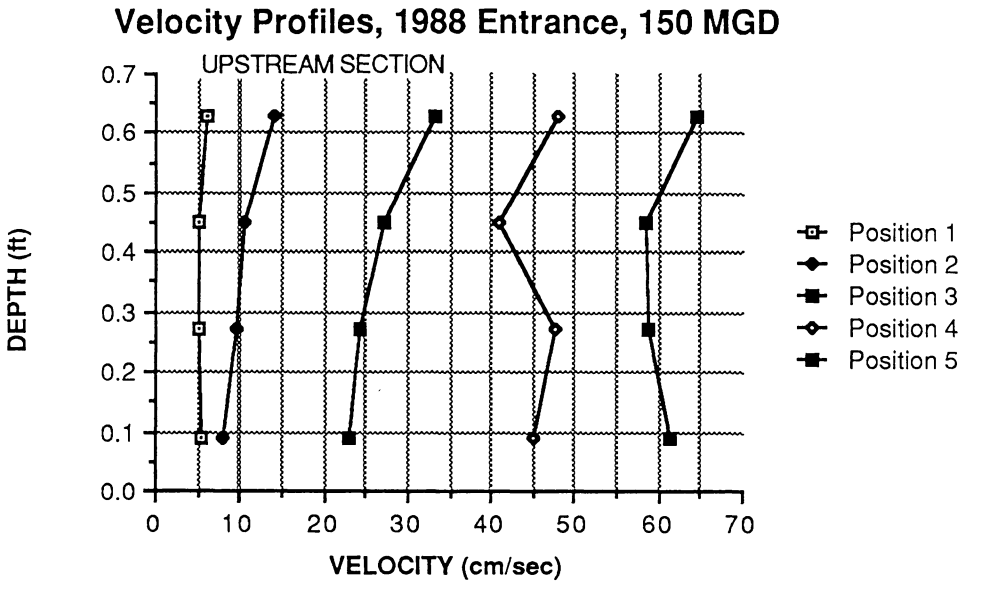

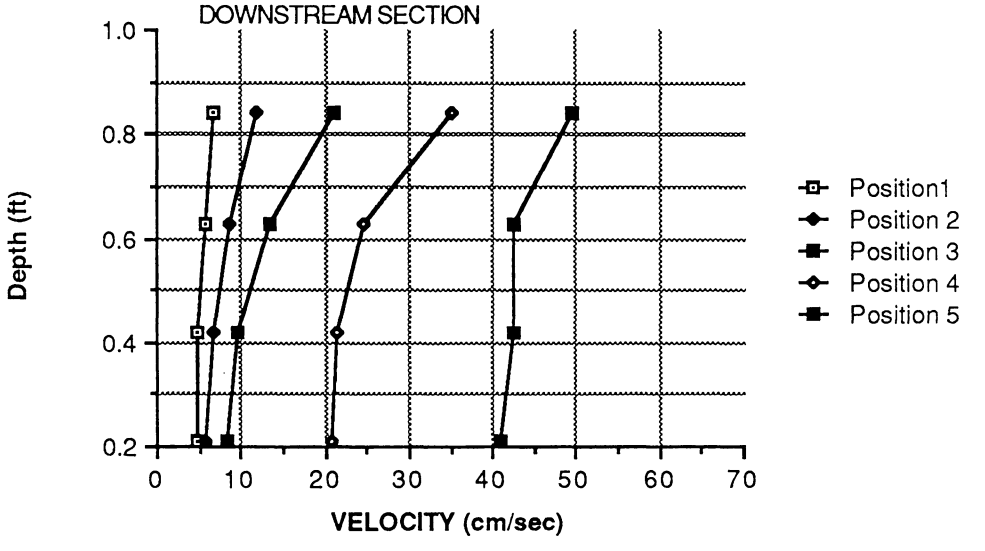

Figure 20. Velocity Distributions, 1988 Entrance, 150 MGD.

a.) Dye Injection at Upstream Access Port on Right Hand Side of Inlet Channel.

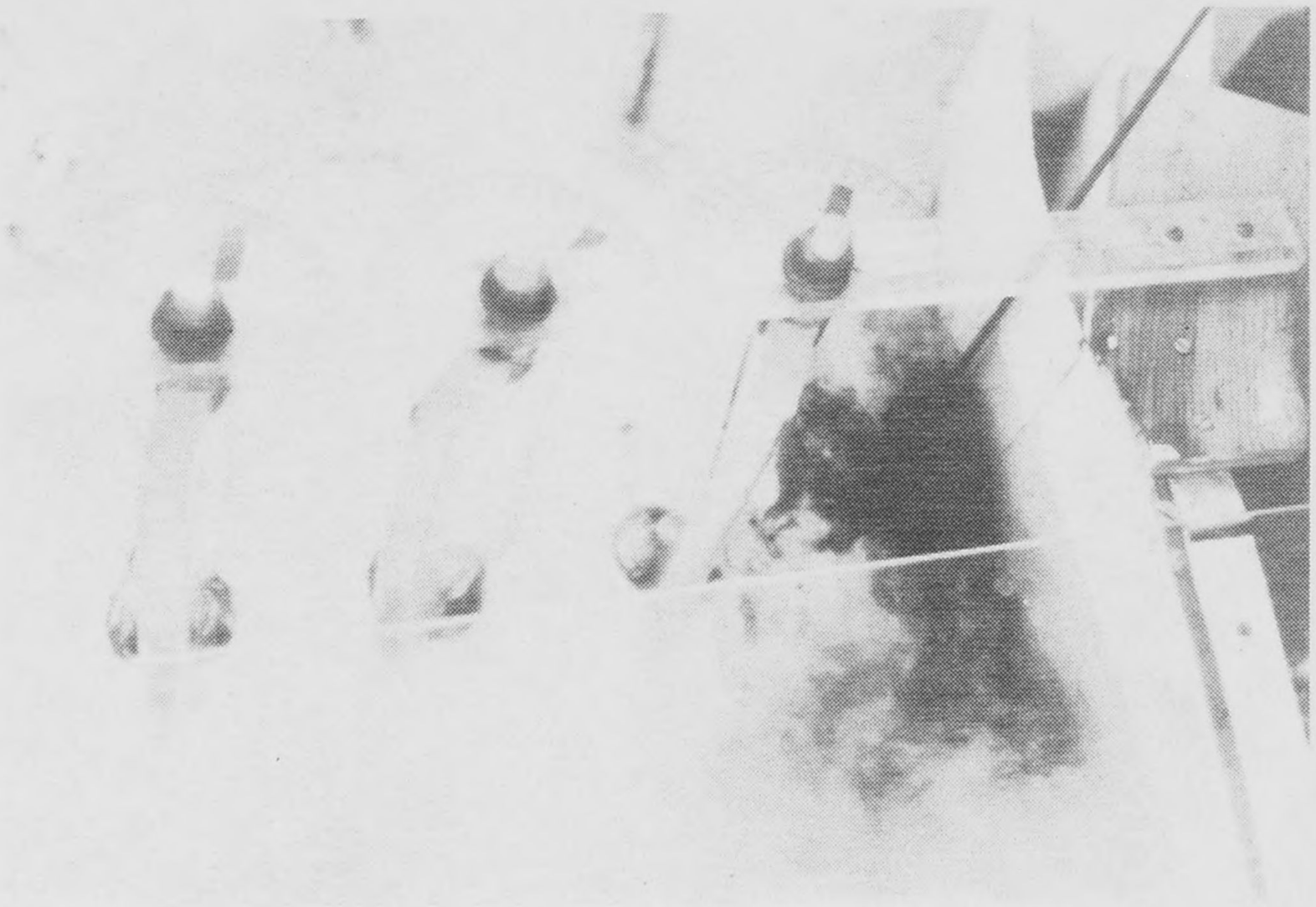

b.) Dye Injection on Upstream Side of Vane A.

Figure 21.

gate openings at the downstream end of the trains. Fig. 22 indicates the nature of this crossover flow which was generally minimal for most flow situations but was always in the direction from Train 2 to 1, for example.

2015 Entrance

The flow is much more uniformly distributed at the upstream end of the channel with the 2015 entrance as indicated in Figs. 23 and 24 for total flow rates of 150 and 300 MGD, respectively. However, by the time the flow has passed to the downstream end of the channel, the velocity distributions are not too dissimilar to those with the 1988 entrance. Again, these profiles have been measured with the vane settings required to obtain an optimal flow distribution. These velocity profiles again concentrate flow to the left side of the channel and indicate the basic cause for the flow distributions observed in the next sections.

Flow Distributions

1988 Entrance

The 1988 entrance configuration consists of cases **1A, B, and C** and **2A, B, and C** as described above. As noted in the preceding section on flow distribution, the velocity in the inlet conduit approaching the vanes tends to be higher on the easterly or left side of the channel looking downstream. When all three trains are in operation, this tends to force a somewhat higher velocity through trains 2 and 3 when compared with 1. This can easily be seen in Fig. 25 which indicates the flow distributions for the range of discharges, with no guide vanes in place, and all downstream overflow weirs open. In this case, the flow should be split evenly between all three trains in an ideal flow distribution; it can be seen that this condition is met to within about 1 percent at a total flow of 50 MGD. However, Train 1 has the lowest flow and Train 3 has the highest flow. This result is found to continue with increasing differences between the individual train flows as the flow rate is increased up to the maximum of 150 MGD. At that flow rate, the maximum deviation is about 3.5 percent of total plant flow with Train 1 low and the other two high with Train 3 the highest.

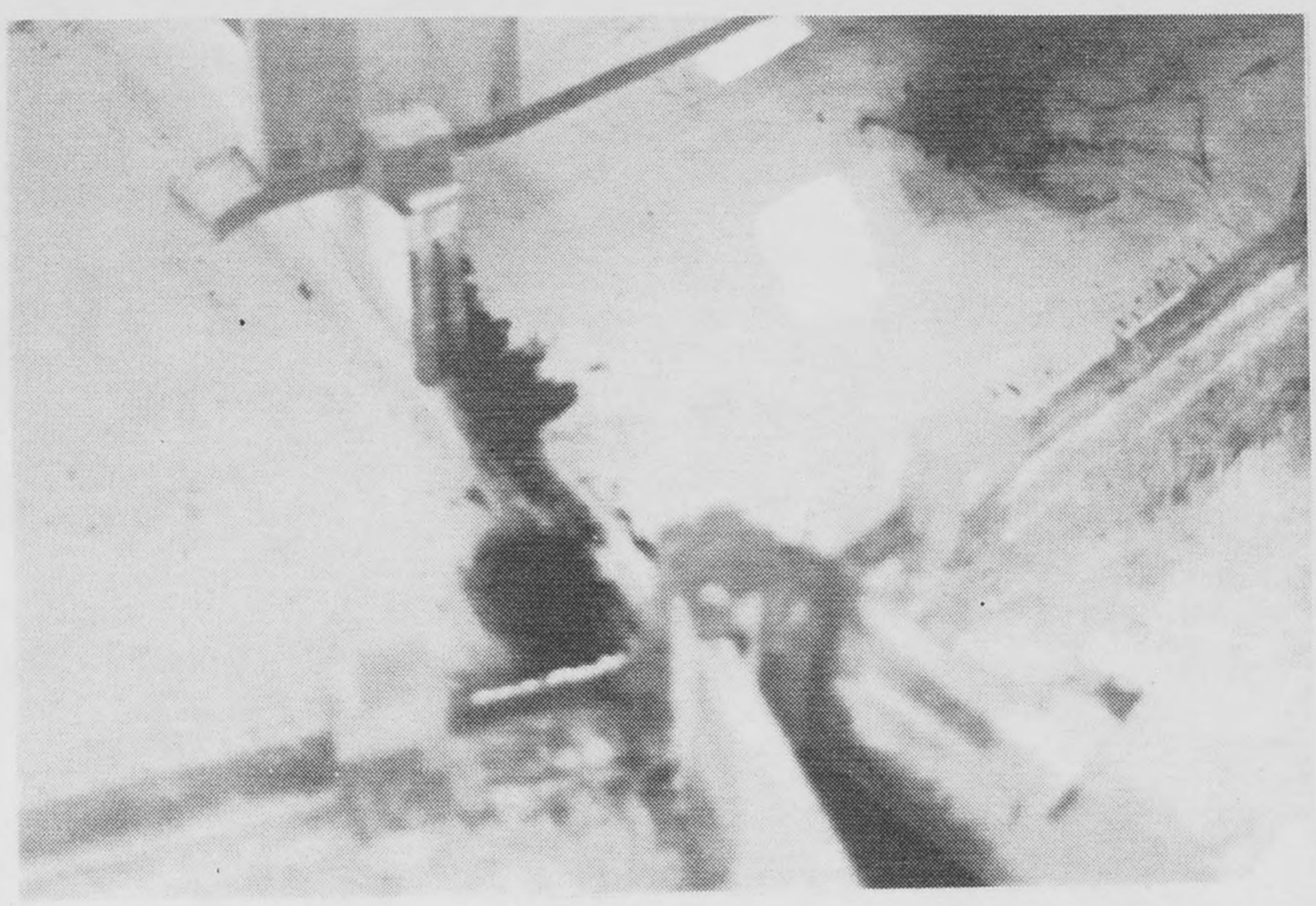

Figure 22. Crossover Flow from Train 2 to Train 1 at Downstream Slide Gate.

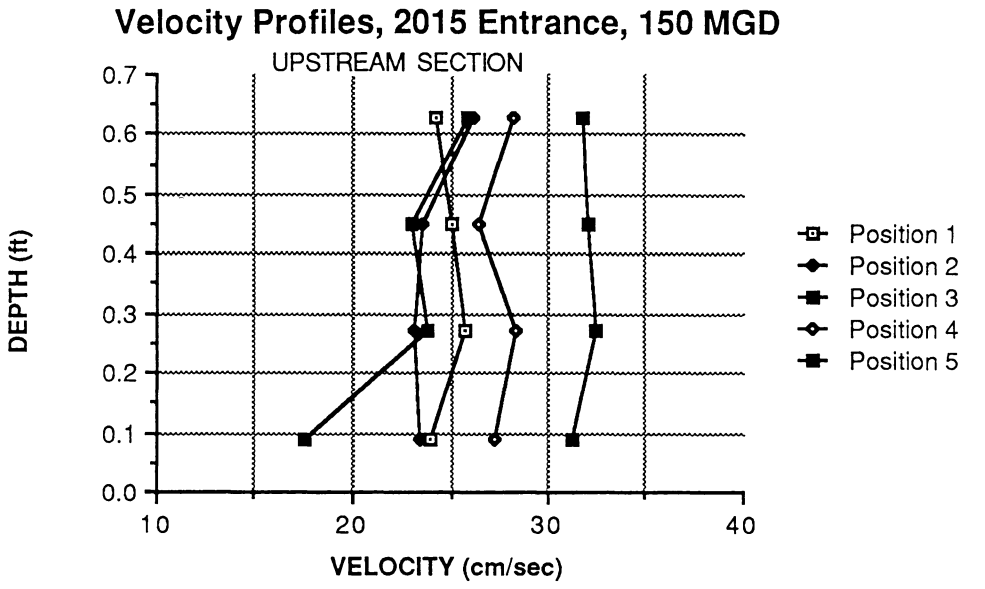

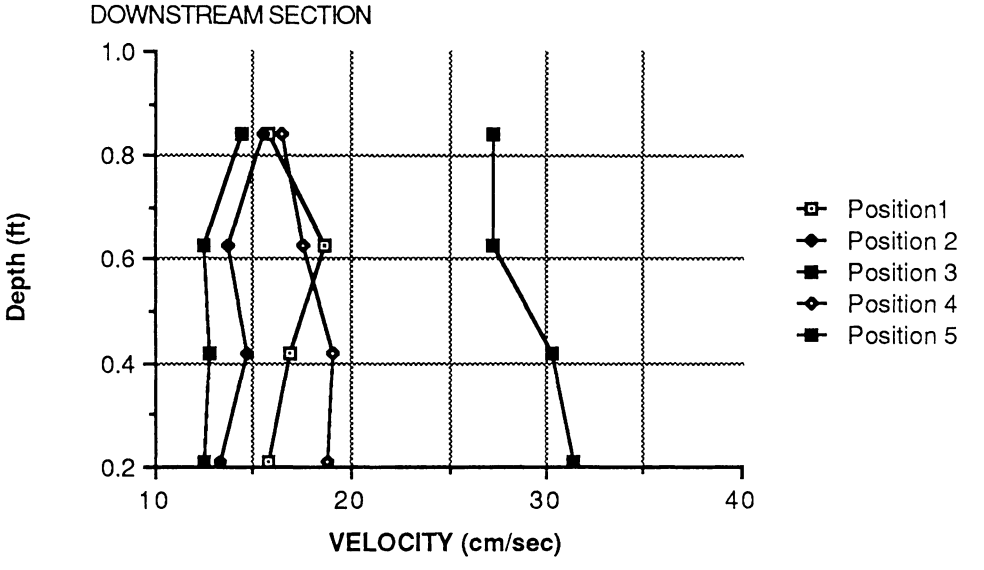

Figure 23. Velocity Distributions, 2015 Entrance, 150 MGD.

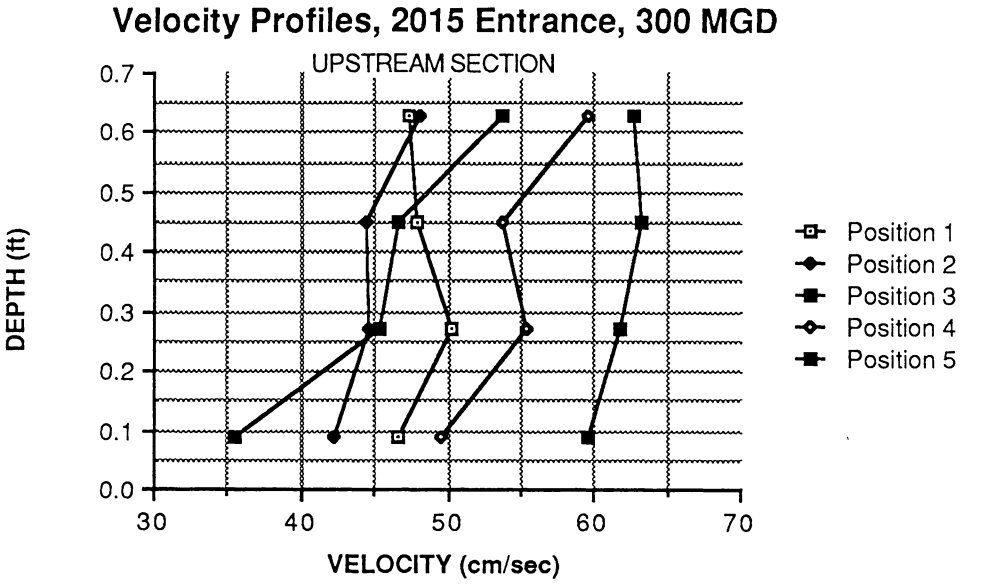

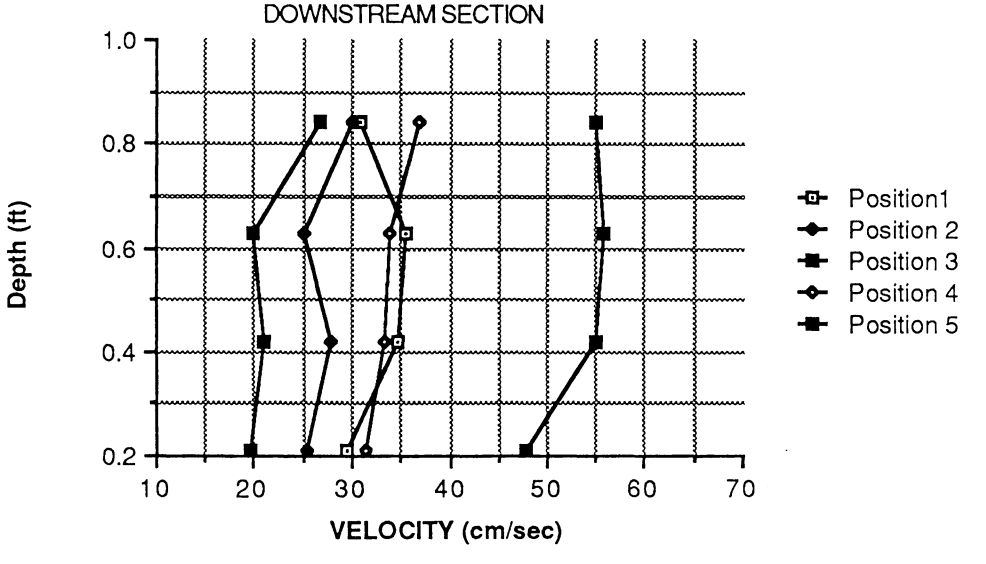

Figure 24. Velocity Distributions, 2015 Entrance, 300 MGD.

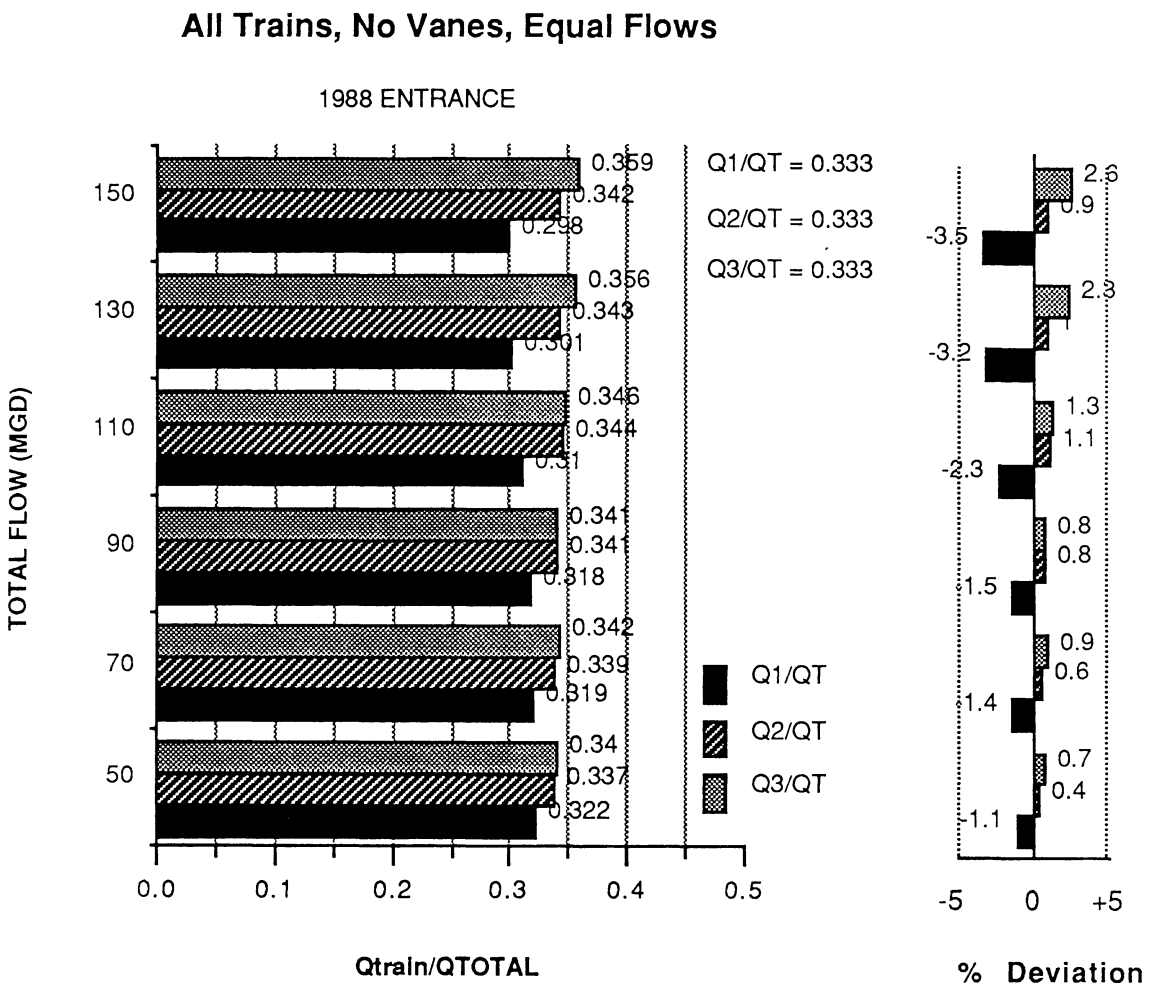

Figure 25. Flow Distributions, 1988 Entrance, No Vanes, Equal Flows.

With the intended operating conditions (Train 2 overflow weir partially blocked) to give the 3/8, 1/4, 3/8 split among the three trains, the same sort of qualitative result is seen in Fig. 26. Here, we can see the fractional Train 1 discharge more or less continuously decreasing and the Train 3 flow increasing with total plant flow. Again, the maximum deviation from the intended flow split occurs at the highest plant flows and is approximately 4 percent of the total plant flow. In general, the partial weir blockage with the slide gate performs as intended with the relative distribution of flows with weir crest length much the same as indicated in Fig. 25. No additional tests with the total weir length open in Train 2 were performed for the 1988 entrance configuration.

With the guide vanes installed, it was generally possible to obtain the desired flow split by experimenting with different vane angles until a suitable flow distribution was obtained. In nearly all cases, clockwise rotations of the vanes were required to divert the flow to the right hand side of the channel. In general, the search for the optimal flow distribution was stopped when either the flows were within the estimated measurement accuracy of the weir boxes or if it became apparent that it would not be possible to achieve the desired flow split. Figure 27 indicates the best flow split achieved for each of the plant flows studied along with the vane positions utilized to obtain that flow distribution and the required vane positions are given in Fig. 28. In all likelihood, there is probably not one single vane setting that would give the same degree of accuracy in the flow split if all three vanes can be adjusted independently. This is most apparent in the results for the 2015 flow entrance with all four trains in operation where two completely different vane settings give nearly the same flow distribution. For the 1988 entrance, it was found that Vane A has relatively little influence on the flow distribution compared to the other two and that most of the flow distribution optimization was performed by adjusting Vanes B and C. In general, it was found that the flow is more sensitive to vane adjustment at the higher flows and thus relatively large changes in vane setting at lower flows may have little influence on the flow distribution. In Fig. 28, it can be seen that the optimal vane angles do not

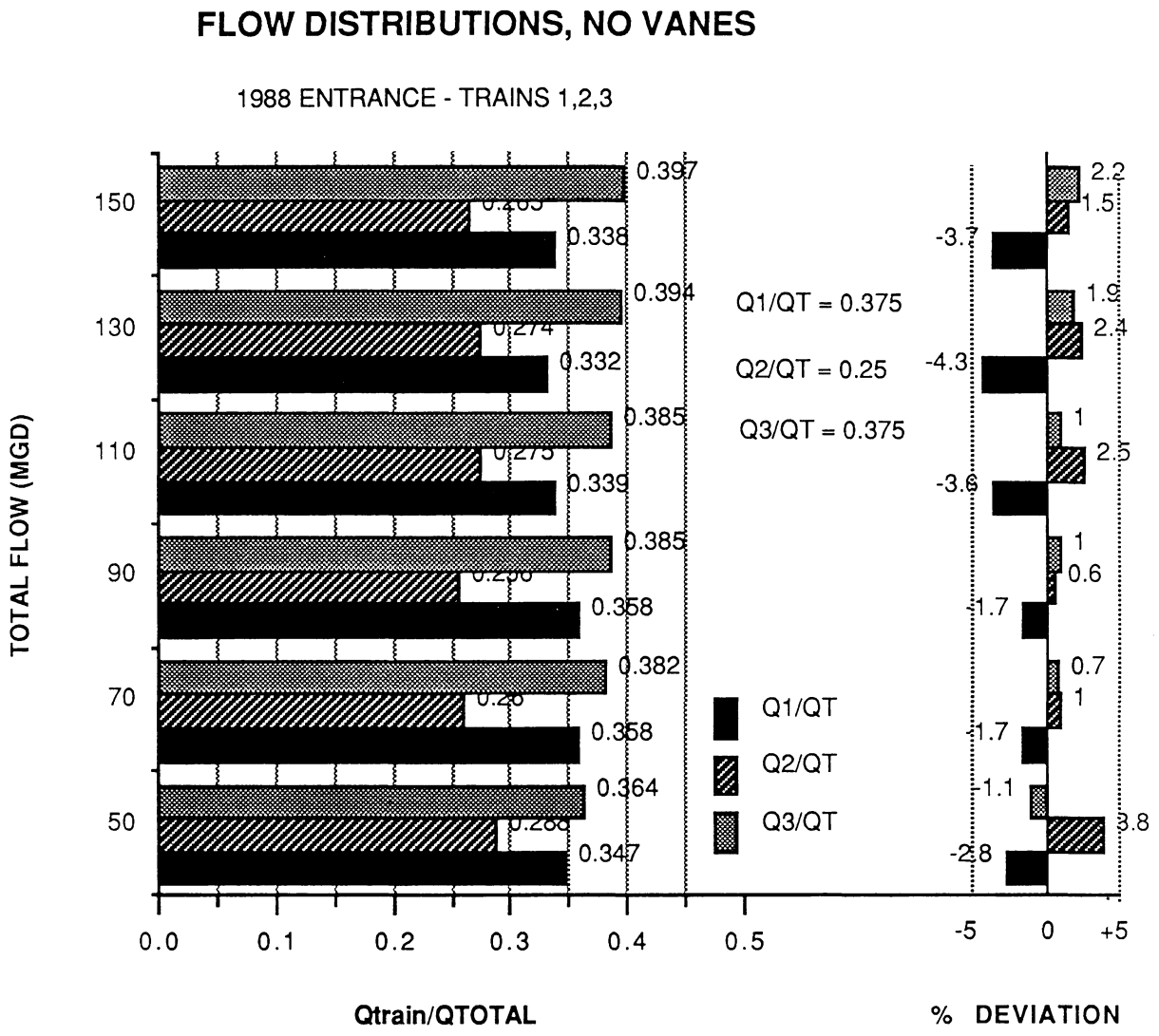

Figure 26. Flow Distributions, 1988 Entrance, No Vanes, Specified Flows.

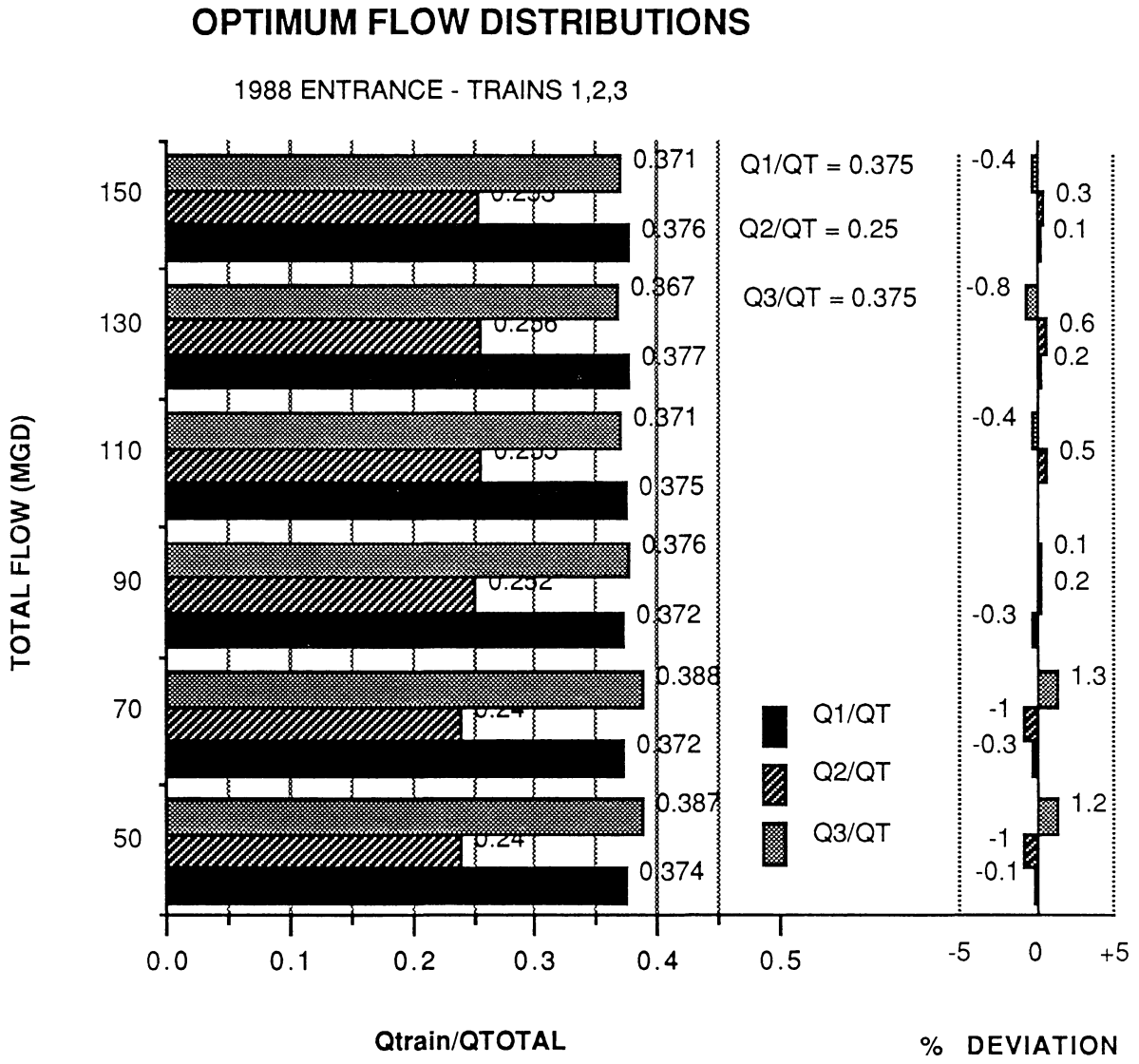

Figure 27. Flow Distributions, 1988 Entrance, Optimum Vane Settings.

VANE ANGLES, OPTIMUM FLOW DISTRIBUTIONS

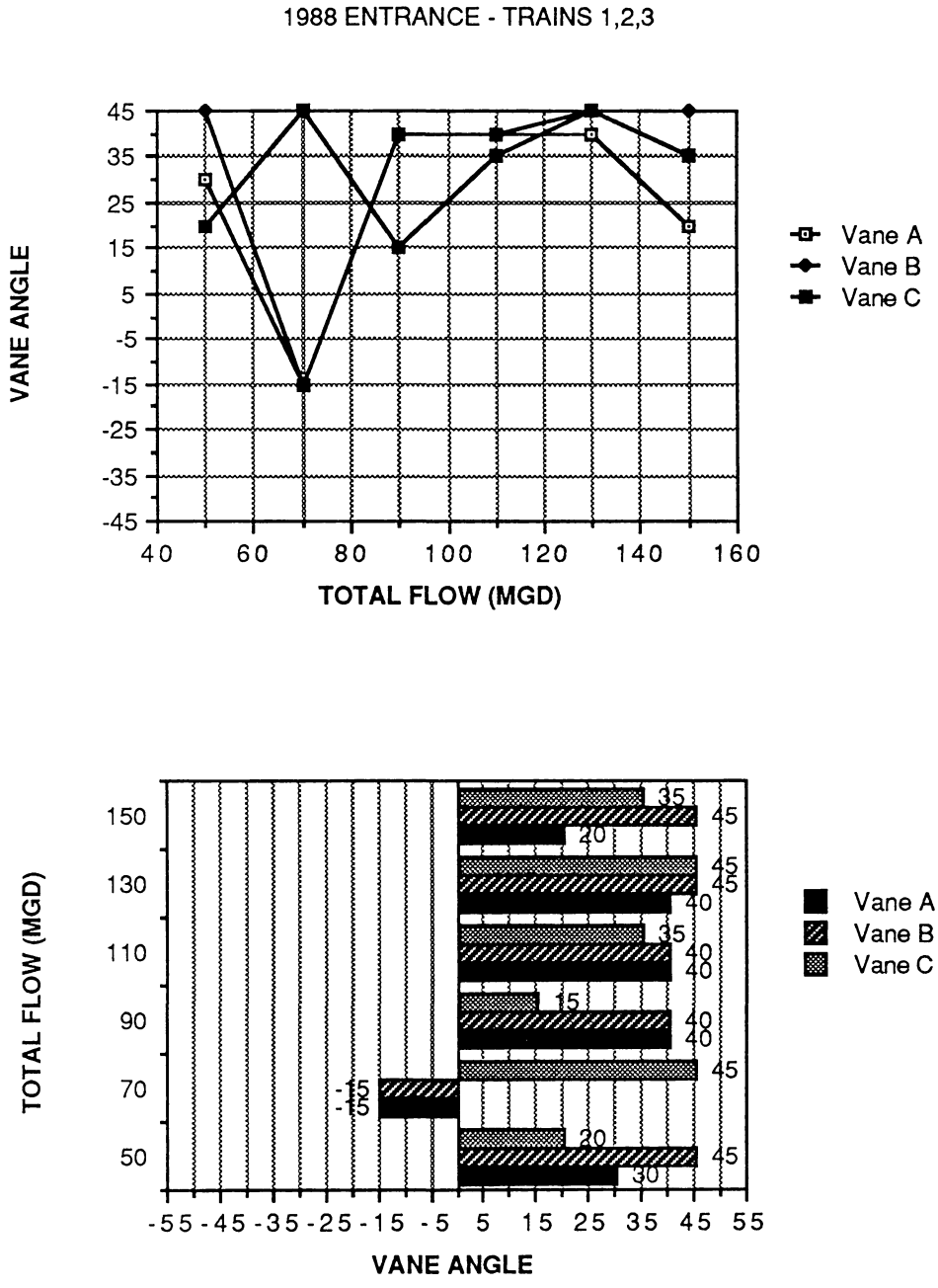

Figure 28. Vane Angles, 1988 Entrance, Optimum Vane Settings.

change much above a flow of 90 MGD while the vane angles for a flow of 70 MGD are quite different. This is felt to be due to some interaction of the flow resulting from the approach bend, but the mechanism is not obvious. In the other cases associated with 2A, B, and C, it was often found that the relative flow distribution at 50 or 70 MGD with no vanes installed did not display a consistent trend with the higher flows and that significantly different vane settings were required to obtain the desired flow distributions.

When it was attempted to select a single vane setting to give a good flow distribution over the entire range of plant flows, the vane settings for the higher flow rates were weighted more heavily in the selection process, since the flow distribution was more dependent upon vane position in those cases. Figs. 29 and 30 present the relative flow distributions for two such vane settings with the second one giving somewhat better overall flow distributions than the first. The vane A setting is that used to obtain the 150 MGD flow split, but as discussed above, the flow distribution is relatively insensitive to that setting. The vanes B and C settings are more or less average values over the three highest flow rates with a 5° higher vane setting used in the second case for Vane C. It is seen that the greater Vane C orientation generally increases the relative fraction of flow passing through Trains 1 and 2. The maximum deviations were all associated with a total flow of 70 MGD which is consistent with the results presented in Fig. 27 and the maximum deviation is approximately 2.5 percent of total plant flow or about 10 percent of desired train flow. All other flow conditions are within about 1.5 percent of total plant flow or 6 percent of desired train flow and most are significantly better than that. Therefore, it appears feasible to use a single vane setting to obtain the desired flow distribution of the range of plant flows for a given configuration of different trains in operation. This conclusion is based on the fact that the largest deviations in flow distribution occur at the lower plant flows, when there will be excess treatment capacity and longer detention times in the treatment process.

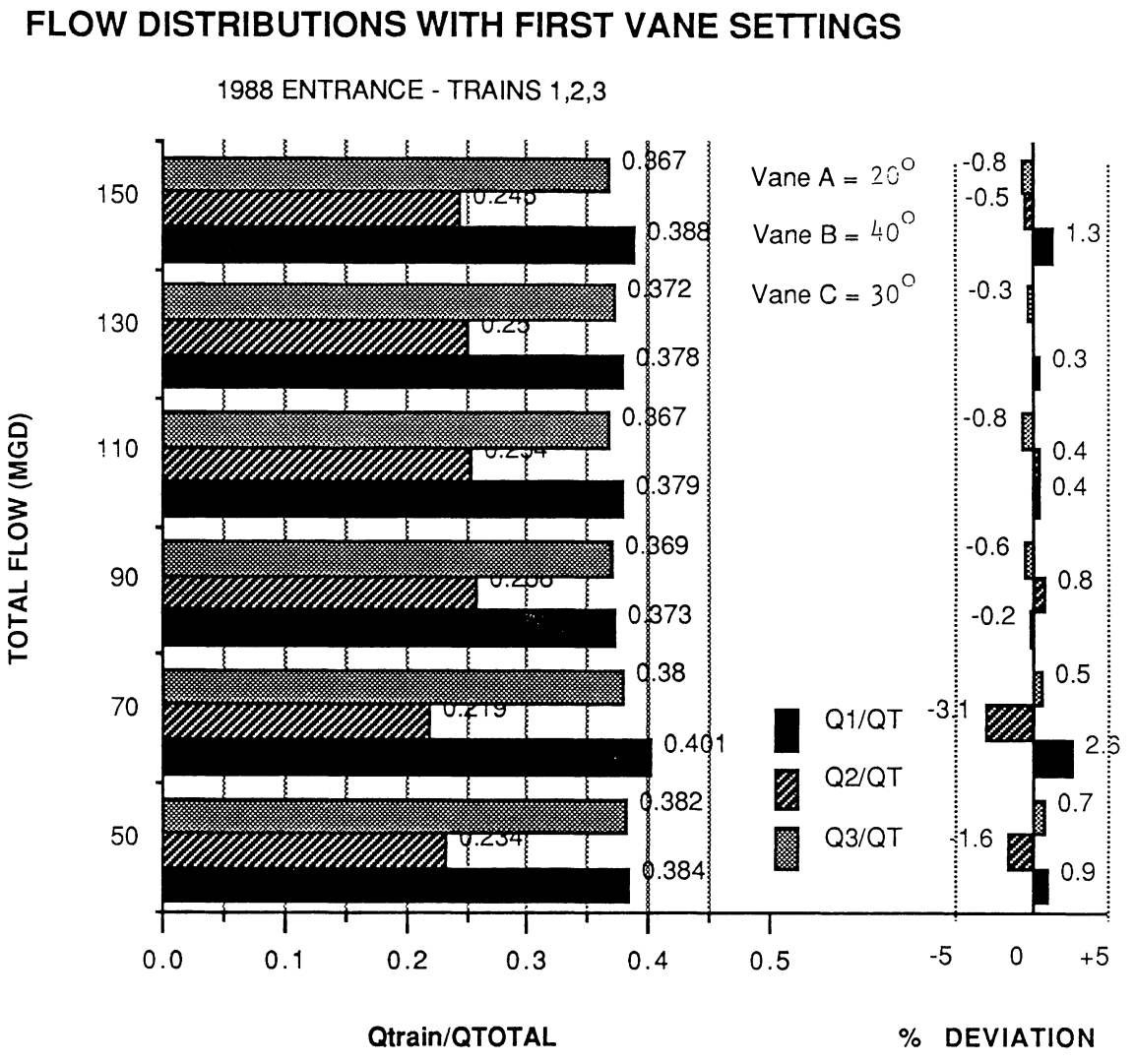

Figure 29. Flow Distributions, 1988 Entrance, Single Vane Setting 1.

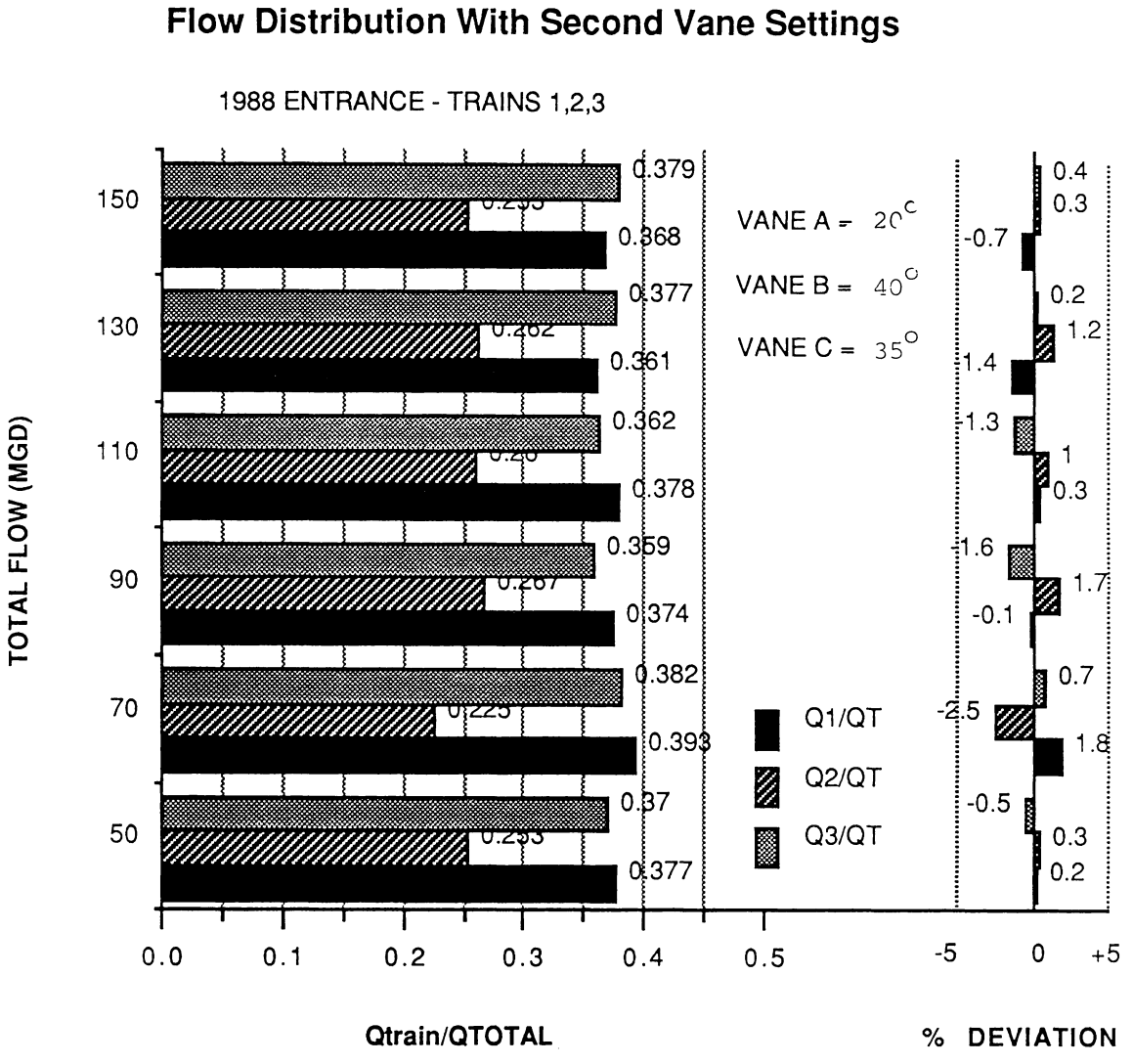

Figure 30. Flow Distributions, 1988 Entrance, Single Vane Setting 2.

Similar results are found for the various combinations of two trains in operation. These results are presented in Figs. 31-42 and consist of plots for 1.) the flow distribution with no vanes for each of the three combinations of two trains; 2.) the optimal flow distributions and 3.) the vane angles to obtain those distributions; and 4.) the flow distribution measured with a single "optimized" set of vane positions. A brief discussion of those results follows.

With Trains 1 and 2 in operation, a disproportionate amount of the flow passes into Train 1 at the 50 MGD flow which is different from the other flows. It was impossible to bring up that flow to the desired flow split with the vanes in place and thus this represents one of the few cases in which the vanes would not perform the desired function. However, since this is at a low total flow rate, the influence on treatment plant efficiency should not be important. With the exception of this flow state, a single flow setting can obtain a flow split within a deviation of 3.5 percent of the total plant flow or 8 percent of the desired train flow.

With trains 1 and 3 in operation and no vanes present, the individual train flows are relatively close to the desired flow split at low flow and are 10 percent from the desired flows at 150 MGD. By optimizing the vane settings for each flow, the flow distribution can be made equal to the desired split to within the measurement accuracy and the vane settings are not significantly different for any of the flow rates. Therefore a single vane setting can achieve the desired flow split to within 1 percent of the total plant flow or 2 percent of the train flow and clearly performs in a most satisfactory manner.

Finally, with Trains 2 and 3 in operation and no vanes, the flow split is weighted towards Train 3. Again at the lowest flow rate, it is not possible to achieve the desired flow split, but the other flows can be brought into a suitable range although the vane settings to achieve this vary considerably with flow rate. With a single vane setting, however, flows to within 1.6 percent of the plant flow or 4 percent of the desired train flow except at the low flow of 50 MGD are obtained.

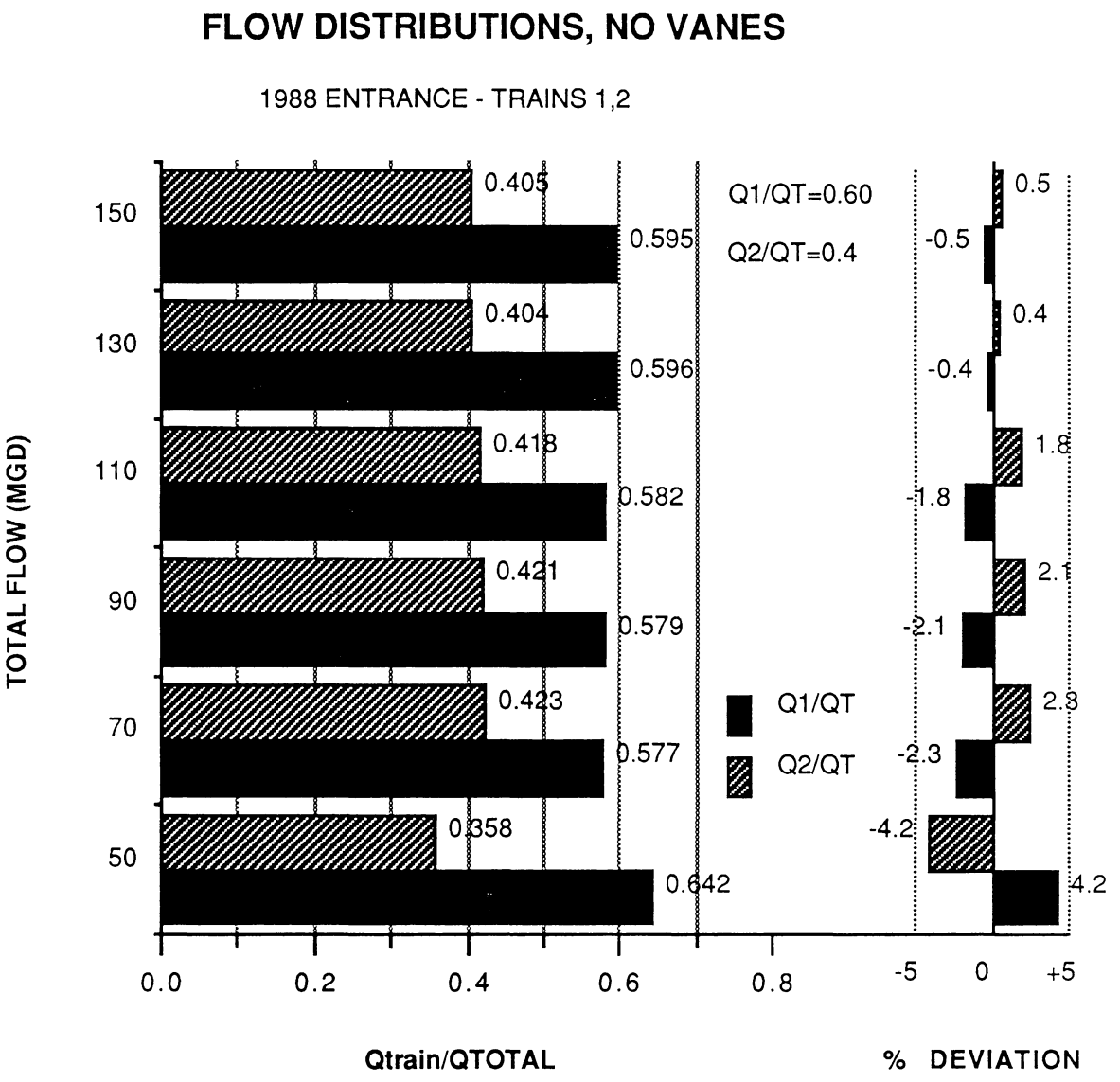

Figure 31. Flow Distributions, 1988 Entrance, Trains 1,2, No Vanes.

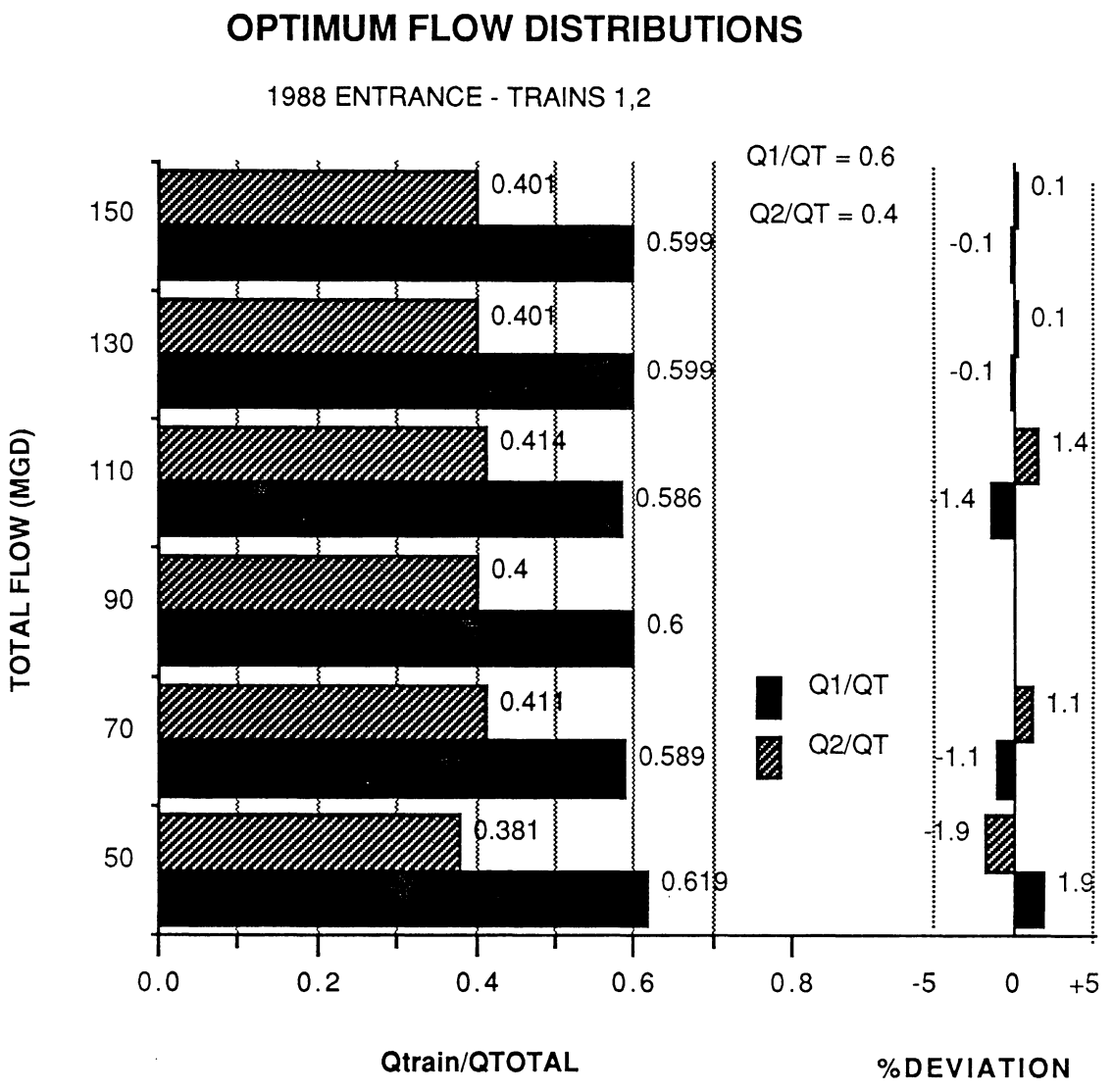

Figure 32. Flow Distributions, 1988 Entrance, Trains 1,2, Optimum Vane Settings.

VANE ANGLES, OPTIMUM FLOW DISTRIBUTIONS

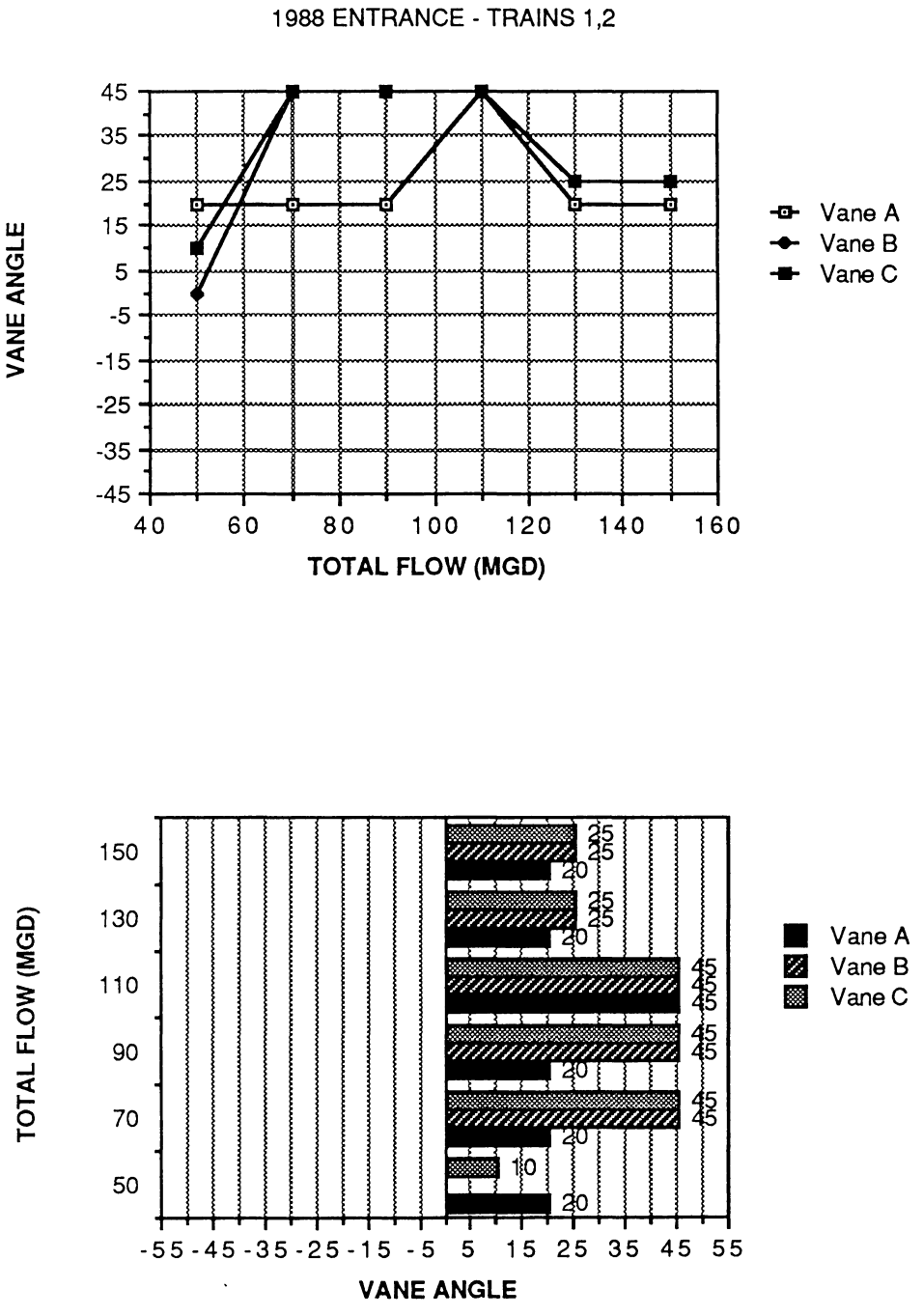

Figure 33. Vane Angles, 1988 Entrance, Trains 1,2, Optimum Vane Settings.

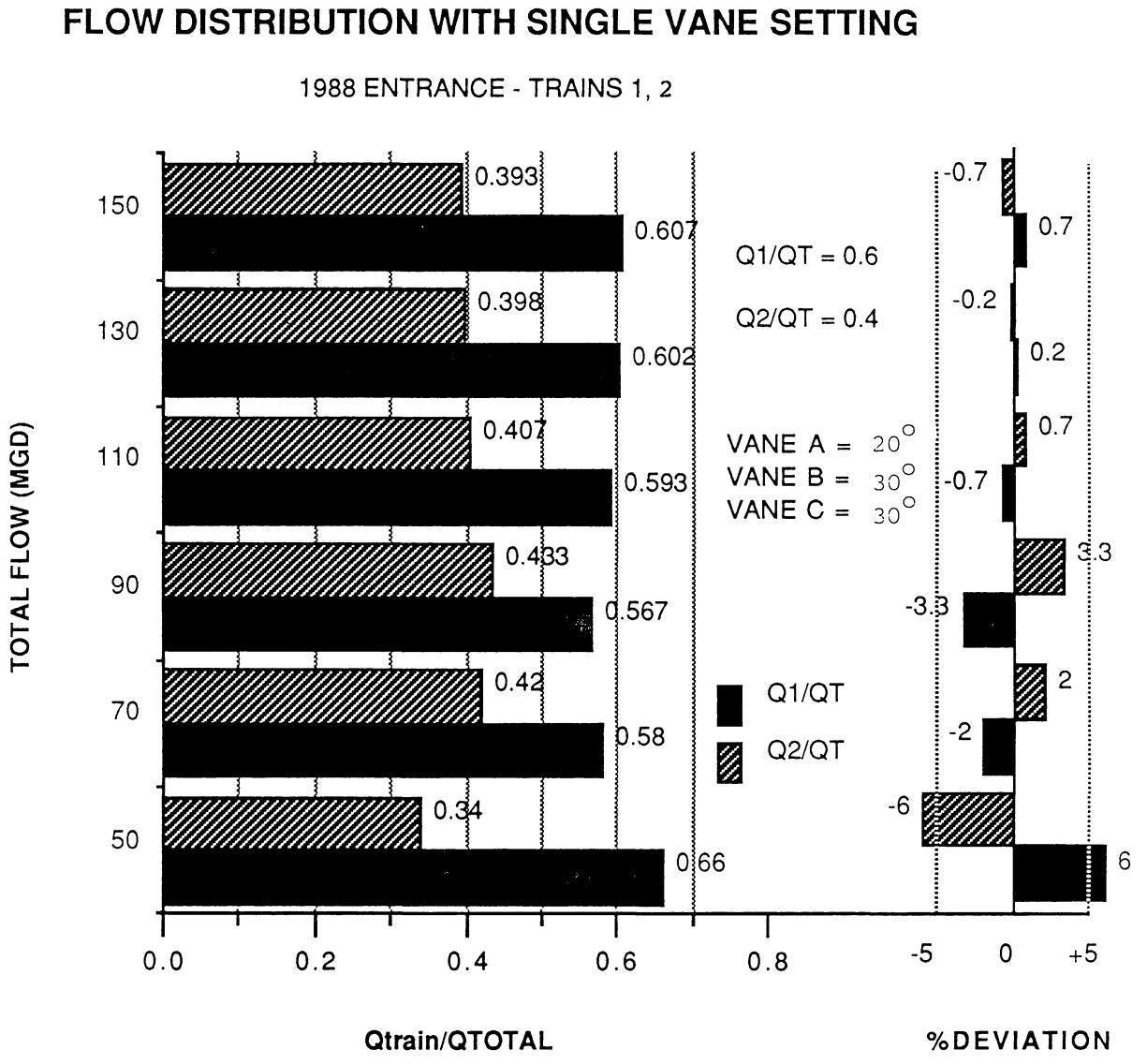

Figure 34. Flow Distributions, 1988 Entrance, Trains 1,2, Single Vane Setting.

FLOW DISTRIBUTIONS, NO VANES

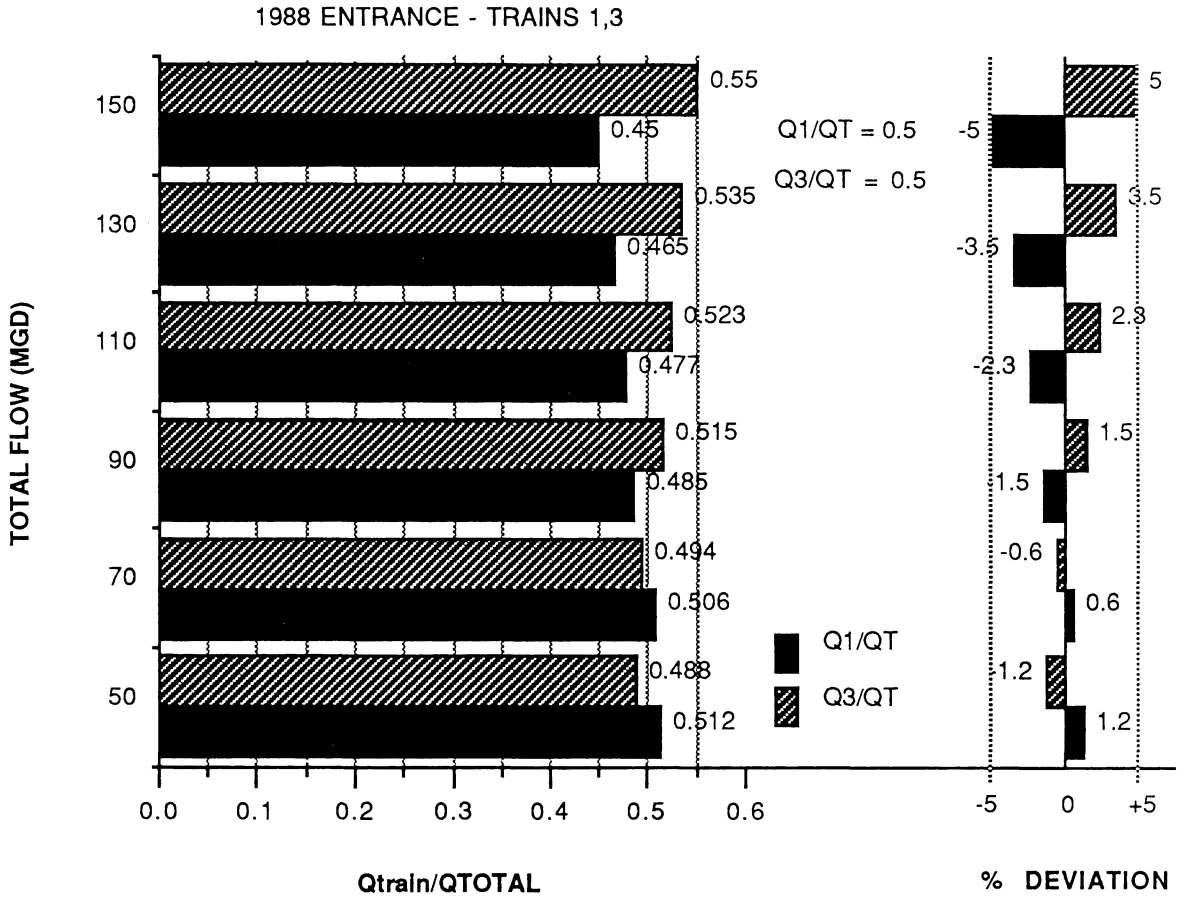

Figure 35. Flow Distributions, 1988 Entrance, Trains 1,3, No Vanes.

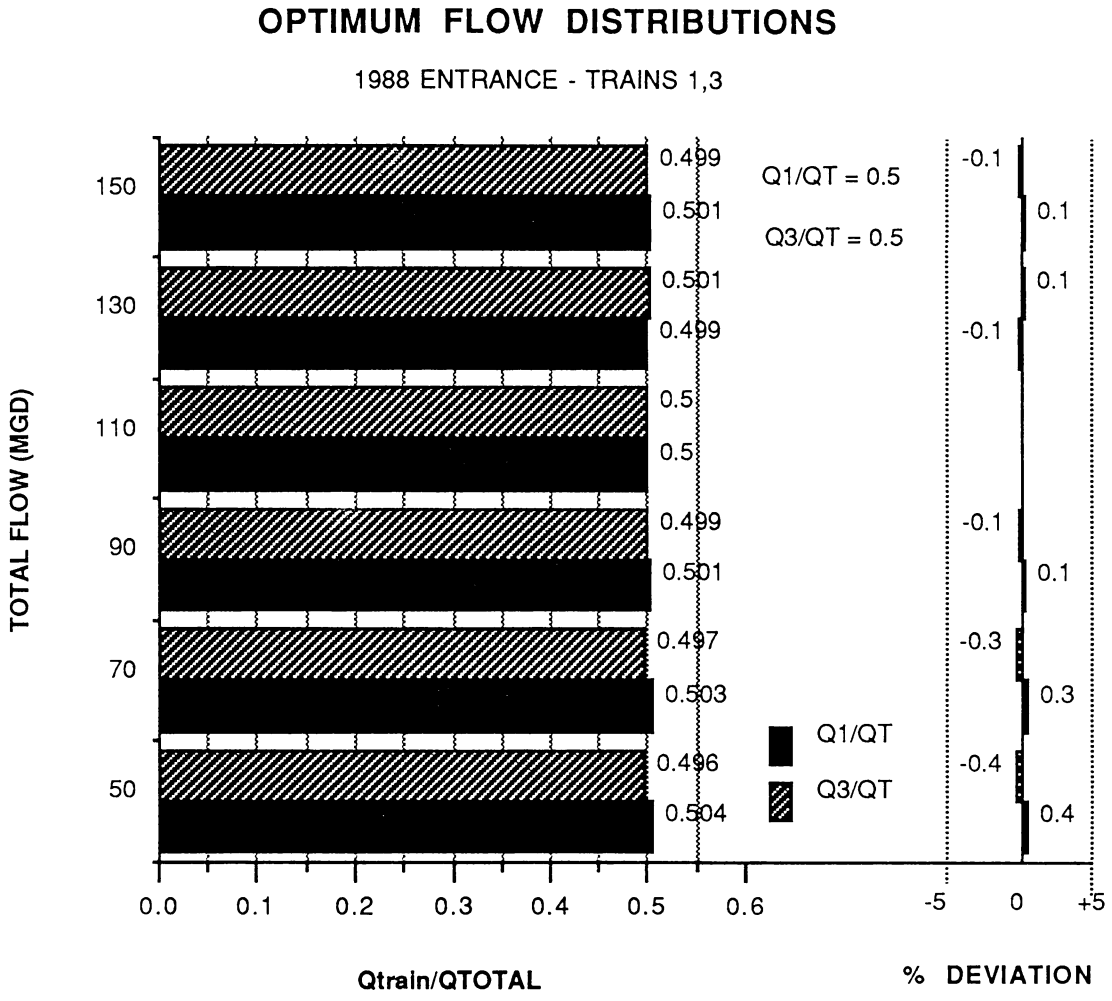

Figure 36. Flow Distributions, 1988 Entrance, Trains 1,3, Optimum Vane Settings.

VANE ANGLES, OPTIMUM FLOW DISTRIBUTIONS

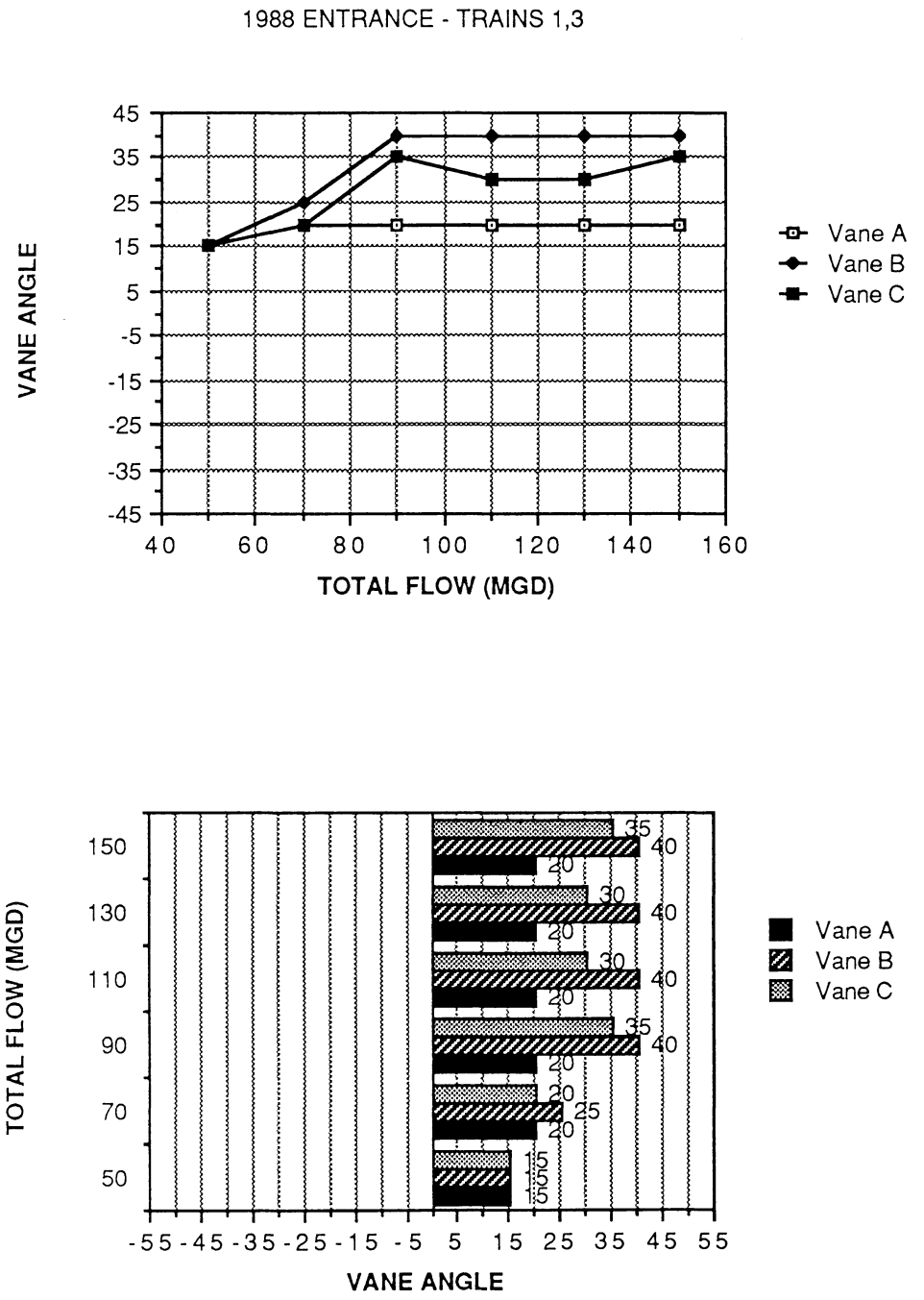

Figure 37. Vane Angles, 1988 Entrance, Trains 1,3, Optimum Vane Setings.

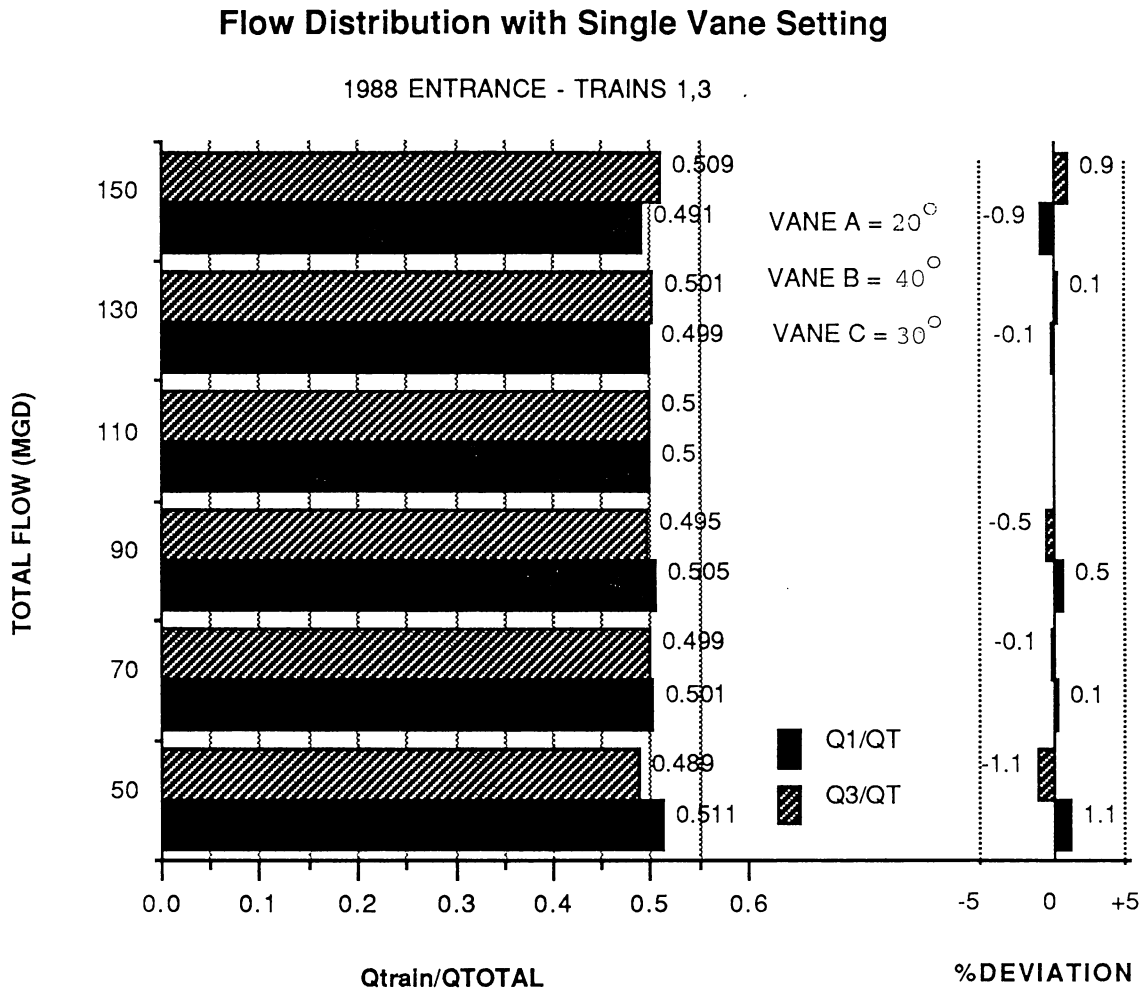

Figure 38. Flow Distributions, 1988 Entrance, Trains 1,3, Single Vane Settings.

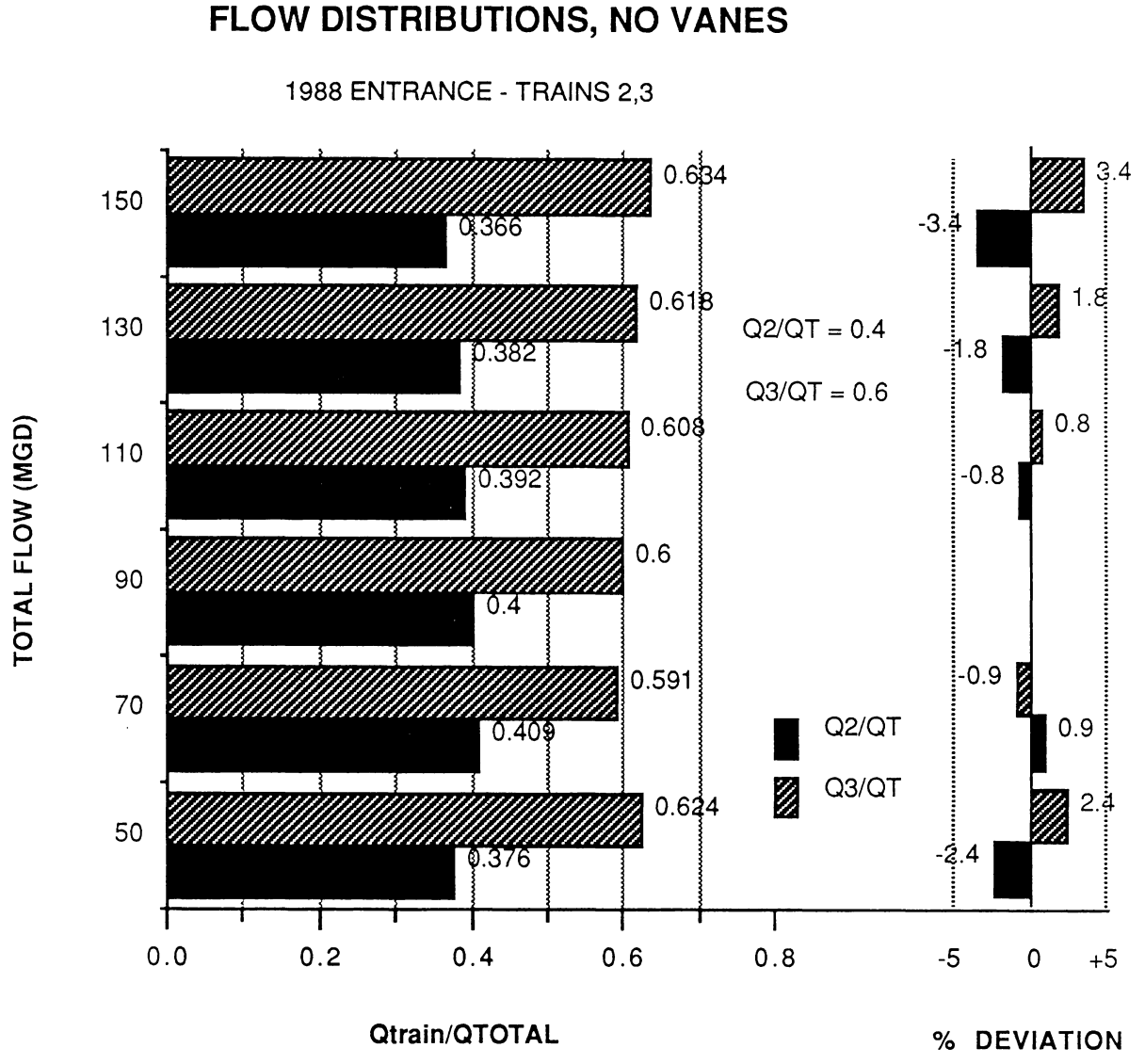

Figure 39. Flow Distributions, 1988 Entrance, Trains 2,3, No Vanes

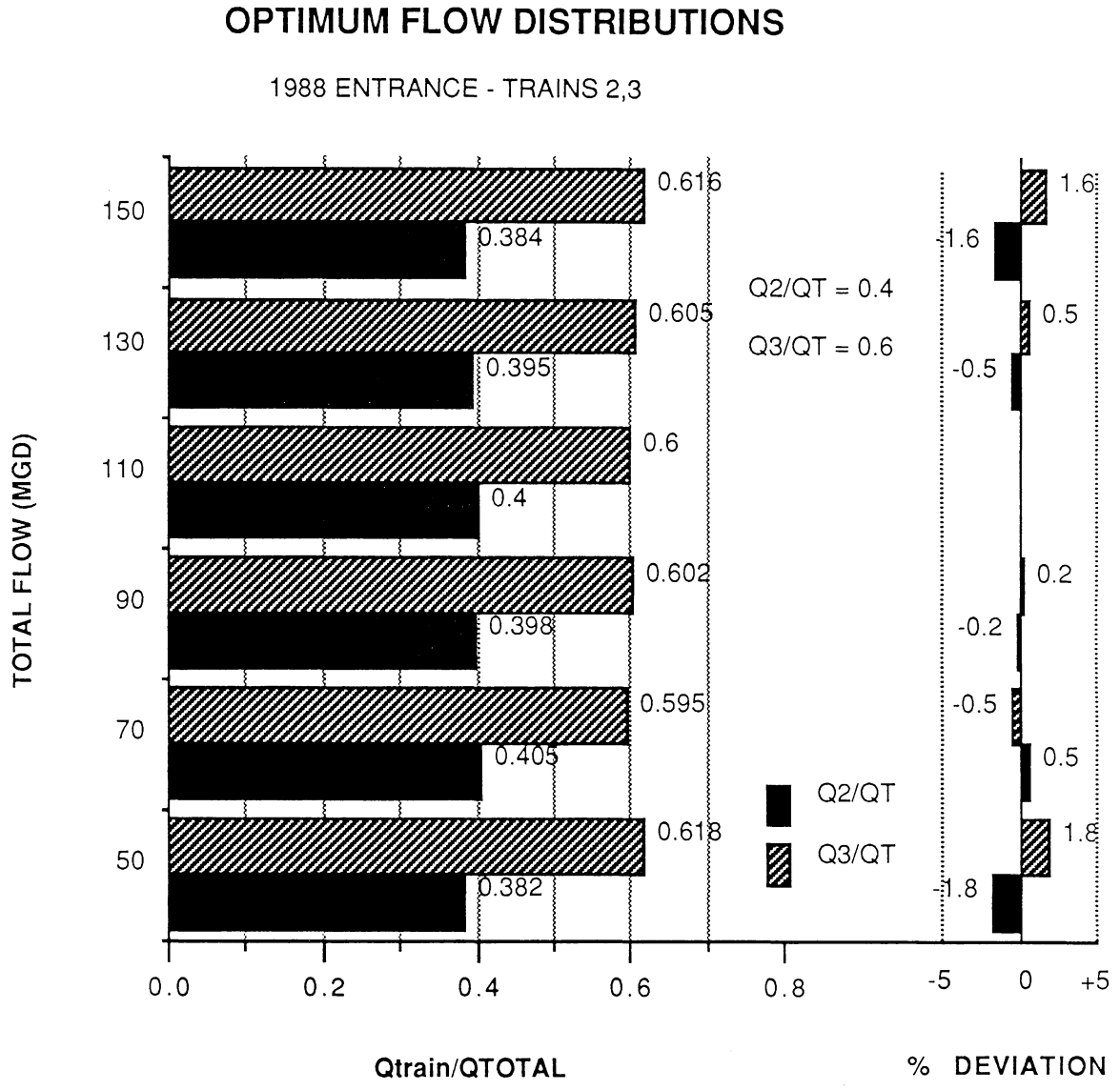

Figure 40. Flow Distributions, 1988 Entrance, Trains 2,3, Optimum Vane Settings.

VANE ANGLES, OPTIMUM FLOW DISTRIBUTIONS

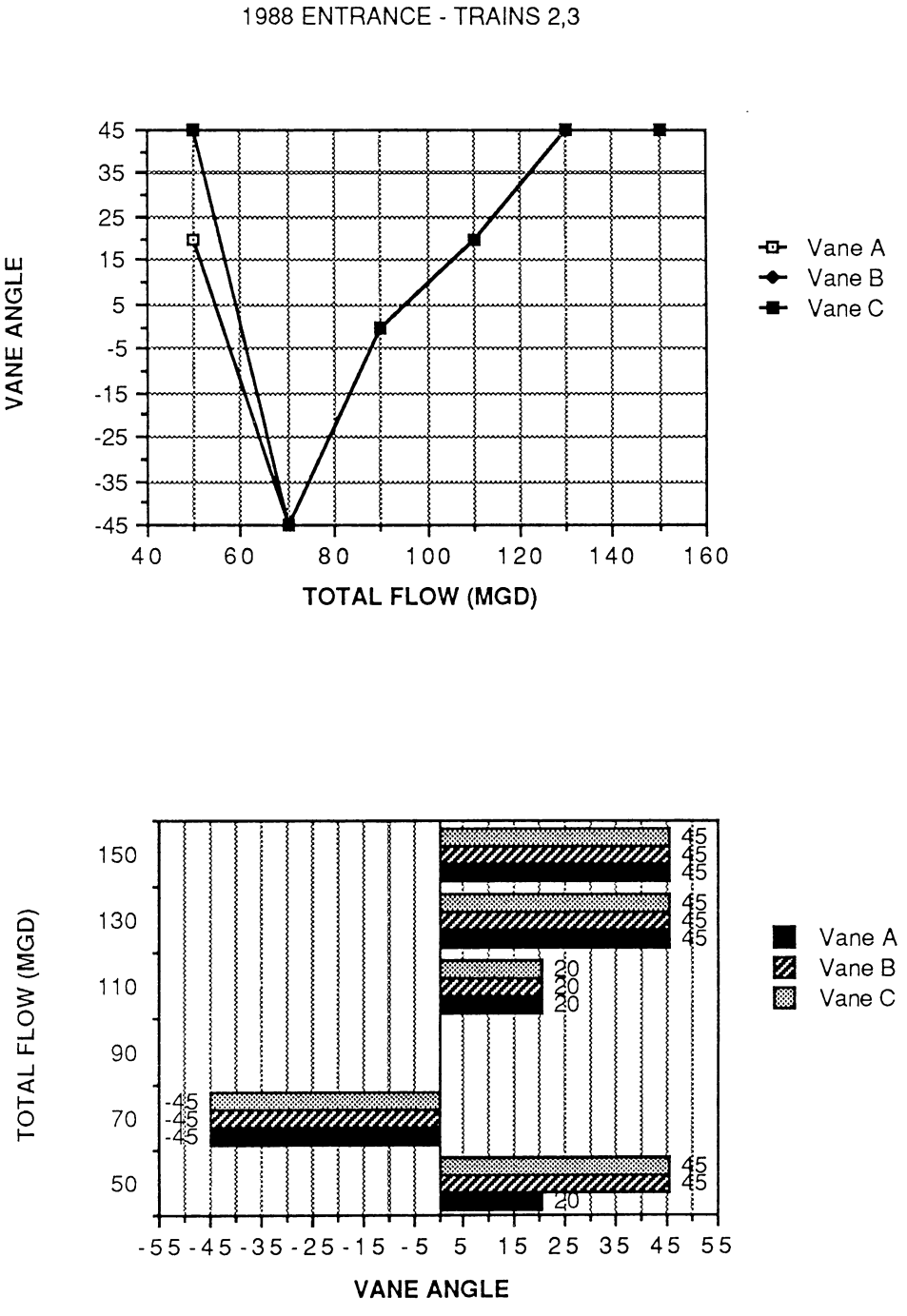

Figure 41. Vane Angles, 1988 Entrance, Trains 2,3, Optimum Vane Settings.

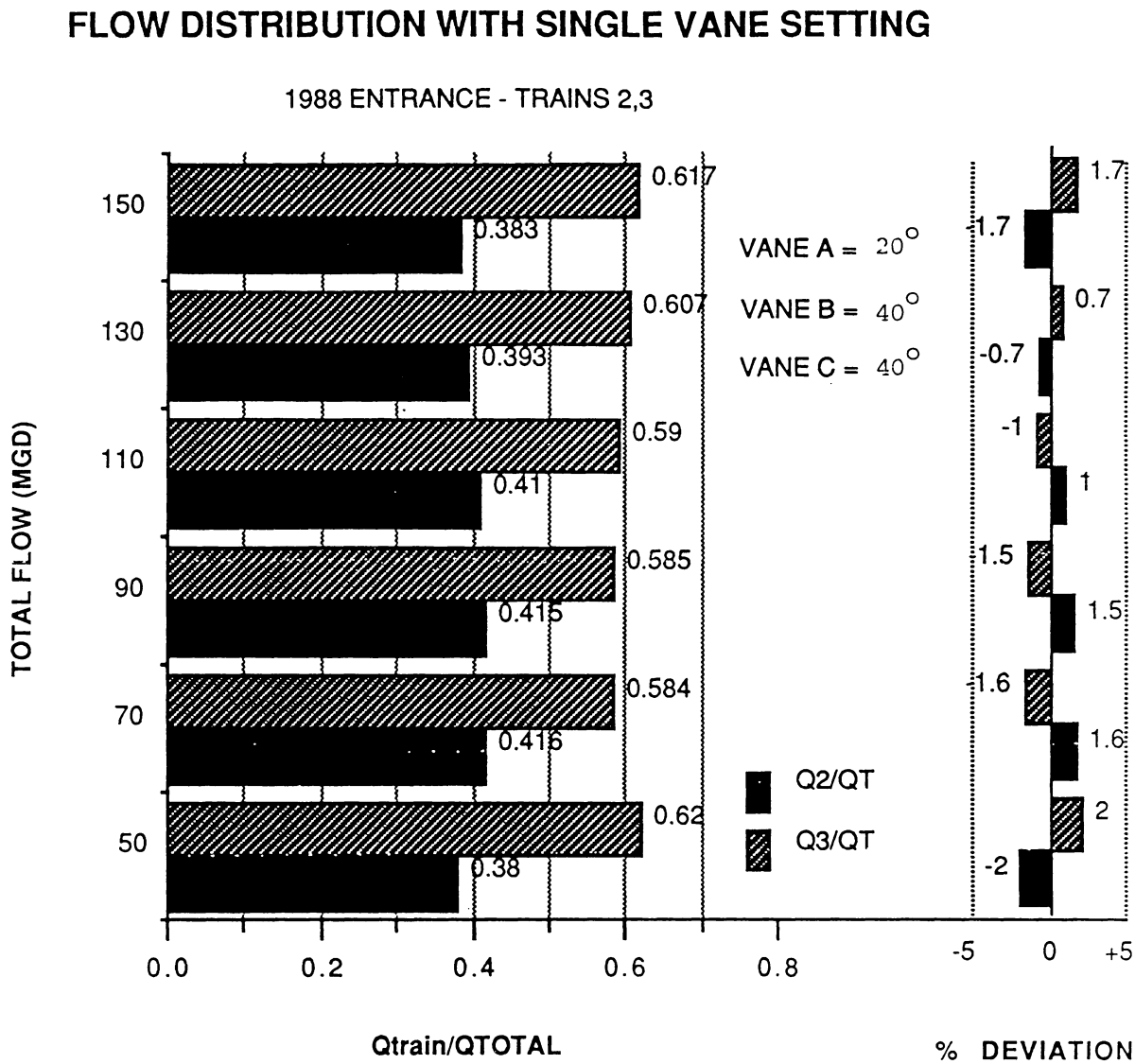

Figure 41. Flow Distributions, 1988 Entrance, Trains 2,3, Single Vane Setting

A summary of the vane angles that yield the required flow distribution over the range of plant discharges is presented in Table 1, including the single vane setting that was used to provide a reasonable flow distribution for all discharges.

TABLE 1. Summary of Vane Angles Determined to Provide Required Flow Distributions, 1988 Entrance.

Trains	Flow	Vane A	Vane B	Vane C
1,2,3	50	30	45	20
	70	-15	-15	45
	90	40	40	15
	110	40	40	35
	130	40	45	45
	150	20	45	35
1,2	50	20	0	10
	70	20	45	45
	90	20	45	45
	110	45	45	45
	130	20	25	25
	150	20	25	25
1,3	50	15	15	15
	70	20	25	20
	90	20	40	35
	110	20	40	30
	130	20	40	30
	150	20	40	35
2,3	50	20	45	45
	70	-45	-45	-45
	90	0	0	0
	110	20	20	20
	130	45	45	45
	150	45	45	45
SINGLE VANE SETTINGS				
1,2,3		20	40	35
1,2		20	30	30
1,3		20	40	30
2,3		20	40	40

2015 Entrance

The 2015 entrance and flow conditions represent a situation where the approach flow is more uniform than with the 1988 entrance, but with higher flow velocities so that the flow distribution is more dependent upon the geometry in the splitter chamber. Consequently, it was found with all four trains in operation and no vanes present, that the flow distribution was relatively good at the lowest flow (150 MGD compared to 50 MGD for the 1988 entrance) but progressively became worse with increasing flow rate. Fig. 43 indicates the flow split for these flows and no vanes present. It can be seen that the flows are within the measurement accuracy at the lowest flows with the deviations generally increasing with flow rates up to a maximum of 3 percent of total plant flow or 12 percent of desired train flow. In general, the inner trains (2 and 3) are favored with respect to the outer ones and the easterly ones (3 and 4) with respect to the westerly ones (1 and 2). The two tendencies trade off against each other and Train 2 is the higher flow at lower flow rates and becomes less than both 3 and 4 at the higher flows. This is due to the approach flow distribution which although not as significant as with the 1988 entrance still favors the east side of the inflow channel.

As with the 1988 entrance, it was possible to obtain the desired flow distribution for each flow by installing the vanes and optimizing the vane positions. The flow distributions and required vane settings are presented in Figs. 44 and 45. It can be seen that the 170 MGD flow has significantly different vane angles than the higher flows. However, it is shown below that there is another vane setting that provides a nearly equivalent flow distribution and indicates that there is no unique solution to the determination of the required vane settings to optimize the flow distribution. Vane A has a much more important influence on the flow distribution with this entrance condition. As close a match as with the 1988 entrance was not obtained, primarily because it was recognized by this point in the testing schedule that the ultimate plant operation would probably involve using a single vane setting for the range of flows associated with any combination of trains in operation. Therefore, more attention was

FLOW DISTRIBUTIONS, NO VANES

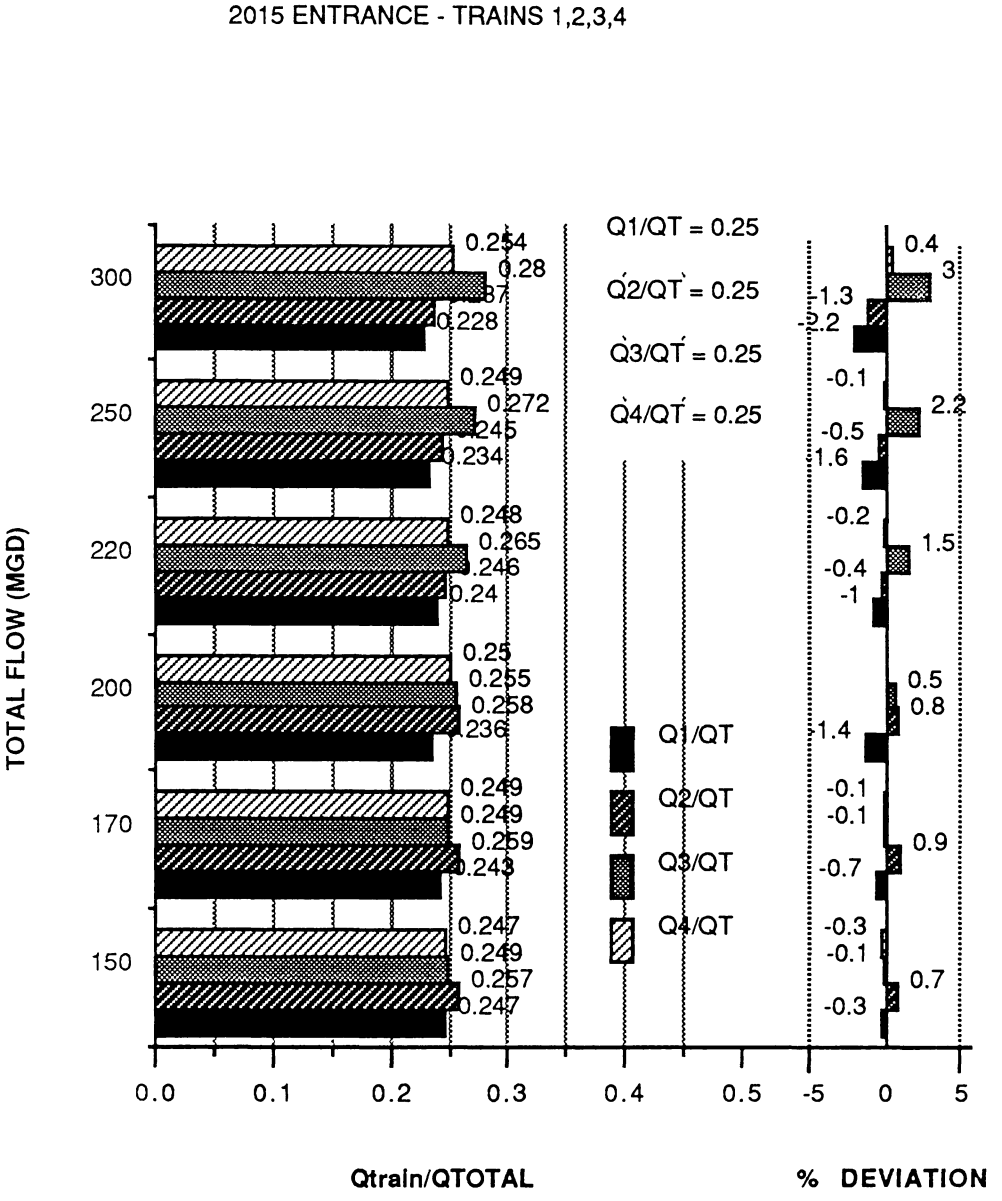

Figure 43. Flow Distributions, 2015 Entrance, No Vanes.

OPTIMUM FLOW DISTRIBUTIONS

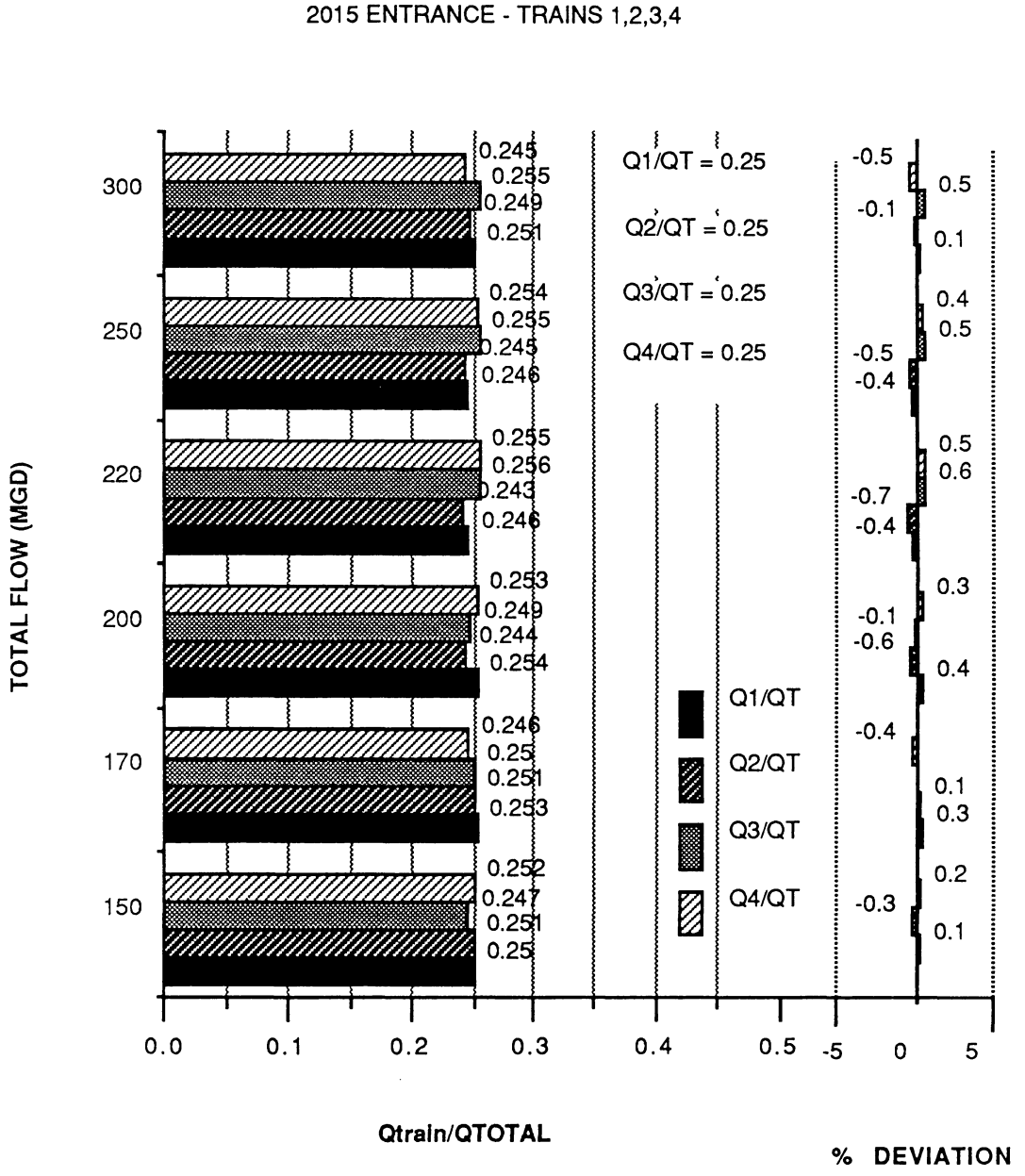

Figure 44. Flow Distributions, 2015 Entrance, Optimum Vane Settings.

VANE ANGLES, OPTIMUM FLOW DISTRIBUTIONS

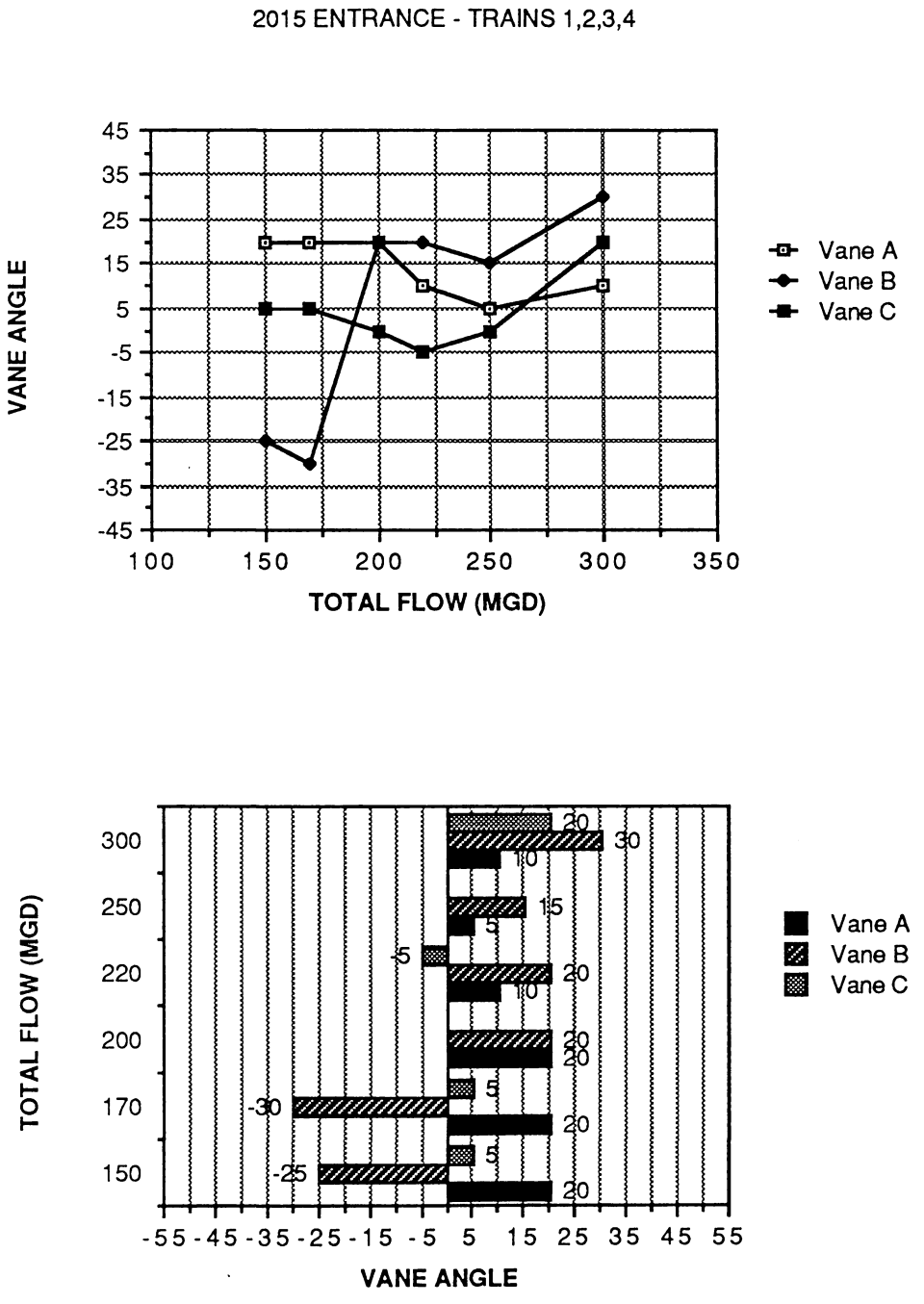

Figure 45. Vane Angles, 2015 Entrance, Optimum Vane Settings.

paid to finding a good flow distribution over the range of flows with a single vane setting and the results of this effort are presented in Fig. 46. Except at the 300 MGD (maximum) flow, all flows are within 1 percent of the total plant flow or 3.6 percent of the desired train flow and thus close to the measurement accuracy. Even at the 300 MGD flow, the worst flow deviation is only 2 percent of the total plant flow. Therefore, the feasibility of utilizing a single vane setting for distributing the flow with all four trains in operation was demonstrated.

When the various combinations of three trains in operations were considered much the same results were developed. For these configurations, the flow distribution with no vanes was not collected. The results are presented in Figs. 47-58 for the four flow states. Similar plots to those presented for the 1988 entrance are developed. It was found that a correct flow distribution, within the accuracy of the measurements, could be developed in all cases, much the same as was found for the 1988 entrance for the higher flow rates. Even with a single vane setting, all flows were within 4 percent of the desired train flow or within 1.3 percent of the total plant flow. These results are generally somewhat better than found with the 1988 entrance. This should hardly be surprising with the straighter entrance condition.

A summary of the vane angles that yield the required flow distribution over the range of plant discharges is presented in Table 2, including the single vane setting that was used to provide a reasonable flow distribution for all discharges.

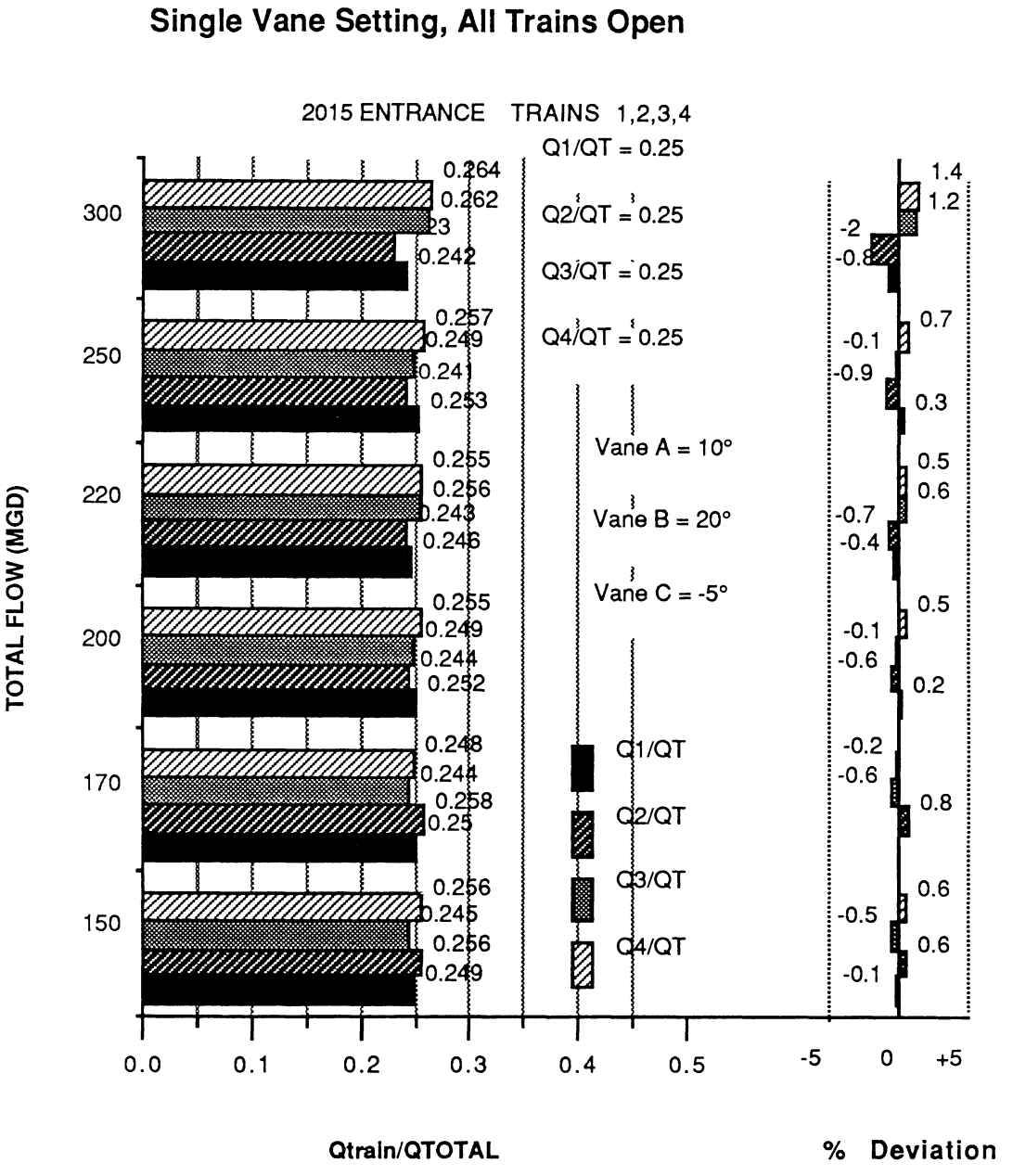

Figure 46. Flow Distributions, 2015 Entrance, Single Vane Setting.

OPTIMUM FLOW DISTRIBUTIONS

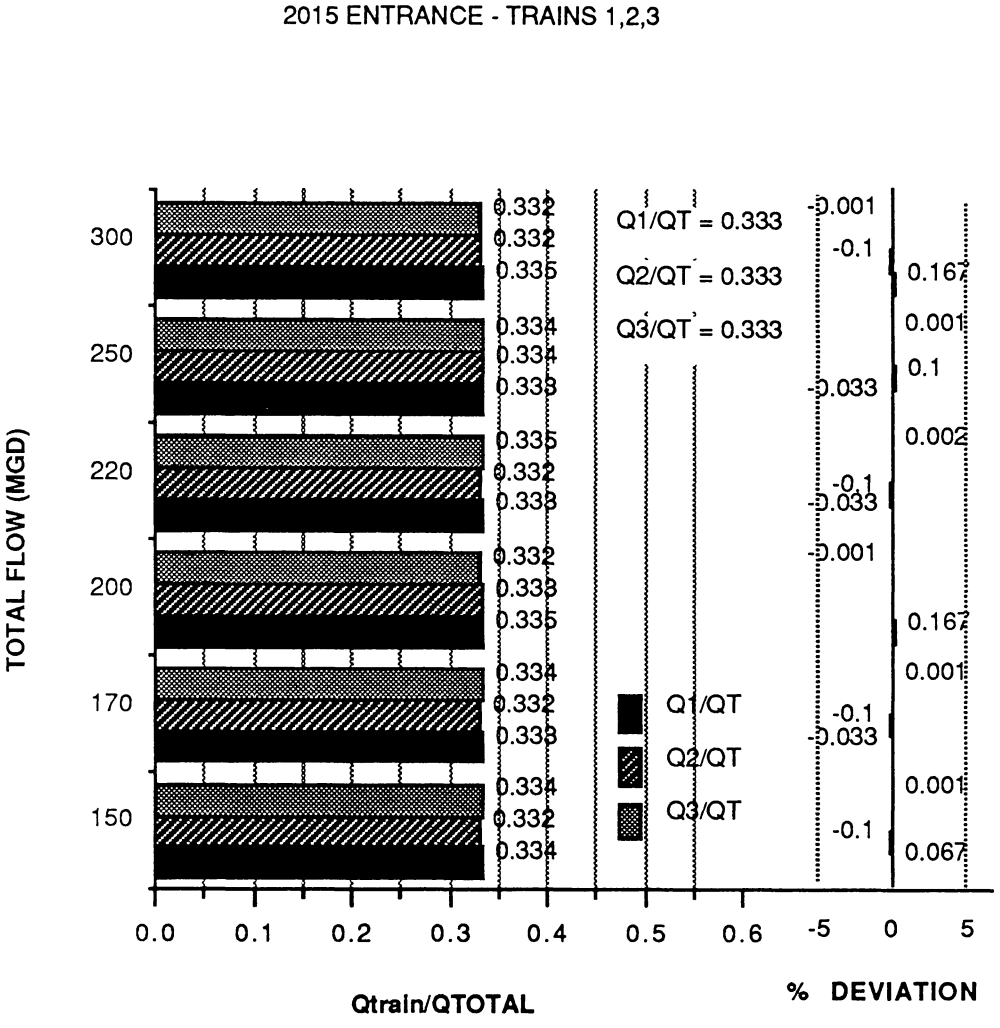

Figure 47. Flow Distributions, 2015 Entrance, Trains 1,2,3, Optimum Vane Setting.

VANE ANGLES, OPTIMUM FLOW DISTRIBUTIONS

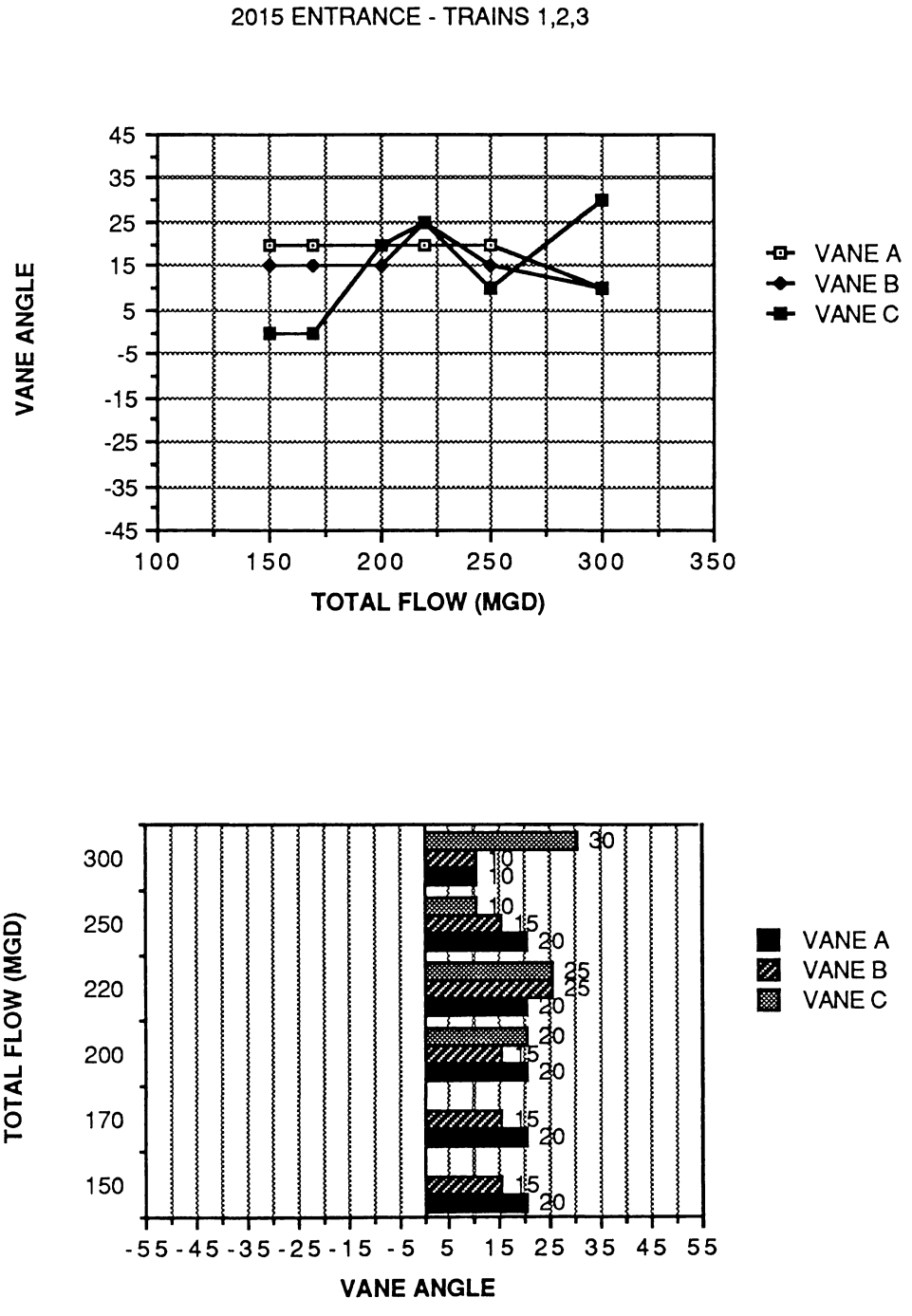

Figure 48. Vane Angles, 2015 Entrance, Trains 1,2,3, Optimum Vane Setting.

FLOW DISTRIBUTIONS, SINGLE VANE SETTING

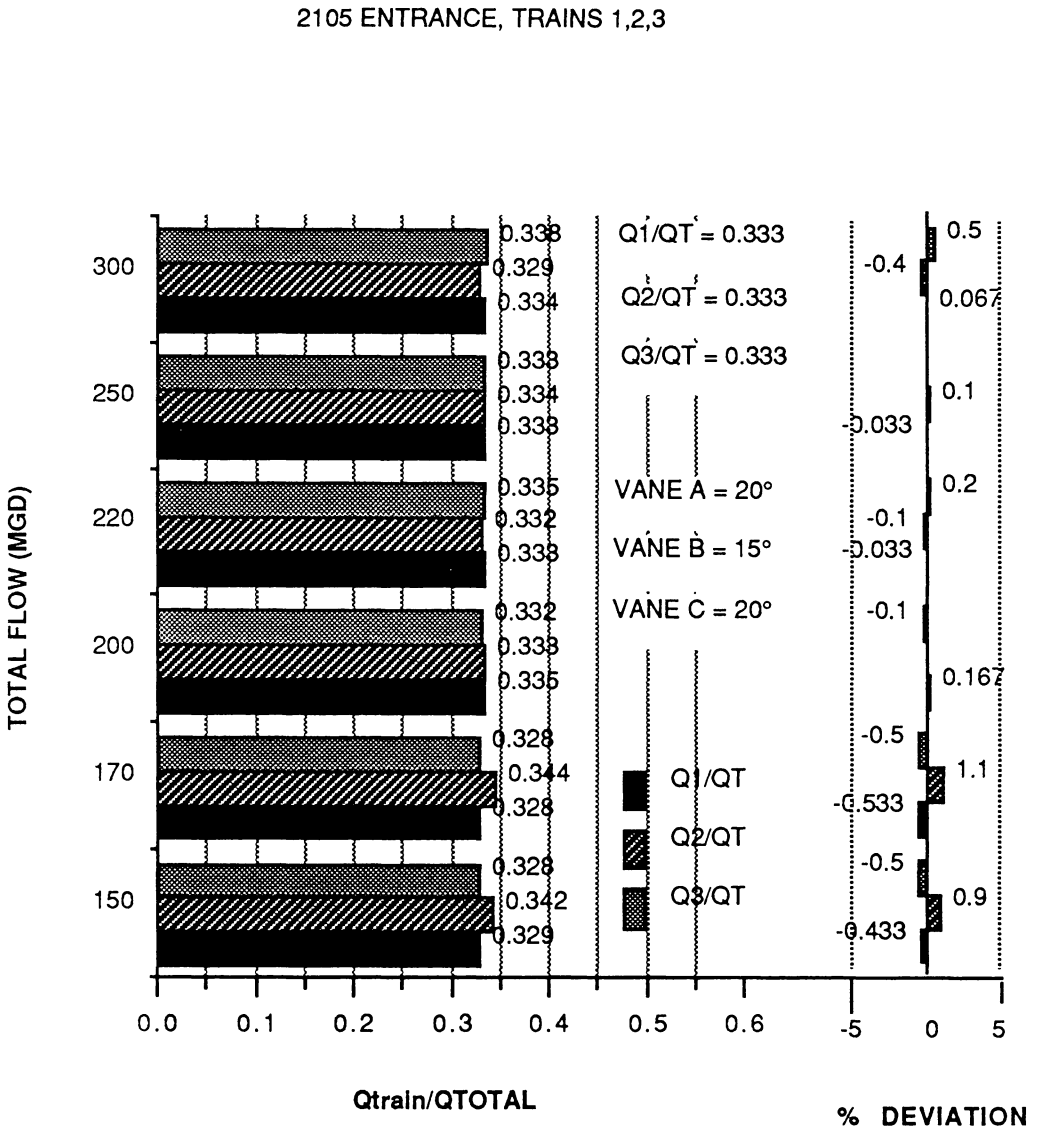

Figure 49. Flow Distributions, 2015 Entrance, Trains 1,2,3, Single Vane Setting.

OPTIMUM FLOW DISTRIBUTIONS

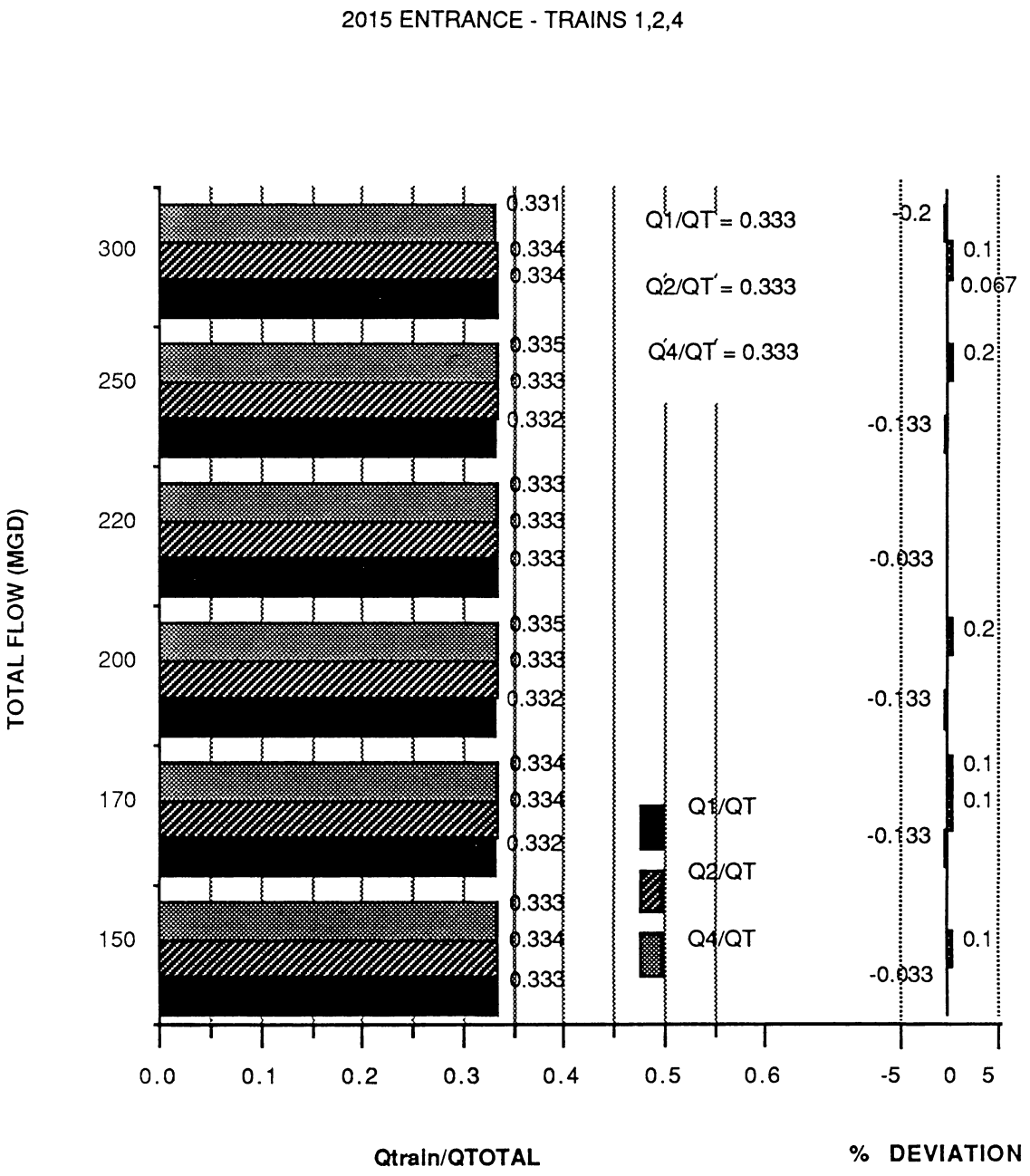

Figure 50. Flow Distributions, 2015 Entrance, Trains 1,2,4, Optimum Vane Setting.

VANE ANGLES, OPTIMUM FLOW DISTRIBUTIONS

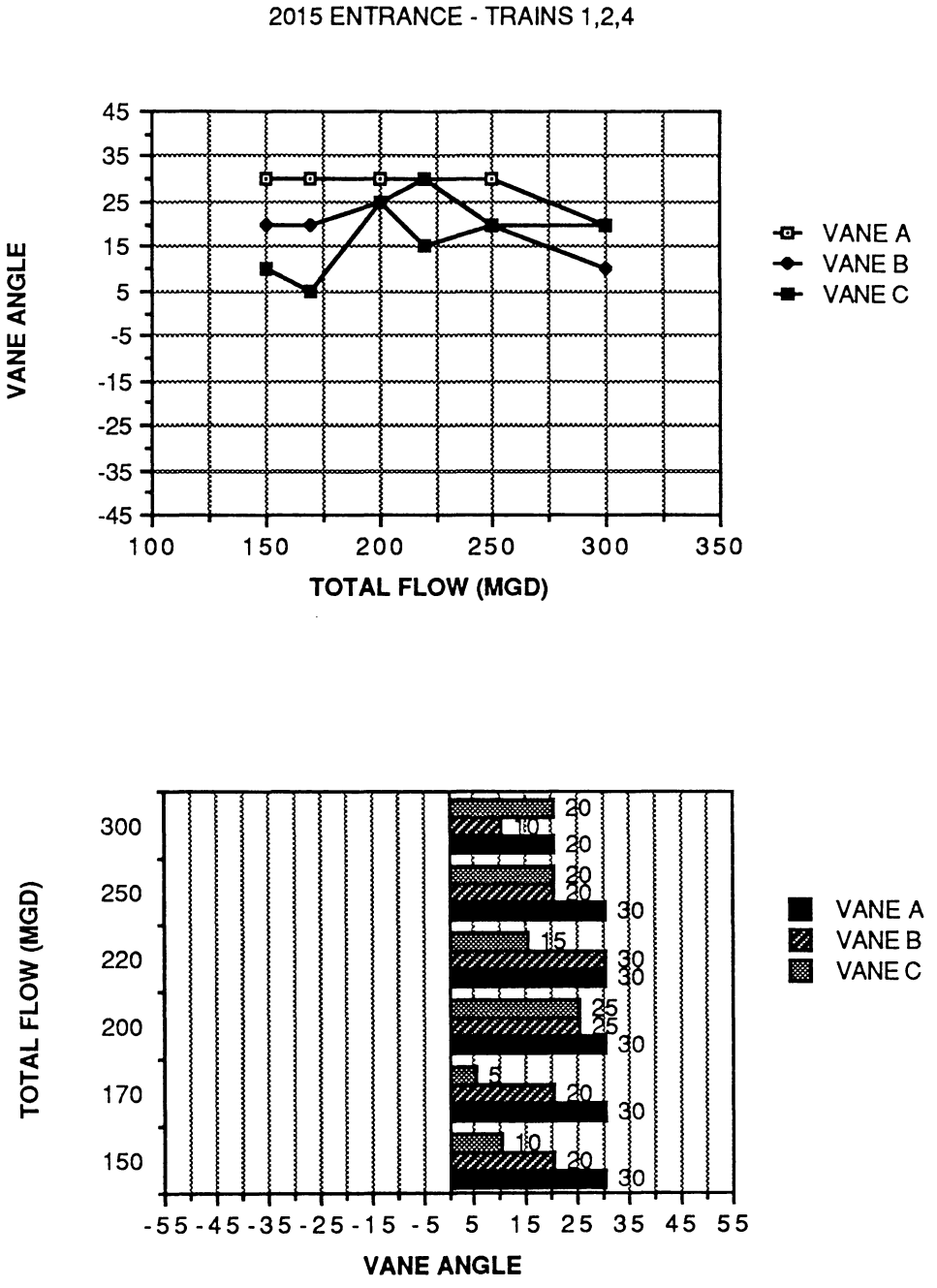

Figure 51. Vane Angles, 2015 Entrance, Trains 1,2,4, Optimum Vane Setting.

FLOW DISTRIBUTIONS, SINGLE VANE SETTING

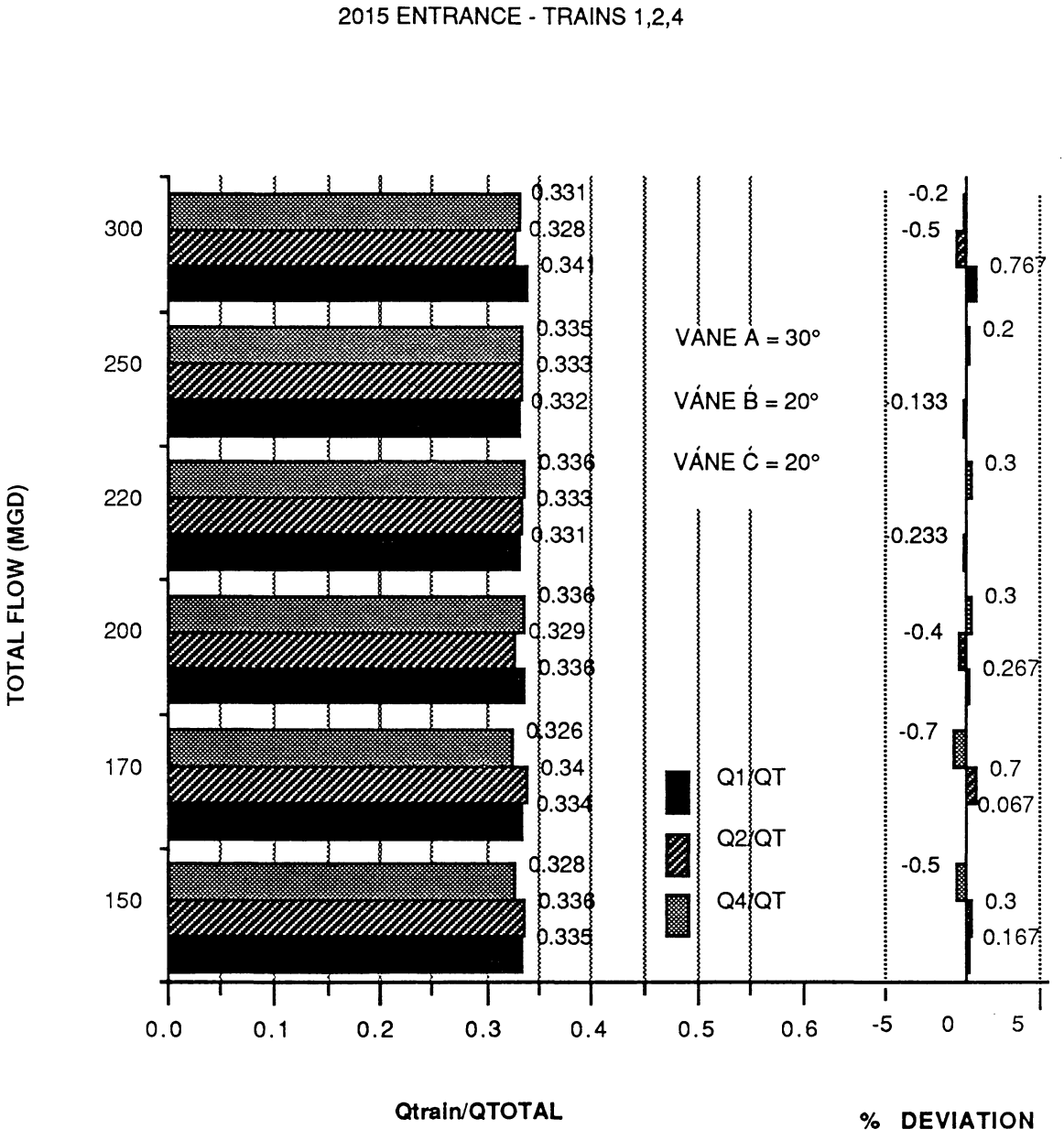

Figure 52. Flow Distributions, 2015 Entrance, Trains 1,2,4, Single Vane Setting.

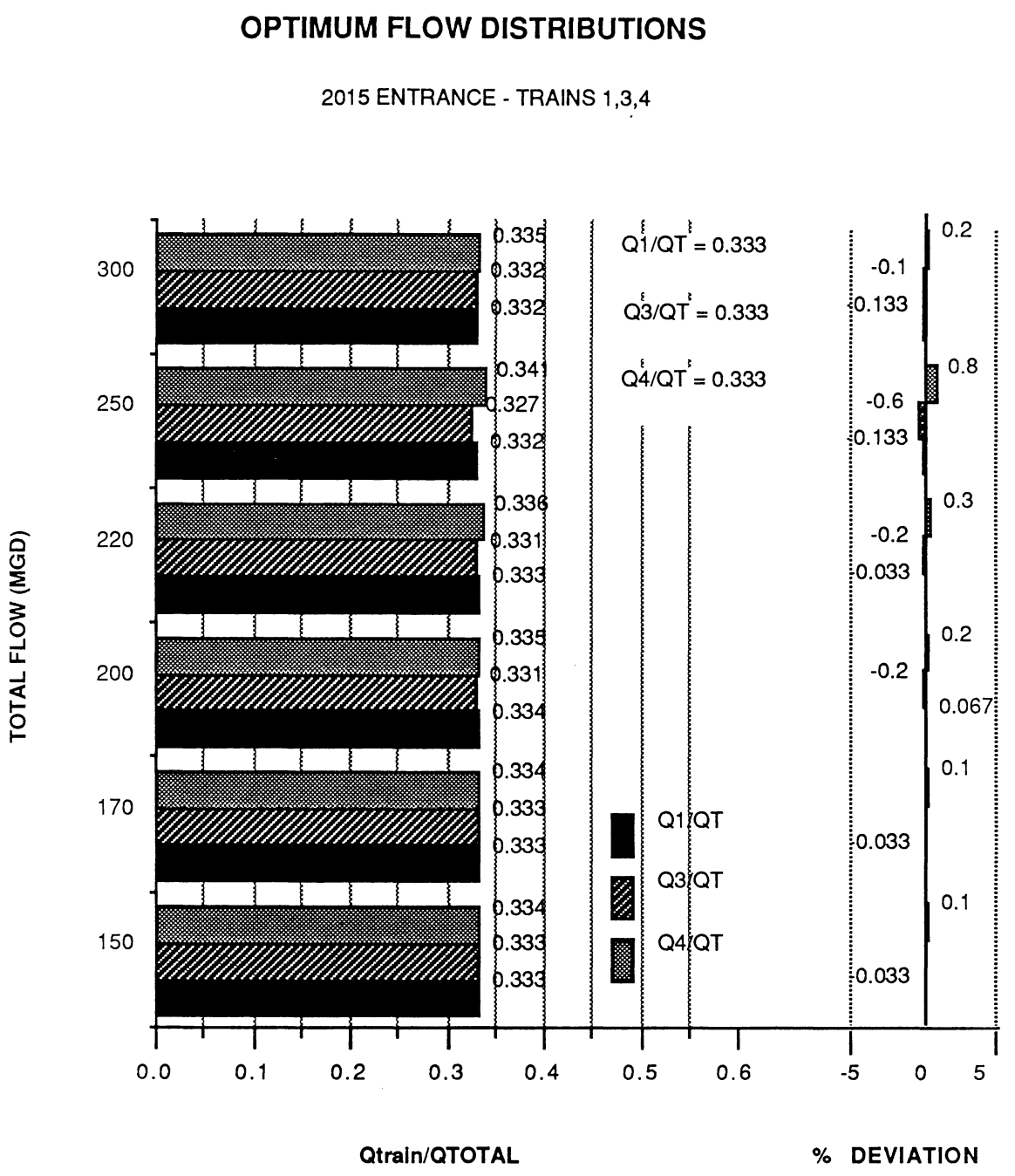

Figure 53. Flow Distributions, 2015 Entrance, Trains 1,3,4, Optimum Vane Setting.

VANE ANGLES, OPTIMUM FLOW DISTRIBUTIONS

2015 ENTRANCE - TRAINS 1,3,4

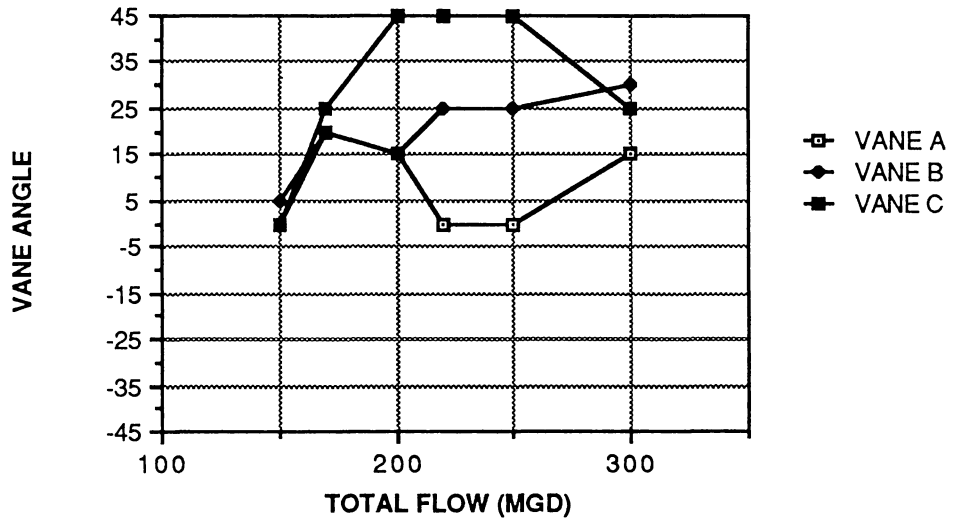

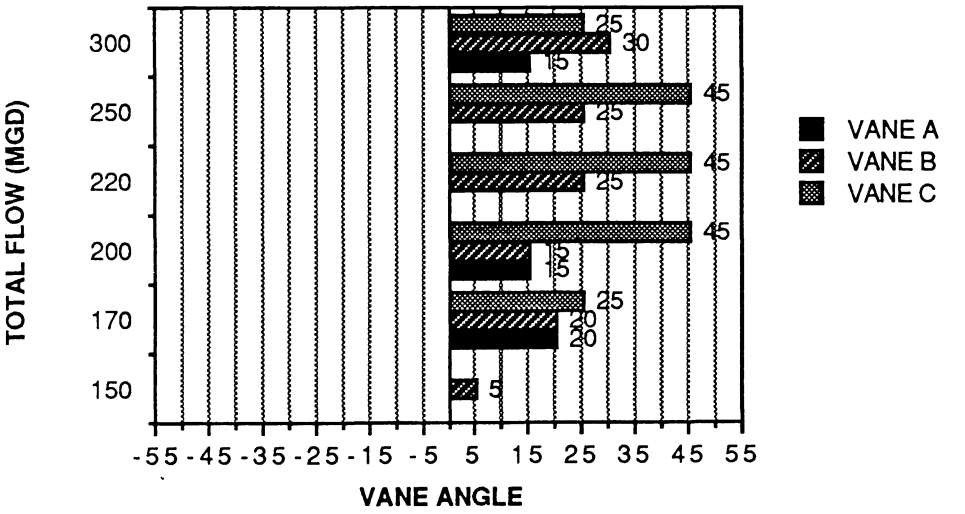

Figure 54.Vane Angles, 2015 Entrance, Trains 1,3,4, Optimum Vane Setting.

FLOW DISTRIBUTIONS, SINGLE VANE SETTING

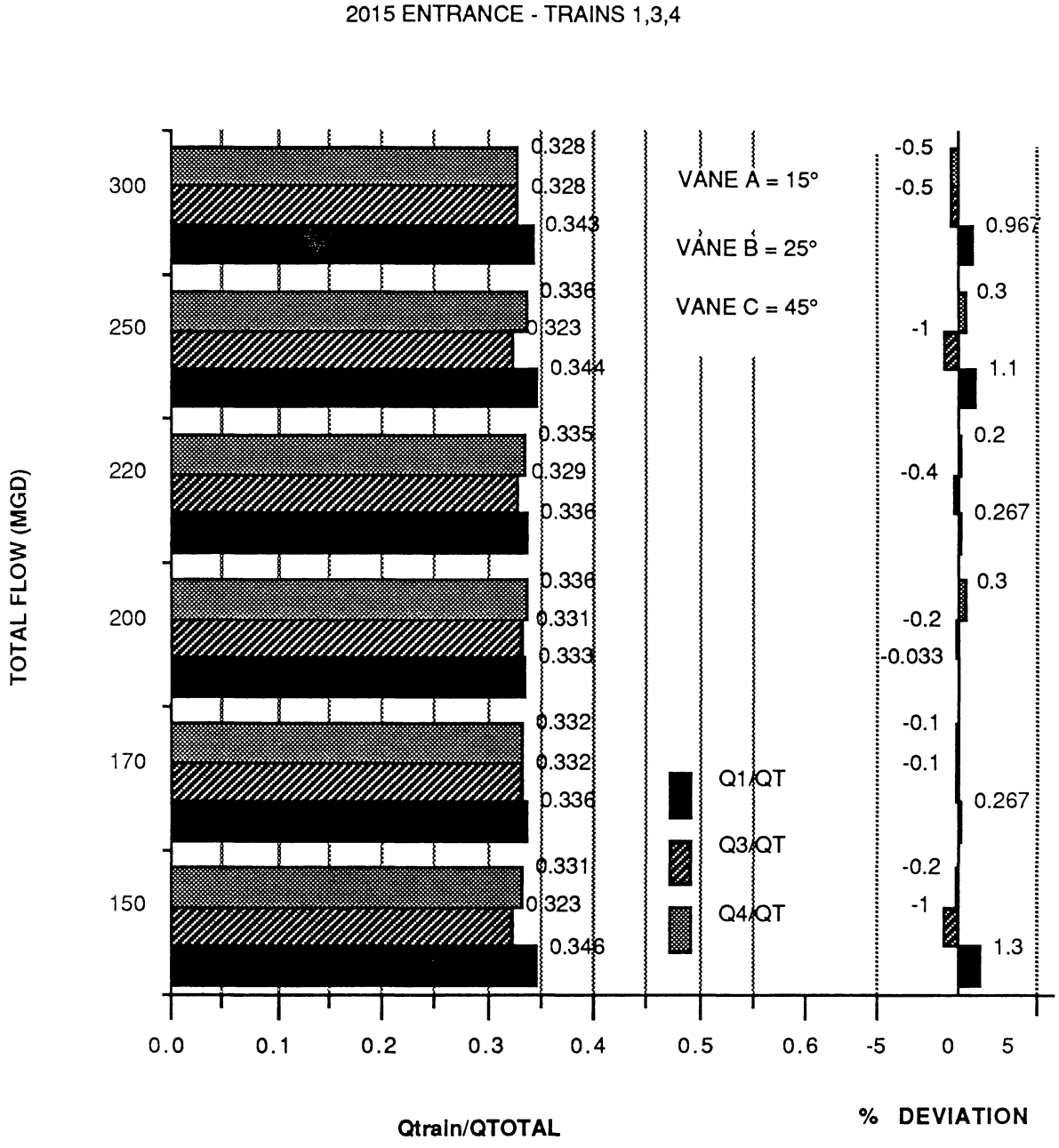

Figure 55.Flow Distributions, 2015 Entrance, Trains 1,3,4, Single Vane Setting.

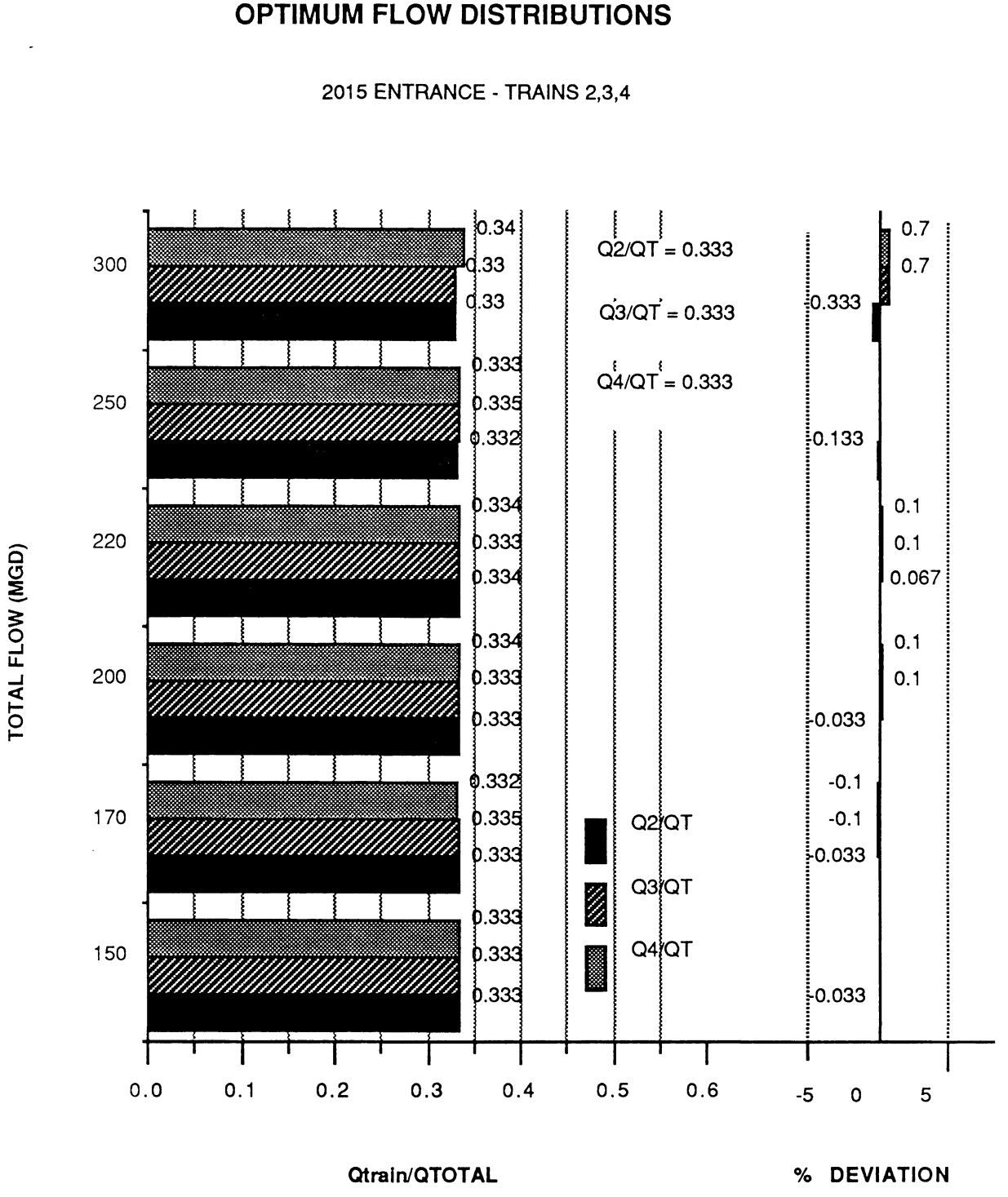

Figure 56.Flow Distributions, 2015 Entrance, Trains 2,3,4, Optimum Vane Setting.

VANE ANGLES, OPTIMUM FLOW DISTRIBUTIONS

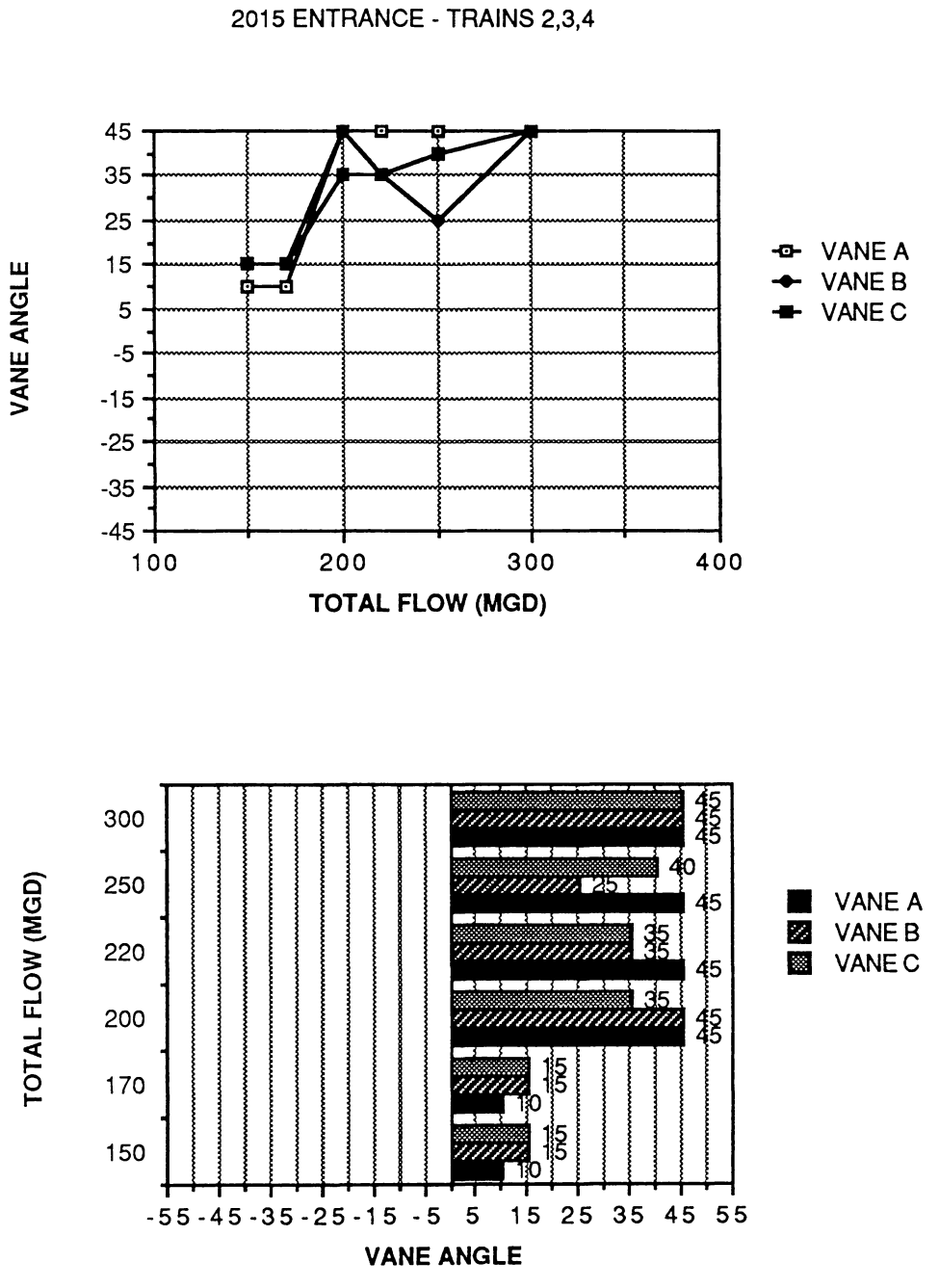

Figure 57. Vane Angles, 2015 Entrance, Trains 2,3,4, Optimum Vane Setting.

FLOW DISTRIBUTIONS, SINGLE VANE SETTING

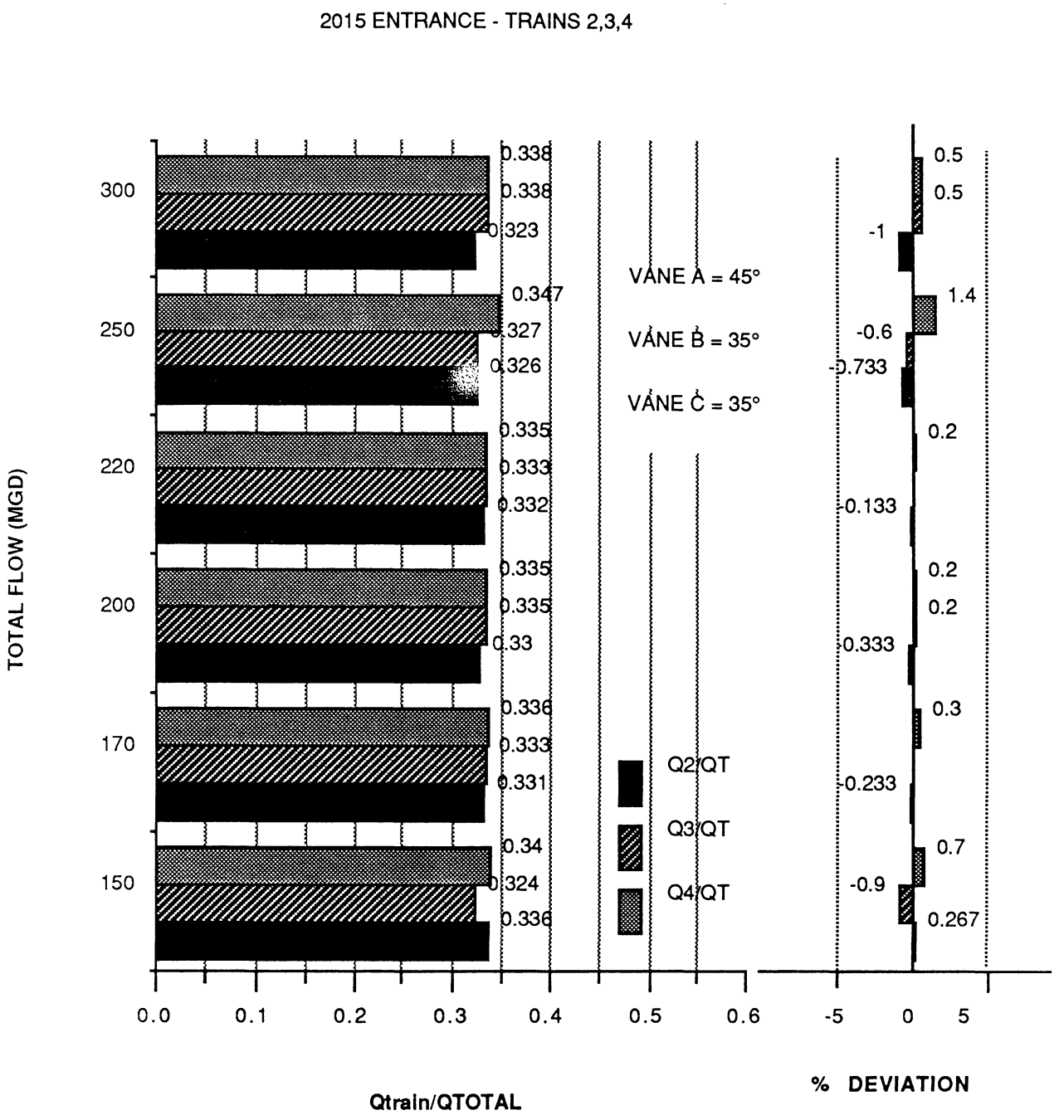

Figure 58. Flow Distributions, 2015 Entrance, Trains 2,3,4, Single Vane Setting.

TABLE 2. Summary of Vane Angles Determined to Provide Required Flow Distributions, 2015 Entrance.

Trains	Flow	Vane A	Vane B	Vane C
1,2,3,4	150	20	-25	5
	170	20	-30	5
	200	20	20	0
	220	10	20	-5
	250	5	15	0
	300	10	30	20
1,2,3	150	20	15	0
	170	20	15	0
	200	20	15	20
	220	20	25	25
	250	20	15	10
	300	10	10	30
1,2,4	150	30	20	10
	170	30	20	5
	200	30	25	25
	220	30	30	10
	250	30	20	20
	300	20	10	20
1,3,4	150	0	5	0
	170	20	20	25
	200	15	15	45
	220	0	25	45
	250	0	25	45
	300	15	30	25
2,3,4	150	10	15	15
	170	10	15	15
	200	45	45	35
	220	45	35	35
	250	45	20	40
	300	45	45	45
SINGLE VANE SETTINGS				
1,2,3,4		10	20	-5
1,2,3		20	15	20
1,2,4		30	20	20
1,3,4		15	25	45
2,3,4		45	35	45

Sedimentation

1988 Entrance

The sedimentation studies were conducted with the vane settings adjusted to give the optimum flow distributions for all three trains in operation, as in Fig. 27. Videotape records were made of the sedimentation process as well as the sediment recovery techniques. Fig. 59, which is for a variety of flows, indicates the general nature of the sedimentation process. A relatively high velocity at the entrance bend tended to sweep out the sediment in that region (Fig. 59a - 110 MGD) with some sedimentation in the dead zone associated with the stub end to be used for the 2015 entrance. Sedimentation occurred further downstream in the wake zone (Fig 59b - 150 MGD) and the region of sediment deposition corresponded with the area delineated in the dye survey. The region of deposition increased in width going down the channel (Fig. 59c - 110 MGD). In the region immediately downstream of the vanes, very little deposition occurred and considerably more occurred in the individual channels (Fig. 59d - 70 MGD). One can see the lack of sediment on the left hand side of Trains 2 and 3; this corresponded to a wake region as discussed above from the dye injection surveys. In this particular case, apparently very little sediment is carried to the wake zone and thus minimal deposition occurs there. The same general observations were made for the lower flow rates with generally more deposition in the upstream locations. In the case of the 50 MGD flow, there was significant deposition along the left side of the inlet channel and very little along the right side. This implies that the sediment was directly deposited and not carried much with the flow. Information regarding the sediment recovery is presented in Table 3. It was found that at the lowest flow of 50 MGD, the sediment was not carried with the flow a significant distance and nearly all settled out upstream from the control vanes. On the other hand, when the flow rate is increased to 150 MGD, most of the sediment deposited was found downstream of the vanes on the upsloping floors in the individual channels. In no case was a significant fraction of the sediment passed over the overflow weirs as a maximum of only 30% was unaccounted for by the recovery technique at the flow of 150

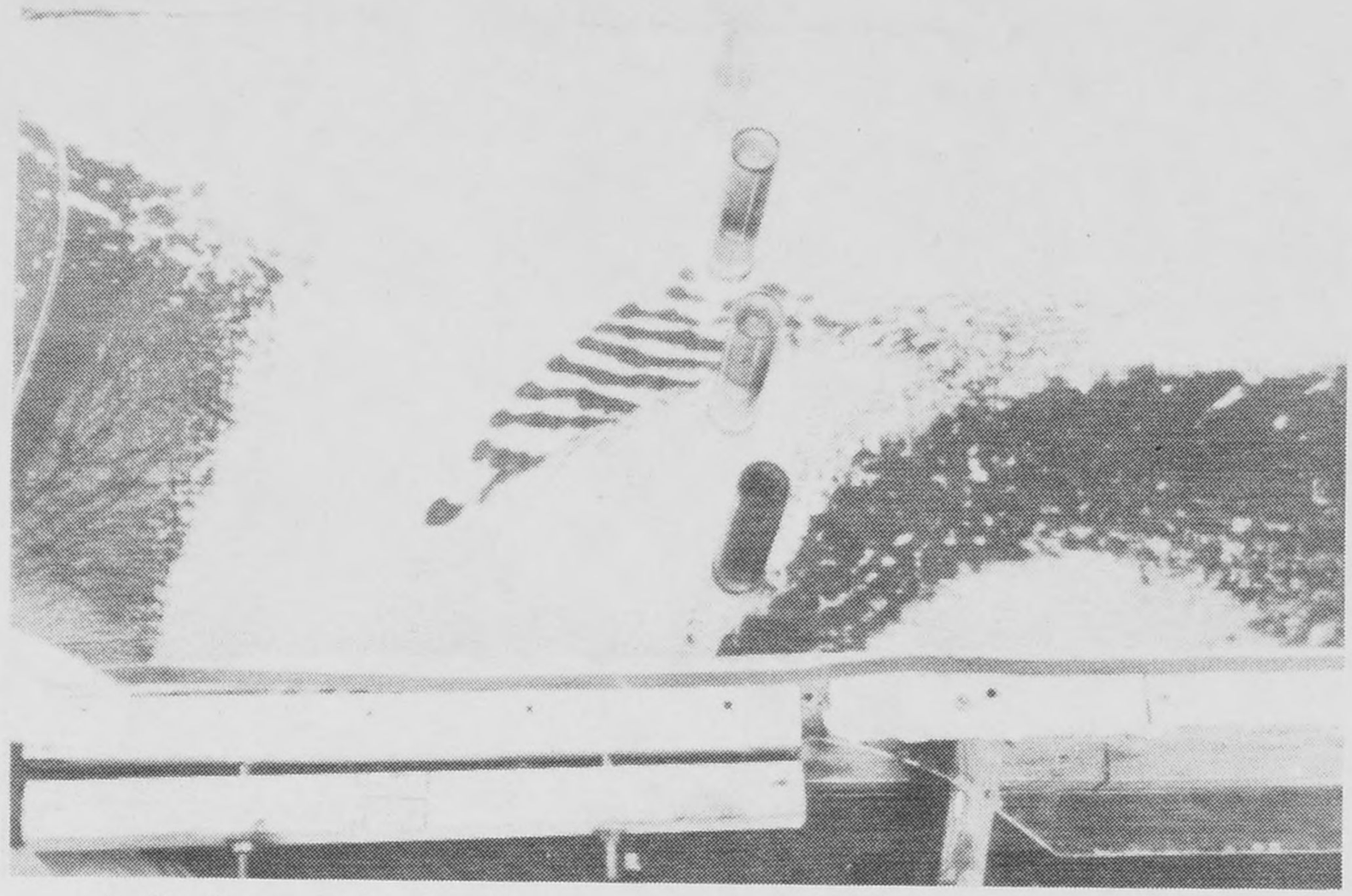

a.) Sediment Deposition at Side Channel Entrance,1988 Entrance, Total Flow = 110 MGD

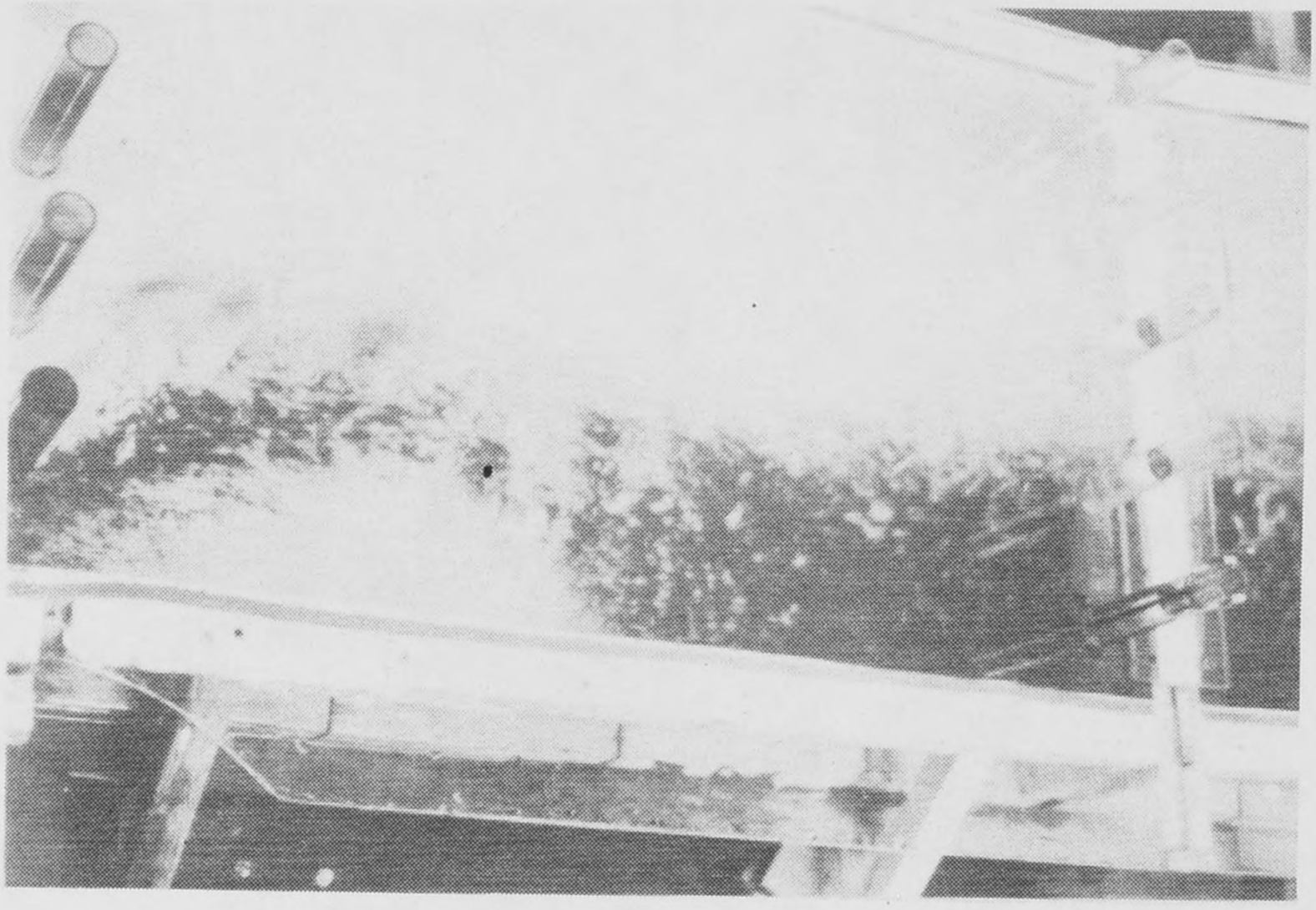

b.) Deposition Between Upstream and Downstream Access Ports.

Figure 59. Sediment Deposition Patterns, 1988 Entrance.

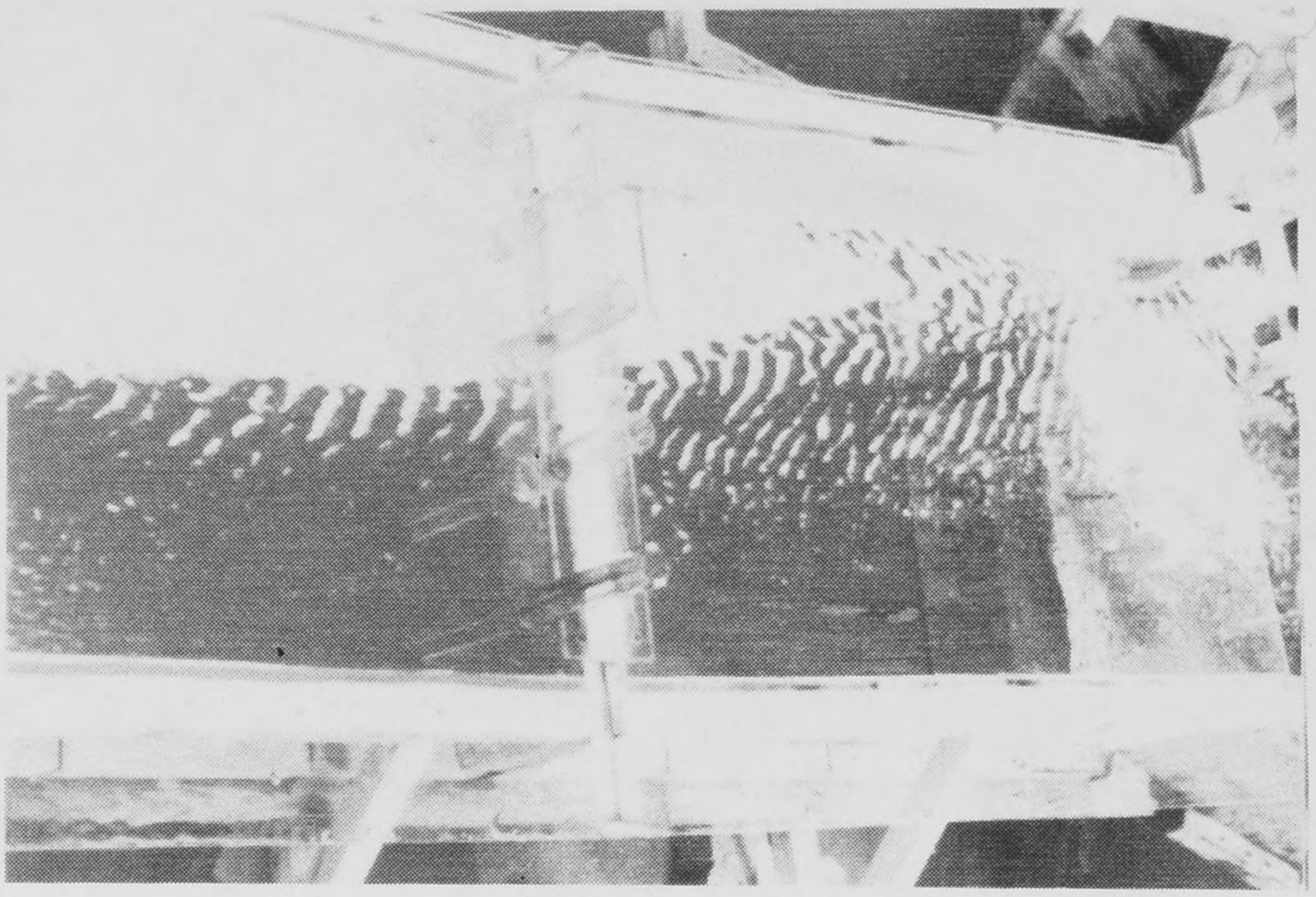

c..) Sediment Deposition Just Ahead of Guide Vanes, Total Flow = 110 MGD

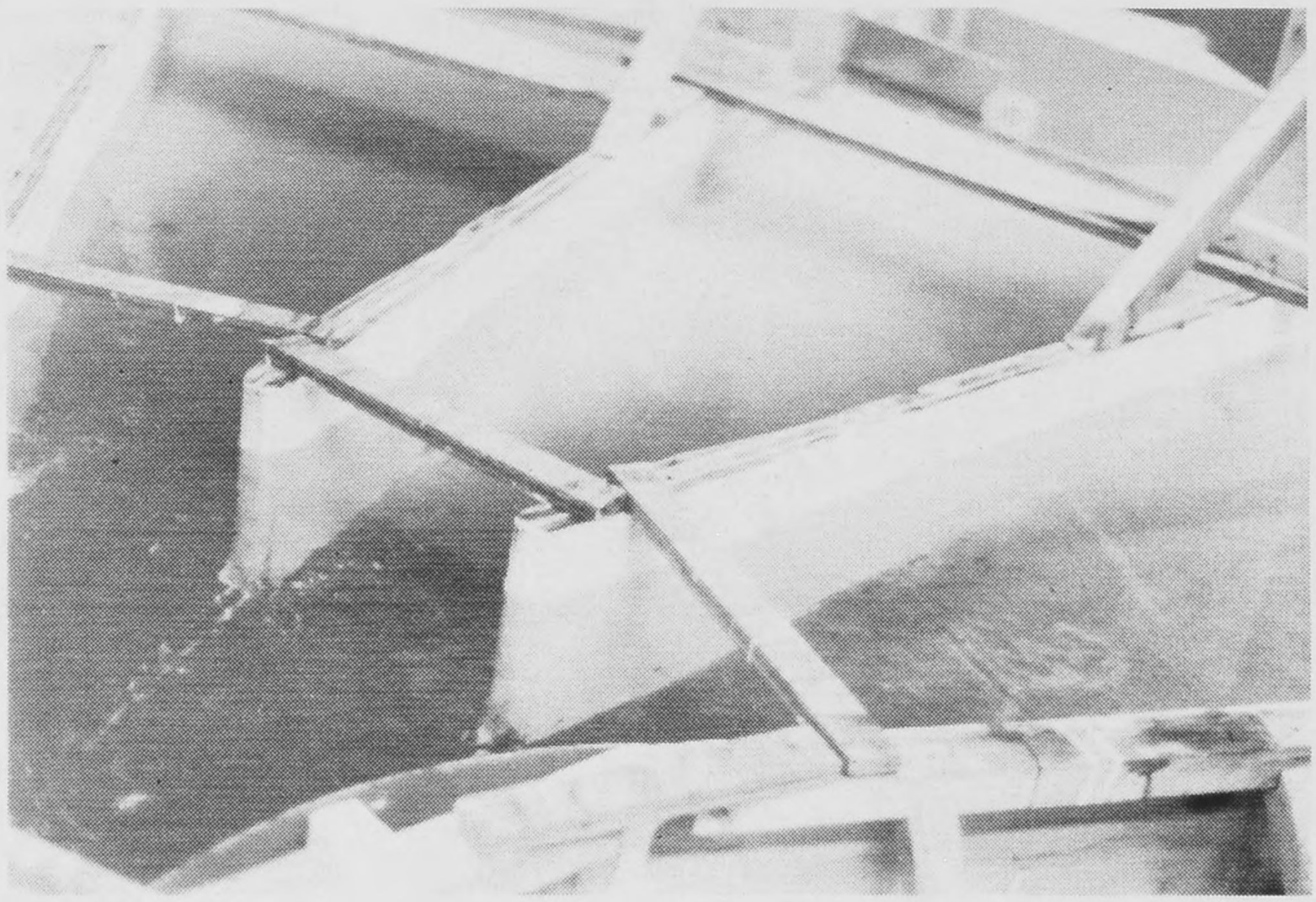

d .) Deposition in Individual Trains, Total Flow = 70 MGD.

Figure 59. Sediment Deposition Patterns, 1988 Entrance.

MGD. At lesser flow rates,an even larger percentage was recovered and the apparent anomaly associated with 50 MGD was clearly associated with sediment lost during the recovery process during the first experiment when the experimental procedure for the recovery process was still being developed.

It is not clear that the model sediment corresponded to the sediment that would be expected in the splitter chamber, as apparently the size fractions provided were from a sample taken from the present plant operation in the grit chamber ahead of the pumping station. Grit removal is to be even more efficient in the new operation and therefore an even smaller size may be removed by sedimentation prior to entry into the splitter chamber. Consequently, too large a grit size may have been used in the model. It is understood that the splitter chamber is presently operating with one train (Train 3) in operation and a flow of approximately 30-50 MGD. In this state, significant sediment deposition was observed in the downstream channel until the air diffuser at the channel bottom was turned on. Therefore, it would appear necessary to maintain this operating condition for most normal flows.

Table 3. Sediment Recovery with 1988 Entrance.

Section	Percent of Introduced Sediment Recovered					
	50 MGD	70 MGD	90 MGD	110 MGD	130 MGD	150 MGD
A	74.1*	67.6	49.0	36.6	22.2	17.3
B	3.7	8.3	13.2	13.3	11.0	9.6
C	0.6	3.7	6.4	10.6	14.1	13.7
D	0.6	4.8	7.4	9.2	12.6	13.2
E	1.7	7.2	11.6	13.0	13.2	16.2
Lost	19.3*	8.3	12.4	17.3	25.9	30.0

* Some sediment was lost during recovery process, smaller fraction actually passed through system.

2015 Entrance

The same general results as observed with the 1988 entrance were also found with the 2015 entrance. Sediment deposition was observed on the right hand side of the entrance channel while the left hand side was scoured relatively clean. Table 4 presents the results of the sediment recovery testing. A relatively constant fraction was left in each of the outlet channels for each flow, and the increased sediment loss came primarily from the inlet channel. As the total flow is increased, less sediment was deposited in the model. At the highest flow of 300 MGD, most of the sediment was carried through the splitter chamber with very little deposited upstream from the guide vanes. No significant differences in splitter chamber performance should be expected with the 2015 entrance as compared to the 1988 entrance.

Table 4. Sediment Recovery with 2015 Entrance.

	Percent of Introduced Sediment Recovered					
Section	150 MGD	170 MGD	200 MGD	220 MGD	250 MGD	300 MGD
A	38.6	28.2	22.2	15.4	9.2	1.6
B	7.2	7.3	7.8	7.0	7.7	1.8
C	12.5	12.7	12.7	12.1	11.4	10.9
D	6.8	7.6	9.1	9.0	8.8	7.9
E	8.0	8.6	8.5	8.7	8.6	8.1
F	9.4	9.7	10.4	10.1	10.6	10.1
Lost	17.6	25.8	29.2	37.6	43.7	59.5

Water Levels

Design information was previously requested regarding the potential location of the water level sensors in the individual channel downstream from the guide vanes

and was transmitted in a letter dated August 13, 1987 to Cosmo Bertino of URS Dalton from Dr. S.J. Wright of The University of Michigan. A copy of the text of that letter is included below to describe the details of that recommendation and for completeness in this report.

There were no obvious flow phenomena that suggested a desired location for the placement of the water level sensor in Train 4. In general, the flows were much more parallel with the 2015 entrance compared to the 1988 entrance and the flow visualization experiments indicated no significant wake zones, so it appears that the sensor placement would be primarily a matter of convenience.

Copy of August 13, 1987 Letter to Cosmo Bertino

This letter is in response to your request for guidance on the placement of the water level sensors in the influent splitter chamber for the Columbus, Ohio WWTP expansion. I have reviewed the results of our model tests to date associated with the 1988 entrance and am making a recommendation based upon those tests. Enclosed is a sketch (Figure 60) of the model and indicated are the locations of the sensors for the West, Center, and East trains.

I am basing this recommendation upon the fact that in the model study, the left side (facing downstream) of Center and East trains were found to exhibit separation zones with well defined wakes in many of the model tests. Although the issue of sediment deposition has apparently not been clearly resolved at present, it appears that there is more likelihood for sediment deposition in these wake regions. Therefore we have chosen to recommend the right side of those respective channels. West train showed no wake region near the downstream end of the channel.

We have made measurements of water level elevations at the positions indicated in the sketch and also at the opposite sides of each train for each of the various flow rates considered in the 88 entrance studies. These readings have indicated that the right side of West train is consistently lower than the readings at the other positions. The reason for this is not entirely clear, but it is apparent that there is flow into West train from Center train at the downstream end so this would be consistent. I have chosen to recommend the left side of West train where the recorded water levels are more consistent with those in the other trains. The other water level measurements are generally consistent to within about a third of an inch (prototype water level measurement) and this is probably near the limit of the measurement accuracy as discrepancies get greater at higher flows where there is more surface disturbance.

Some preliminary efforts were made to use the measured heads to predict the weir discharges and compare them to the measured values. Information on weir coefficients was taken from Brater and King's *Handbook of Hydraulics* by McGraw-Hill. They report a series of tests by Kindsvater and Carter who studied weirs with end contractions and with a square-edged weir crest. A spread sheet (Table 5) is attached which summarizes the results of the comparison with the last row containing the ratio of measured flow to predicted. At the higher flows, the comparison is very good, while we over-predict the discharge for the lower flows. It is not obvious that the empirical formulas of Kindsvater and Carter are valid in the low flow range since their correction for crest length ends up with an increased weir length rather than a decreased one due to the end contractions. Therefore, it is not clear that the comparison means anything. We shall continue to explore this issue however.

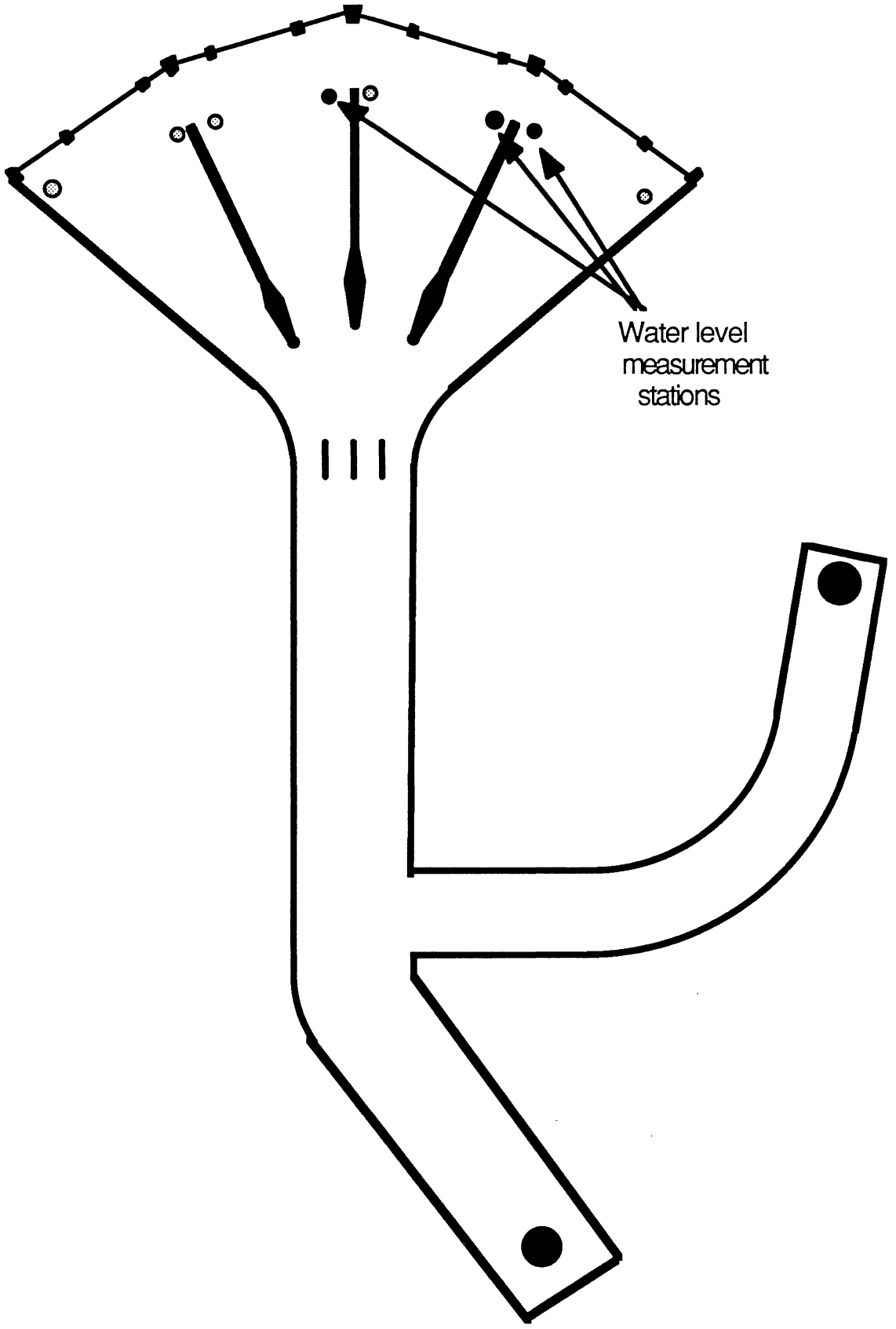

Figure 60. Recommended Water Level Sensor Placement.

	A	B	C	D	E	F	G
1		Q - 50 MGD	Q - 70 MGD	Q - 90 MGD	Q - 110 MGD	Q - 130 MGD	Q - 150 MGD
2							
3	L1	0.467	0.467	0.467	0.467	0.467	0.467
4	L2	0.933	0.933	0.933	0.933	0.933	0.933
5	L3	1.4	1.4	1.4	1.4	1.4	1.4
6	L1/B1	0.74	0.74	0.74	0.74	0.74	0.74
7	L2/B2	0.85	0.85	0.85	0.85	0.85	0.85
8	L3/B3	0.89	0.89	0.89	0.89	0.89	0.89
9	kL1	0.014	0.014	0.014	0.014	0.014	0.014
10	kL2	0.014	0.014	0.014	0.014	0.014	0.014
11	kL3	0.013	0.013	0.013	0.013	0.013	0.013
12							
13	Le1	0.481	0.481	0.481	0.481	0.481	0.481
14	Le2	0.947	0.947	0.947	0.947	0.947	0.947
15	Le3	1.413	1.413	1.413	1.413	1.413	1.413
16							
17	P	0.37	0.37	0.37	0.37	0.37	0.37
18	H1	0.082	0.093	0.107	0.126	0.138	0.151
19	H2	0.081	0.096	0.11	0.127	0.139	0.151
20	H3	0.0835	0.097	0.113	0.13	0.139	0.154
21	H/P	0.22162162	0.25135135	0.28918919	0.34054054	0.37297297	0.40810811
22							
23	Ce1	3.22	3.22	3.23	3.24	3.24	3.24
24	Ce2	3.28	3.29	3.3	3.3	3.31	3.31
25	Ce3	3.29	3.3	3.32	3.33	3.33	3.34
26							
27	kH	0	0	0	0	0	0
28	He1	0.082	0.093	0.107	0.126	0.138	0.151
29	He2	0.0825	0.096	0.11	0.127	0.139	0.151
30	He3	0.0835	0.097	0.113	0.13	0.139	0.154
31							
32	Q1Tr1	0.03636819	0.04392638	0.054378	0.06970211	0.079893	0.09144406
33	Q2Tr1	0.07293645	0.09267289	0.11401263	0.14143911	0.16244269	0.18392611
34	Q3tr1	0.10915882	0.14086844	0.17819598	0.22054714	0.24384205	0.28521326
35	Q1Tr2	0.03670134	0.0460689	0.05668089	0.07053354	0.08076297	0.09144406
36	Q2Tr2	0	0	0	0	0	0
37	Q3tr3	0.11015875	0.13869569	0.17114699	0.21295703	0.24384205	0.27691983
38	Q1tr3	0.03737065	0.04679059	0.05901539	0.07304746	0.08076297	0.09418271
39	Q2Tr3	0.07494688	0.09412467	0.11870844	0.14648021	0.16244269	0.18943449
40	Q3tr3	0.11216769	0.14086844	0.17819598	0.22054714	0.24384205	0.28521326
41							
42	Qtrain1	0.21846346	0.27746771	0.34658661	0.43168835	0.48617773	0.56058343
43	Qtrain2	0.14686008	0.18476458	0.22782788	0.28349057	0.32460502	0.36836389
44	Qtrain3	0.22448522	0.2817837	0.35591981	0.4400748	0.48704771	0.56883046
45	Qtotal	0.58980876	0.74401599	0.9303343	1.15525372	1.29783046	1.49777778
46	Qmeasured	0.503	0.7	0.9	1.096	1.303	1.5
47	Qmea./Qcomp.	0.8528188	0.94083999	0.96739419	0.94870935	1.00398322	1.00148368

TABLE 5. Water Level Sensor Computations.

DESCRIPTION OF COMPUTATIONS OUTLINED IN WORKSHEET ON PAGE 99.

Kindsvater and Carter Equations

$$Q = C_e L_e H_e^{32}$$

where Q is the weir discharge, C_e is the weir coefficient, L_e is the *effective weir length,* and H_e is the *effective weir head.* The latter two variables are in turn computed from

$$L_e = L + k_L$$

and

$$H_e = H + k_H$$

with L and H, the actual weir length and head and k_L and k_H are corrections factors given by

k_H = 0.003 feet

k_L is a graphical function of the weir crest length L divided by the total width between sidewalls B

C_e is also a graphical function of the same ratio and also the H/P ratio

where P is the depth below the weir crest and just upstream of the weir. All terms are consistent in units of feet and seconds.

The spreadsheet is laid out so that computations are performed for each of the three weir crest lengths in each train separately. The width between sidewalls is taken as the distance to the center of the piers dividing the individual weir crests. Section 1 is the short (1/6 length) weir opening, Section 2 is the longer (2/6) one, and Section 3 is the center (1/2 length) weir opening.

Separate L/B ratios are computed (rows 6-8), k_L values recorded (rows 9-11), and effective lengths computed (rows (13-15)

Head ratios H/P are (with heads from the water level measurements) then computed (rows 17-21)

Weir Coefficients are recorded (rows 23-24) and effective heads computed (rows 27-30)

Finally, flow rates for each of the individual weir openings in each of the three trains are computed (rows 32-40), individual train flows summed (rows 42-44) total flow summed (row 45) and compared with the measured flow rate (rows 46-47).

Vortex Shedding

The studies on vortex shedding by the vane were made to determine the likelihood of possible resonant interactions associated with vane vibration. It was felt in the early phases of the study that this was not likely to be a significant problem and the physical model was used to verify that assumption rather than to obtain detailed information regarding the vortex shedding properties for a wide variety of vane configurations. In particular, to obtain Reynolds numbers in the range of those expected in the prototype, it was not possible to model all three vanes simultaneously. Rather, the flow around a single vane was modeled. A previous study by Abernathy (2) was used to help interpret the results of the present study. The study by Abernathy considered the flow around a flat plate which was oriented at an angle to the free stream in a confined flow, i.e. with side walls relatively close to the plate edges. The effect of the relative blockage of the flow by the plate was studied as was the effect of varying the plate angle to the approach flow. In the study the variation of the Strouhal Number $S_t = \omega L \cos\alpha/U$ was studied, where L is the length of the plate and $L \cos\alpha$ is the length projected normal to the free stream. It was found that S_t varied within a fairly narrow range of 0.143 - 0.193 for approach angles in the same range considered in the present study and for a wide range of blockage conditions and other influences. In fact, the variations can be expected to be minor for a flat plate in which the separation points are fixed at the leading and trailing edges of the plate.

A significant difference between the flat plate and the present vane shape would not be expected because the separation points are still likely to be at the leading and trailing edges of the vane. Therefore, it is reasonable to expect that similar Strouhal numbers would result in the present study. This was found to be the case as indicated for the two vane angles studied (35° and 45°) in Fig. 61. The variation in flow velocity is

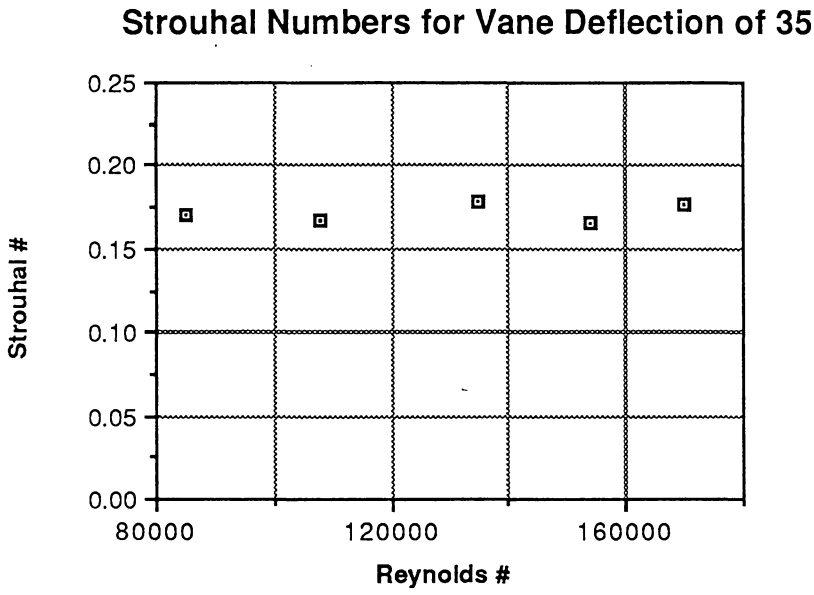

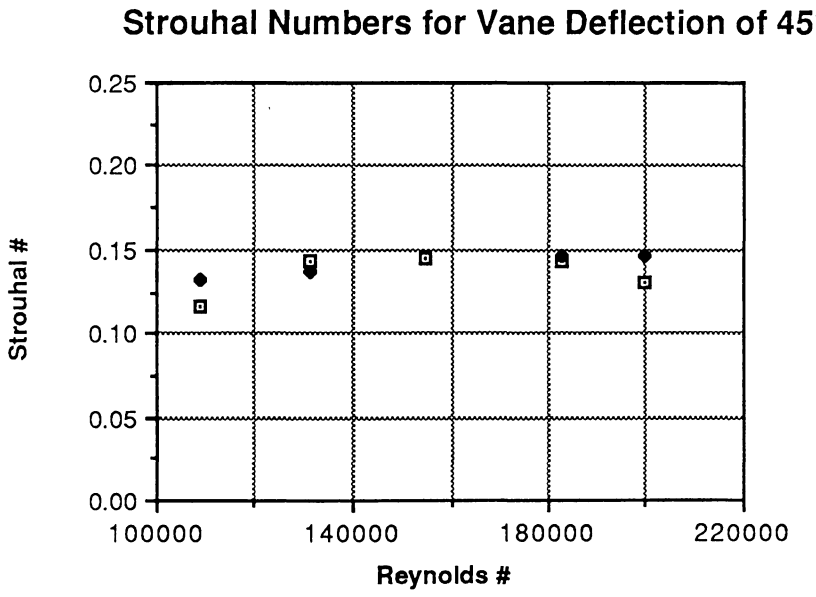

Figure 61. Strouhal Number for Guide Vane at Different Angles of Attack Versus Reynolds Number.

presented in terms of the Reynolds Number $R_e = ULcos\alpha/\nu$, with ν the kinematic viscosity of the fluid. Generally, it has been found in previous studies that the Strouhal number is independent of Reynolds Number (at least at large Reynolds Numbers) and this is also the case in the present study. Therefore, the results can be extended to any arbitrary approach velocity. Furthermore, the magnitude of the Strouhal Number is only slightly dependent on the vane orientation, with a value of approximately 0.165 for a vane deflection of 35° and 0.14 for a vane angle of 45°. The two sets of data for the vane angle of 45° represent estimates from the spectrum analyzer signal and from the analog pressure traces. Tentative experiments were performed with smaller vane angles and it became increasingly difficult to deduce the vortex shedding frequencies because the pressure signals were dominated by the higher frequency turbulence. However, it is highly unlikely that the Strouhal numbers change significantly from the indicated range.

In order to appreciate the indicated prototype performance, consider the average approach velocities associated with the limiting flows of 50 and 300 MGD. Given the flow depth at the vanes, the average approach velocities should range between roughly 0.5 and 3.5 ft/sec. At a vane angle of 45° and Strouhal Number of 0.14, the vortex shedding frequencies should range between about 0.025 and 0.15 Hz. Since the response analysis for the vane indicated that the frequency associated with the lowest vibration mode is 65 Hz, this makes the vortex shedding and structural response frequencies over a factor of 400 apart and therefore, no possibility for resonant interactions of vane vibration and vortex shedding can possibly be anticipated.

SUMMARY

A variety of different measurements were made in the two physical models. These included the flow distributions for various splitter chamber flows and configurations, the variations of vane angles required to achieve the desired flow split, the velocity profiles in the inlet conduit preceding the control vanes, the sedimentation patterns at various flows, water level variations upstream from the overflow weirs,

and the vortex shedding frequencies for flow past the control vanes. The results of the physical modelling allow fairly definite conclusions in most cases.

It was found that the flow distributions without the control vanes are satisfactory for some configurations and flow rates, but not for all conditions. However, with proper adjustment of the control vanes, a reasonable flow distribution in nearly all cases can be attained. In general, a single combination of vane settings can distribute the flow satisfactorily over the entire range of flows associated with a given splitter chamber configuration, i.e. with a given entrance and combination of trains in operation. This combination of angles varies with the flow configuration and was established as a result of the study.

Other findings included the establishment that free vibration modes of the vanes were associated with frequencies a factor of at least 400 higher than the vortex shedding frequencies for anticipated flows past the vanes. The sedimentation studies were more ambiguous in that significant sedimentation within the splitter chamber was observed. However, the model sediment was scaled from a specified size that may not be representative of the grit that will actually pass through the splitter chamber, so it is not entirely clear that the model results indicate this to be a real problem. Finally, locations for the placement of water level sensors in each of the flow trains were recommended.

ACKNOWLEDGEMENTS

A number of different students and technicians were involved in various phases of the model construction and testing. Technicians Kevin Schmidt and Merrick Burch provided valuable help in the model construction. Students Robert Koch, Timothy Finley, Samer Maamari, Farhang Aslani, and Chi-Lin Chang were involved in various phases of the model testing in addition to the authors. The help of all is gratefully acknowledged.

REFERENCES

1. "Sedimentation Engineering," *American Society of Civil Engineers Manuals and Reports on Engineering Practice,* No. 54, 1975

2. F.H. Abernathy, "Flow Over an Inclined Plate," *Transactions, ASME, Journal of Basic Engineering,* Vol. 84, 1962, pp. 380-388.

APPENDIX A

RESULTS OF FINITE ELEMENT ANALYSIS
FREE VIBRATION ANALYSIS FOR VANE
WITH SAP - 80*

* Structural Analysis Program -
Finite Element Analysis of Static and Dynamic Structures
By E.L. Wilson and A. Haibibullah
Computers and Structures, Inc.
San Francisco, California
(415) 845-2177

Page Missing in Original Volume

VANE MODELING FOR NATURAL FREQUENCY - FOR PROF. SJW (VANE67)

E I G E N S Y S T E M P A R A M E T E R S

NUMBER OF EQUATIONS	=	561
NUMBER OF MASSES	=	264
NUMBER OF VALUES TO BE EVALUATED	=	5
SIZE OF SUBSPACE	=	9

E I G E N V A L U E S

EIGENVALUE NUMBER	EIGENVALUE (RAD/SEC)**2	CIRCULAR FREQ (RAD/SEC)	FREQUENCY (CYCLES/SEC)	PERIOD (SEC)
1	.169920E+06	.412213E+03	65.605772	.015243
2	.223878E+06	.473157E+03	75.305327	.013279
3	.304747E+06	.552039E+03	87.859767	.011382
4	.362210E+06	.601839E+03	95.785638	.010440
5	.366071E+06	.605038E+03	96.294825	.010385

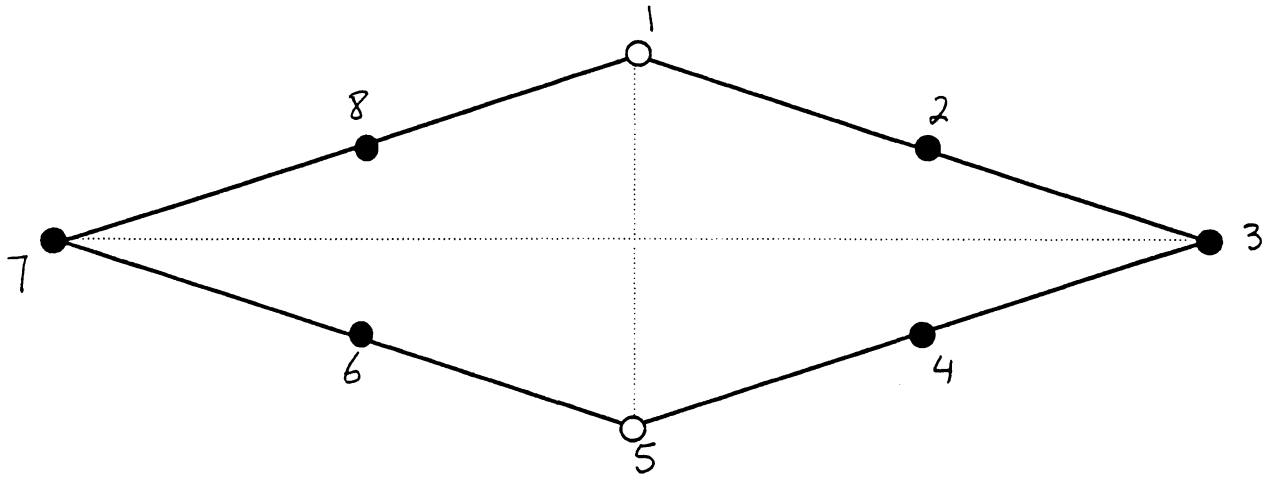

FINITE ELEMENT MODEL OF THE SECTION

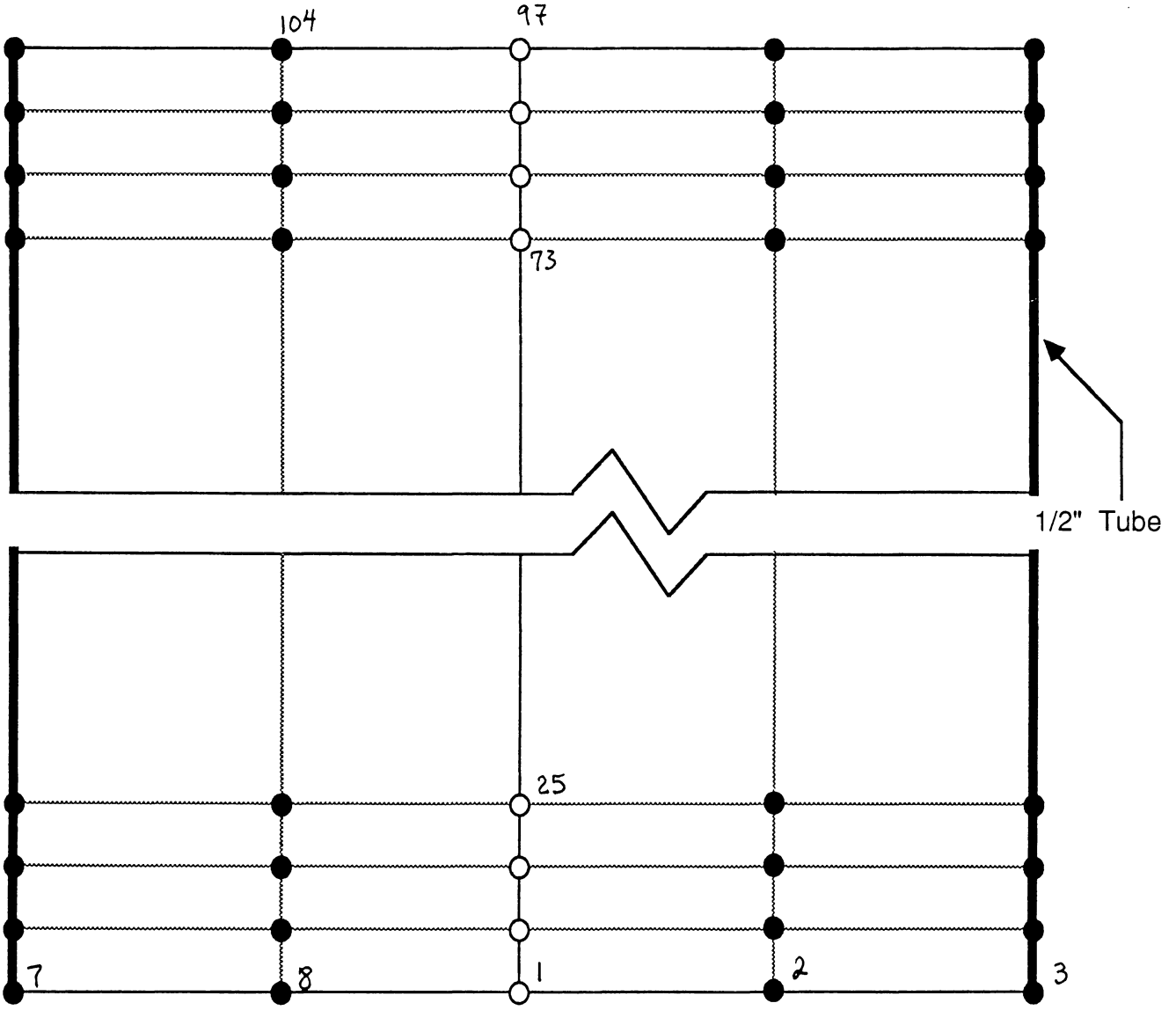

FINITE ELEMENT MODEL OF THE ELEVATION

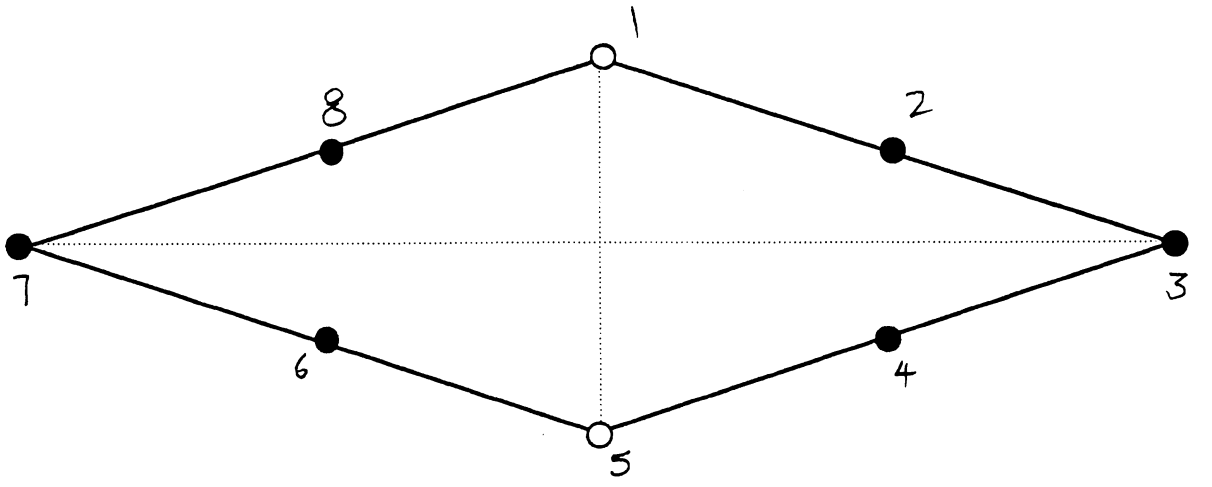

FINITE ELEMENT MODEL OF THE SECTION

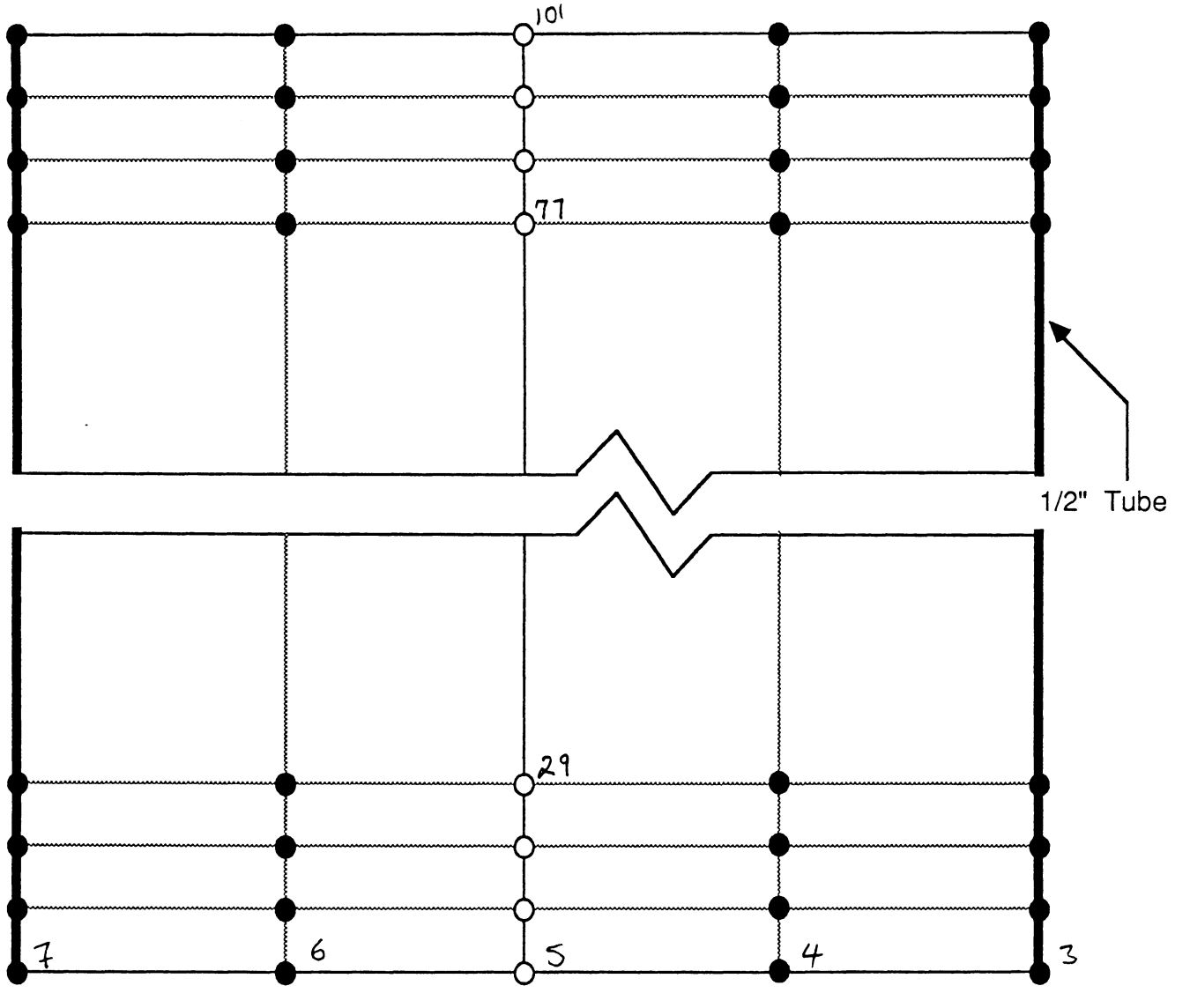

FINITE ELEMENT MODEL OF THE ELEVATION

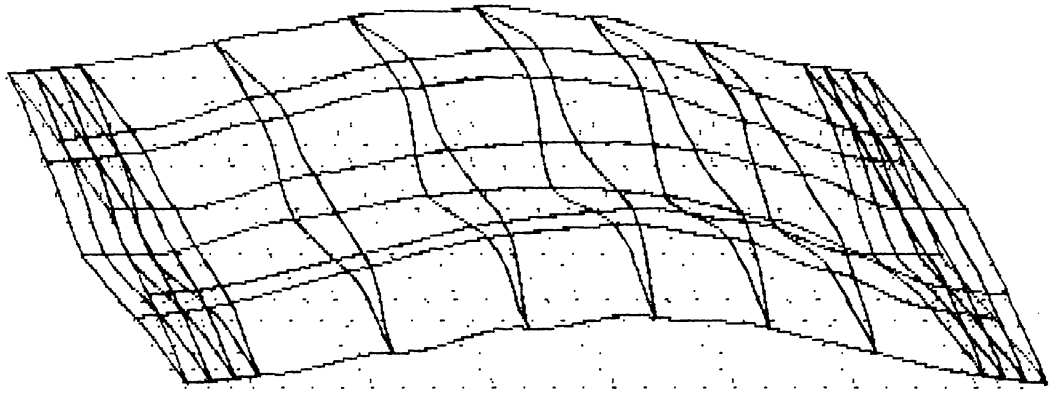

SAP80

FILE : VANE7

MODE NUMBER : 1

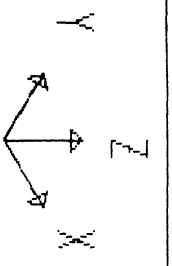

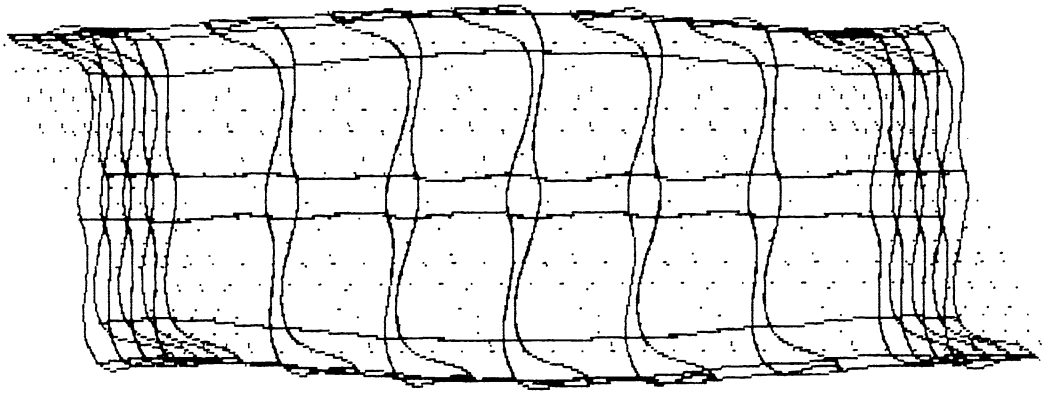

SAP80

FILE : VANE7

MODE NUMBER : 2

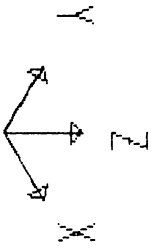

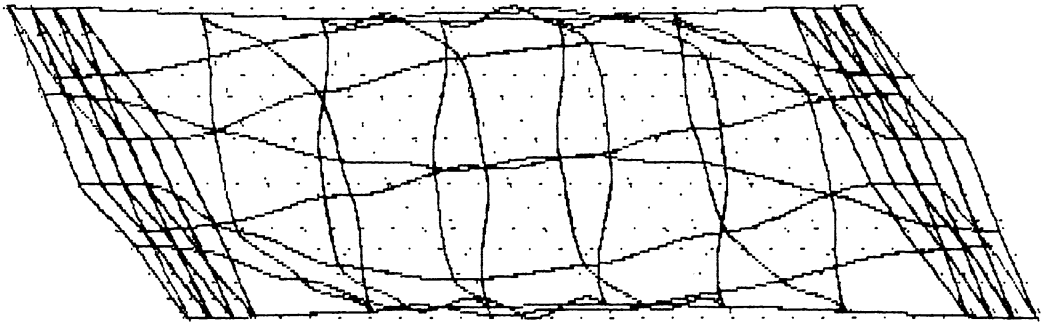

SAP80

FILE : VANE7

MODE NUMBER : 3

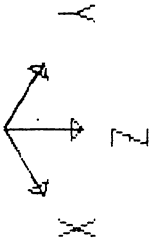

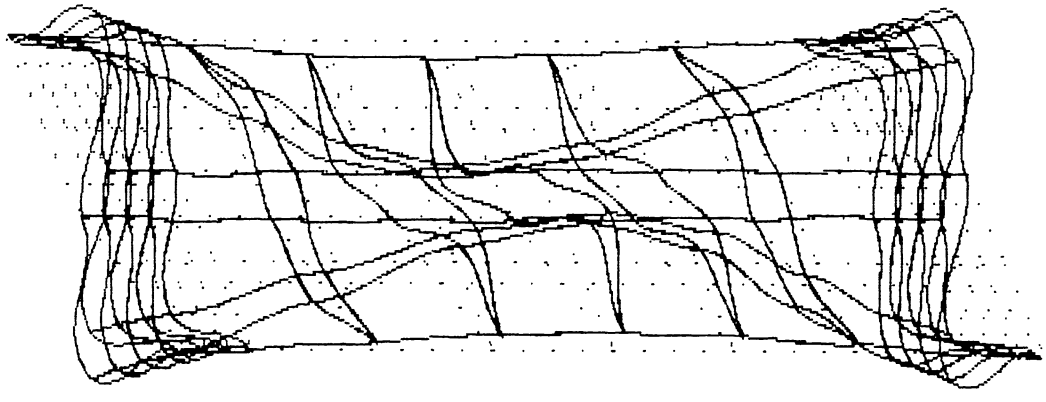

SAP80

FILE : VANE7

MODE NUMBER : 4

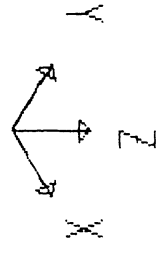

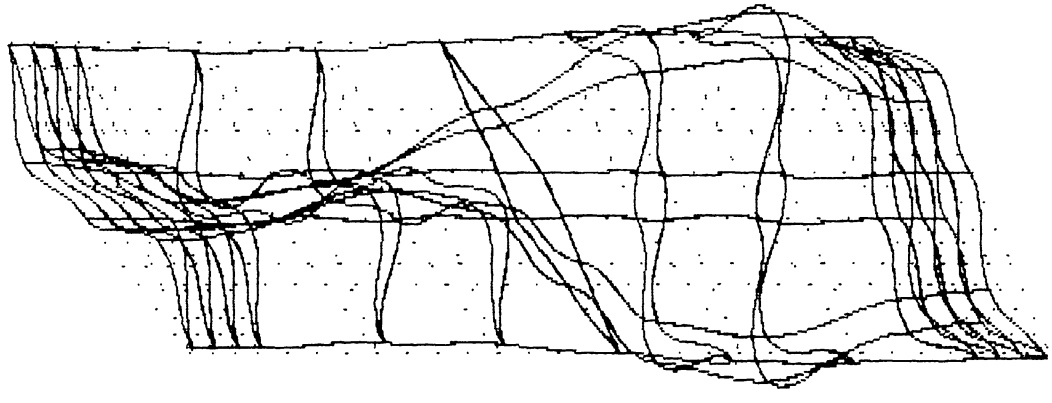

SAP80

FILE : VANE7

MODE NUMBER : 5

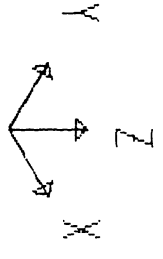

```
VANE MODELING FOR NATURAL FREQUENCY - FOR PROF. SJW (VANE67)
SYSTEM
N= 104        V= 5
JOINTS
1       X= 0     Y= +3.5     Z= 0
5       X= 24    Y= 0                    G= 1,3
9       X= 0     Y= -3.5                 G= 3,5
7       X= -24   Y= 0                    G= 5,7
8       X= -12   Y= +3.5/2
C
25      X= 0     Y= 3.5      Z= 9        G= 1,25,8
73                           Z= 106      G= 25,73,8
97                           Z= 115      G= 73,97,8     F= 1,7,12,1,8

RESTRAINTS
1,25,8              R=1,1,1,0,0,0
73,97,8             R=1,1,1,0,0,0
5,29,8              R=1,1,1,0,0,0
77,101,8            R=1,1,1,0,0,0

CONSTRAINTS
9,25,8              C=0,0,0,0,0,1
73,97,8             C=0,0,0,0,0,1
5,29,8              C=0,0,0,0,0,1
77,101,8            C=0,0,0,0,0,1

FRAME
NM=1
1 A= 2.66   I= 1.31,1.31     J=2.62        E= 30E+03      M=21E-07
1   3   11      M=1   LP=2,0      G= 11,1,8,8
16  7   15                        G= 11,1,8,8

SHELL
NM=1
1       E=30E+03             M=7.286E-07     U=.3
1       JQ= 1,2,9,10          ELTYP=2       M=1   TH=.5     LP=0      G= 7,12
85      JQ= 8,1,16,9                                                   G= 1,12
```

AIIM SCANNER TEST CHART # 2

Spectra

4 PT ABCDEFGHIJKLMNOPQRSTUVWXYZabcdefghijklmnopqrstuvwxyz:'',./?$0123456789

6 PT ABCDEFGHIJKLMNOPQRSTUVWXYZabcdefghijklmnopqrstuvwxyz;:'',./?$0123456789

8 PT ABCDEFGHIJKLMNOPQRSTUVWXYZabcdefghijklmnopqrstuvwxyz;:'',./?$0123456789

10 PT ABCDEFGHIJKLMNOPQRSTUVWXYZabcdefghijklmnopqrstuvwxyz;:'',./?$0123456789

Times Roman

4 PT ABCDEFGHIJKLMNOPQRSTUVWXYZabcdefghijklmnopqrstuvwxyz;:'',./?$0123456789

6 PT ABCDEFGHIJKLMNOPQRSTUVWXYZabcdefghijklmnopqrstuvwxyz;:'',./?$0123456789

8 PT ABCDEFGHIJKLMNOPQRSTUVWXYZabcdefghijklmnopqrstuvwxyz;:'',./?$0123456789

10 PT ABCDEFGHIJKLMNOPQRSTUVWXYZabcdefghijklmnopqrstuvwxyz;:'',./?$0123456789

Century Schoolbook Bold

4 PT **ABCDEFGHIJKLMNOPQRSTUVWXYZabcdefghijklmnopqrstuvwxyz;:'',./?$0123456789**

6 PT **ABCDEFGHIJKLMNOPQRSTUVWXYZabcdefghijklmnopqrstuvwxyz;:'',./?$0123456789**

8 PT **ABCDEFGHIJKLMNOPQRSTUVWXYZabcdefghijklmnopqrstuvwxyz;:'',./?$0123456789**

10 PT **ABCDEFGHIJKLMNOPQRSTUVWXYZabcdefghijklmnopqrstuvwxyz;:'',./?$0123456789**

News Gothic Bold Reversed

4 PT ABCDEFGHIJKLMNOPQRSTUVWXYZabcdefghijklmnopqrstuvwxyz;:'',./?$0123456789

6 PT ABCDEFGHIJKLMNOPQRSTUVWXYZabcdefghijklmnopqrstuvwxyz;:'',./?$0123456789

8 PT ABCDEFGHIJKLMNOPQRSTUVWXYZabcdefghijklmnopqrstuvwxyz;:'',./?$0123456789

10 PT ABCDEFGHIJKLMNOPQRSTUVWXYZabcdefghijklmnopqrstuvwxyz;:'',./?$0123456789

Bodoni Italic

4 PT ABCDEFGHIJKLMNOPQRSTUVWXYZabcdefghijklmnopqrstuvwxyz;:'',./?$0123456789

6 PT ABCDEFGHIJKLMNOPQRSTUVWXYZabcdefghijklmnopqrstuvwxyz;:'',./?$0123456789

8 PT ABCDEFGHIJKLMNOPQRSTUVWXYZabcdefghijklmnopqrstuvwxyz;:'',./?$0123456789

10 PT ABCDEFGHIJKLMNOPQRSTUVWXYZabcdefghijklmnopqrstuvwxyz;:'',./?$0123456789

Greek and Math Symbols

4 PT ΑΒΓΔΕΞΘΗΙΚΛΜΝΟΠΦΡΣΤΥΩΧΨΖαβγδεξθηικλμνοπφρστυωχψζ≧∓'',. / ≦±=≠°><⊁⊀⩾⩽≡

6 PT ΑΒΓΔΕΞΘΗΙΚΛΜΝΟΠΦΡΣΤΥΩΧΨΖαβγδεξθηικλμνοπφρστυωχψζ≧∓'',. / ≦±=≠°><⊁⊀⩾⩽≡

8 PT ΑΒΓΔΕΞΘΗΙΚΛΜΝΟΠΦΡΣΤΥΩΧΨΖαβγδεξθηικλμνοπφρστυωχψζ≧∓'',. / ≦±=≠°><⊁⊀⩾⩽≡

10 PT ΑΒΓΔΕΞΘΗΙΚΛΜΝΟΠΦΡΣΤΥΩΧΨΖαβγδεξθηικλμνοπφρστυωχψζ≧∓'',. / ≦±=≠°><⊁⊀⩾⩽≡

White

Black

Isolated Characters

e	m	1	2	3	a
4	5	6	7	o	°
8	9	0	h	I	B

A4 Page 6543210

MESH HALFTONE WEDGES

65

85

100

110

133

150

A4 Page 6543210

RIT ALPHANUMERIC RESOLUTION TEST OBJECT, RT-1-71

PRODUCED BY GRAPHIC ARTS RESEARCH CENTER

ROCHESTER INSTITUTE OF TECHNOLOGY, ONE LOMB

MEMORIAL DRIVE, ROCHESTER, NEW YORK 14623